Unfolding, crosslinking and co-polymerization of Camelina protein
and its use as wood adhesives

by

Xiangwei Zhu

B.S., Huazhong Agricultural University, 2010
M.S., Huazhong Agricultural University, 2012

AN ABSTRACT OF A DISSERTATION

submitted in partial fulfillment of the requirements for the degree

DOCTOR OF PHILOSOPHY

Department of Grain Science and Industry
College of Agriculture

KANSAS STATE UNIVERSITY
Manhattan, Kansas

2017

Abstract

Oilseed protein is a promising renewable source to be used as the replacement of petroleum-based materials for adhesion purpose, and it has drawn increasing attention since soy-based adhesives were developed for wood glues. However, soy protein comprises a portion of humans' diets, thereby creating competition between utilization of soy protein for protein-based products or human food. Therefore, alternative bio-resources must be discovered. Proteins from camelina sativa provide such potential. Similar to other protein-based polymers, low mechanical strength and poor water resistance are the major drawbacks limiting camelina protein's further applications. In this research, camelina protein (CP) was modified by unfolding, crosslinking, and co-polymerization treatment for improved flow-ability, adhesion properties and water resistance, which facilitates the industrialization of camelina as an alternative to soy-based adhesives. The physicochemical properties and microstructures of CP were also investigated.

To increase the reactivity of CP adhesive, the first step is to denature the folded structure of native proteins. Camelina protein was extracted from defatted camelina meal through alkali solubilization and acid precipitation and modified with varying amount of $NaHSO_3$ (0-12% of the protein dry base) and Gdm.Cl (0-250% of the protein dry base). $NaHSO_3$ treatment broke the disulfide bonds of the CP and thus increased its free sulfhydryl content and surface hydrophobicity. As $NaHSO_3$ concentration increased, the viscosity, elastic modulus (G') and water resistant of $NaHSO_3$-modified camelina protein (SMCP) dispersion decreased, and the protein became hydrophobic. Gdm.Cl treatment broke the CPI's hydrogen bonds but decreased their surface hydrophobicity. Similarly, viscosity, G', and water resistant of Gdm.Cl-modified camelina protein (GMCP) dispersions decreased as Gdm.Cl increased and protein became to aggregate. The reducing effect of $NaHSO_3$ was more obvious than Gdm.Cl to disrupt CPI's intermolecular protein interaction but less obvious than Gdm.Cl to reduce the viscosity and water resistant.

To further increase the CP's water resistance, a coupling agent, Ethyl-3-(3-dimethyl-aminopropyl-1-carbodiimide) (EDC), was applied to stabilize the protein structure by crosslinking the free carboxyl groups and amino groups. The cross-linked CP exhibited increased molecular weight and particle size. Microstructures of modified CP also became rigid and condensed. Accordingly, CP's increased intermolecular protein interaction resulted in its higher elastic modulus, viscosity and water resistance. The ultrasound pretreatment further increased the

crosslink degree of CP, which resulted in protein's increased aggregation behaviors and compact micro-structures. Consequently, the elastic modulus, viscosity, and water resistance of CP increased accordingly.

Copolymerization with hydrophobic enhancers was also an effective method to improve CP's water resistance. In this study, kraft lignin was oxidized by H_2O_2 and then copolymerized with CP as wood adhesives, which exhibited increased wet strength. In the presence of ultrasound irradiation, the H_2O_2-depolymerized kraft lignin exhibited reduced particle size, thermal stability and increased content of hydroxyl groups. Fluorescence spectroscopy analysis revealed that after coupling with pristine or de-polymerized lignin, CP exhibited increased hydrophobicity due to lignin's increased reactivity with camelina protein. Accordingly, the water resistance of CP-based adhesives improved. In the optimized condition, when CP was copolymerized with ultrasound-induced oxidized lignin, it had increased wet shear adhesion strength from 0.28 MPa to 1.43 MPa, with wood panels passing the three-cycle water soaking test.

Unfolding, crosslinking and co-polymerization of Camelina protein
and its use as wood adhesives

by

Xiangwei Zhu

B.S., Huazhong Agricultural University, 2010
M.S., Huazhong Agricultural University, 2012

A DISSERTATION

submitted in partial fulfillment of the requirements for the degree

DOCTOR OF PHILOSOPHY

Department of Grain Science and Industry
College of Agriculture

KANSAS STATE UNIVERSITY
Manhattan, Kansas

2017

Approved by:

Major Professor
Xiuzhi Susan Sun

Copyright

Abstract

Oilseed protein is a promising renewable source to be used as the replacement of petroleum-based materials for adhesion purpose, and it has drawn increasing attention since soy-based adhesives were developed for wood glues. However, soy protein comprises a portion of humans' diets, thereby creating competition between utilization of soy protein for protein-based products or human food. Therefore, alternative bio-resources must be discovered. Proteins from camelina sativa provide such potential. Similar to other protein-based polymers, low mechanical strength and poor water resistance are the major drawbacks limiting camelina protein's further applications. In this research, camelina protein (CP) was modified by unfolding, crosslinking, and co-polymerization treatment for improved flow-ability, adhesion properties and water resistance, which facilitates the industrialization of camelina as an alternative to soy-based adhesives. The physicochemical properties and microstructures of CP were also investigated.

To increase the reactivity of CP adhesive, the first step is to denature the folded structure of native proteins. Camelina protein was extracted from defatted camelina meal through alkali solubilization and acid precipitation and modified with varying amount of $NaHSO_3$ (0-12% of the protein dry base) and Gdm.Cl (0-250% of the protein dry base). $NaHSO_3$ treatment broke the disulfide bonds of the CP and thus increased its free sulfhydryl content and surface hydrophobicity. As $NaHSO_3$ concentration increased, the viscosity, elastic modulus (G') and water resistant of $NaHSO_3$-modified camelina protein (SMCP) dispersion decreased, and the protein became hydrophobic. Gdm.Cl treatment broke the CPI's hydrogen bonds but decreased their surface hydrophobicity. Similarly, viscosity, G', and water resistant of Gdm.Cl-modified camelina protein (GMCP) dispersions decreased as Gdm.Cl increased and protein became to aggregate. The reducing effect of $NaHSO_3$ was more obvious than Gdm.Cl to disrupt CPI's intermolecular protein interaction but less obvious than Gdm.Cl to reduce the viscosity and water resistant.

To further increase the CP's water resistance, a coupling agent, Ethyl-3-(3-dimethyl-aminopropyl-1-carbodiimide) (EDC), was applied to stabilize the protein structure by crosslinking the free carboxyl groups and amino groups. The cross-linked CP exhibited increased molecular weight and particle size. Microstructures of modified CP also became rigid and condensed. Accordingly, CP's increased intermolecular protein interaction resulted in its higher elastic modulus, viscosity and water resistance. The ultrasound pretreatment further increased the

crosslink degree of CP, which resulted in protein's increased aggregation behaviors and compact micro-structures. Consequently, the elastic modulus, viscosity, and water resistance of CP increased accordingly.

Copolymerization with hydrophobic enhancers was also an effective method to improve CP's water resistance. In this study, kraft lignin was oxidized by H_2O_2 and then copolymerized with CP as wood adhesives, which exhibited increased wet strength. In the presence of ultrasound irradiation, the H_2O_2-depolymerized kraft lignin exhibited reduced particle size, thermal stability and increased content of hydroxyl groups. Fluorescence spectroscopy analysis revealed that after coupling with pristine or de-polymerized lignin, CP exhibited increased hydrophobicity due to lignin's increased reactivity with camelina protein. Accordingly, the water resistance of CP-based adhesives improved. In the optimized condition, when CP was copolymerized with ultrasound-induced oxidized lignin, it had increased wet shear adhesion strength from 0.28 MPa to 1.43 MPa, with wood panels passing the three-cycle water soaking test.

Table of Contents

List of Figures

List of Tables

Acknowledgements

I would like to express my sincere gratitude to my major professor, Dr. Xiuzhi Susan Sun for her continuous encouragement, valuable advice, and insightful guidance during my PhD period in Department of Grain Science and Industry at Kansas State University. What I learned from Dr. Sun, such as her persistent focus to the science and enthusiasm attitude, would become to the fortune to lead my future study and work. Four years ago, I feel so lucky and excited to join Dr. Sun's group; In BTL, I was trained to be a qualified scientist, and now I appreciate every day I worked here. I would also like to thank Dr. Donghai Wang, Dr. Yonghui Li, Dr. Michal Zolkiewski, and Dr. Paul Smith for their interest to serve as my supervisory committee and providing valuable suggestions.

An expression of appreciation and thanks to all my fellows in Dr Sun's research group, Yonghui, Guangyan, Cong, Haijing, Jonggeun, Quan, Duanbin, Yizhou for their help and friendship. Also, I would like to thank my dear friends Dr. Ke Zhang and, Dr. Ningbo Li, Sarocha Pradyawong for their sincere friendship. Further thanks go to all the staff and graduate students in Grain Science Department for their continuous support.

At last, I deeply express my appreciation and gratitude to my parents and my wife Xi Chen, who give me unconditional and everlasting love. Thank you.

Chapter 1 - INTRODUCTION

1.1 General background

The global markets for adhesive and sealants have witnessed remarkable growth during the past few years: it would grow at a CARG of 4.72% between 2015 and 2020 and finally increase to $ 59.75 billion. Currently, petroleum-based polymers such as urea-formaldehyde, phenol-formaldehyde, polyvinyl chloride have been widely used in plywood, particleboard, labeling, packaging, and sizing (Mekonnen, Mussone, & Bressler, 2014). Adhesive produced from these chemicals exhibited strong bonding strength and resistance to moisture condition. However, the shrinking fuel resources and corresponding environmental problems caused by the petroleum manufacturing urged us to develop alternative bio-based materials (Guangyan Qi & Sun, 2010b; X. S. Sun, 2011). Some oilseed proteins, such as soy, have exhibited its process-ability and biocompatibility in fabricating the biodegradable polymers with bulk and surface modification. However, inherent characteristics such as and insufficient reactivity, modest strength and modulus, poor water resistance, high viscosity at high solid content have limited its use.

1.1.1 Problems for plant protein as adhesives

Petroleum-based synthetic adhesives prevailed in the current wood adhesive market, and most of them are based on the substrate such as urea formaldehyde (UF), phenol formaldehyde (PF), resorcinol-formaldehyde, polyvinyl acetate (PVA), or their derivates. All of these substrates contained the aldehyde groups that are highly reactive and potential to bond with wood surface. Compared with PVA, bonding strength for UF and PF is even stronger due to their presence of aldehyde groups and phenolic hydroxyl with increased reactivity(Song, Tang, Wang, & Wang, 2011). However, compared with those petroleum-based materials, the reactivity for plant proteins is much lower; several other inherent characteristics of proteins such as modest strength and modulus, poor water resistance, high viscosity at high solid content further limited their commercial applications. Unlike the chain structure polymers, most plant proteins are globular shape with complex secondary, tertiary and quaternary structures in the molecular level. Thus, except for the peptide bond within protein's primary structures, most protein subunits were non-covalently bonded together by hydrogen bond, hydrophobic interaction, ionic interaction, Van Der Waals interaction. This problem was even obvious when exposed to the water. In the aquatic environment the protein-substrate interaction was weakened. Thus, while natural proteins

already exhibited comparable wood bonding strength to the synthetic polymers, developing the water resistant protein adhesives became increasingly important to their applied values(Mo, Wang, & Sun, 2011a; Ren & Soucek, 2014).

1.1.2 Modifications to plant protein as adhesives

Based on protein's polymeric structure, there are five major methods to resolve these problems: 1) crosslink protein structures, 2) unfold protein structure with increased reactivity, 3) hydrophobic enhancers, 4) forming interpenetrating network, or 5) nano-particle enhancers. Unfolding treatment and introducing cross-linkers into protein dispersions are the most widely used and facile method to increase protein's wet bonding strength. Because, the pristine plant protein is a globular molecule with limited reactive functional groups exposed, after unfolding treatment, protein may exhibit (1) increased reactivity due to the exposed free functional groups such as free SH, (2) enhanced surface hydrophobicity to increase water resistance, or (3) decreased viscosity of protein solution to facilitate further processing(J.-M. Wang et al., 2011)(X. S. Sun, 2011). Typical unfolding reagents including sodium bisulfite, urea, guanidine-HCl, SDS, and crosslinking agents such as glutaraldehyde, were also systematically reported by our group to modify plant protein's structures, and corresponding functional properties(W. Huang & Sun, 2000a; Ningbo Li, Qi, Sun, Stamm, & Wang, 2011; Ying Wang, Mo, Sun, & Wang, 2007).

Although crosslinking and unfolding treatment could stimulate the polymerization and adhesion of protein based adhesive, the hydrophilic nature of modified polymers are still undesirable. Thus, In order to obtain a more hydrophobic polymer, incorporation of some hydrophobic enhancers (such as filler, copolymer or form interpenetrate network) would be a feasible approach. Some typical hydrophobic components include many fatty acids with long alkyl group, lignin or its derivate oligomers, monomers that rich in hydrophobic phenolic compound.

1.1.3 Camelina as an alternative to soy

Oilseed protein is a promising renewable source to be used as the replacement of petroleum-based materials for adhesion purpose, and it has drawn increasing attention since soy-based adhesives were developed for wood glues. Soybeans, primarily an industrial crop with high oil and protein contents, were first developed into adhesives in 1923 from the meal ground into flour (Kumar, Choudhary, Mishra, Varma, & Mattiason, 2002). By then, soy protein has been studied as

an adhesive for wood and paper, coating binders, and paints, and as emulsifiers in colloidal rubber products (Hettiarachchy, Kalapathy, & Myers, 1995; Messina, Gardner, & Barnes, 2002; Myers, 1993). Currently, it was commercialized for the interior wood binding and decoration. However, soy protein comprises a portion of humans' diets, thereby creating competition between utilization of soy protein for protein-based products or human food. Therefore, alternative bio-resources must be discovered.

Proteins from camelina provide such potentials. Camelina sativa, an easy-cultivated oilseed crop, has been primarily used for biodiesel (Kasetaite, Ostrauskaite, Grazuleviciene, Svediene, & Bridziuviene, 2014). Recently, the crop has drawn increasing attention due to its abundance in high quality oil, namely the omega-3 and polyunsaturated fatty acids, which is potential sources for animal feedings and film manufacturing. Accordingly, the demand for biofuels and unsaturated camelina oil resulted in increased production of camelina meal (CM) as protein resources for value-added products (Reddy, Jin, Chen, Jiang, & Yang, 2012). CM, a by-product of camelina seed's oil extraction process, typically contains 10-15% residual oil, 40% crude protein, 5% minerals, and 10-12% crude fiber.

Camelina protein (CP) is a mixture of 2S (albumin storage protein) and 12S fraction (cruciferin), which are linked by disulfide bonds (Nguyen et al., 2013). Li et al. (N Li et al., 2014) isolated four fractions of CP from the meal: albumins (water-soluble), globulins (5% NaCl-soluble), prolamins (70% ethanol-soluble), and glutelins (0.1 N NaOH-soluble). Acid-sedimentation could also be used to extract glutelin, the primary fractions, as soy protein for further processing. Similar to soy protein isolate (SPI), ongoing studies have investigated application of CM and its protein isolate for the biodegradable materials. Zhao et al. (Zhao et al., 2014)developed CP-based water-stable films with potential for tissue engineering in a cytocompatibility study. Reddy (Reddy et al., 2012) used vinyl-grafted CM for thermoplastic application. However, information about the extraction and modification of CP is still limited.

1.2 Objectives

The overall goals of this research are to overcome the intrinsic drawbacks of camelina protein-based such as poor water resistance, high viscosity. In addition, the physicochemical properties and microstructure of camelina protein were also investigated, which facilitates further development and commercialization of camelina protein as an alternative to the soy protein-based adhesive. The specific objectives are:

1) Camelina protein isolate (CPI) was extracted from the camelina meal and was unfolded by sodium bisulfite and guanidine-HCl. To optimize the unfolding conditions by evaluating the unfolding degree and surface hydrophobicity as well as characterization of the physicochemical properties with potential for adhesive applications.

2) To stabilize CPI structures by the coupling agent for improved water resistance. The cross-linked CPI exhibited increased molecular weight and particle size. Evaluate the improved water resistance of modified CPI by water soaking test and characterize the physicochemical properties of modified CPI.

3) Prepare and characterize the functionalized lignin from kraft lignin by H_2O_2 de-polymerization, and then copolymerize it with CPI. Evaluate the mechanical performance and water resistance of the copolymer-based wood adhesives.

1.3 Reference

Hettiarachchy, N., Kalapathy, U., & Myers, D. (1995). Alkali-modified soy protein with improved adhesive and hydrophobic properties. *Journal of the American Oil ….* Retrieved from http://link.springer.com/article/10.1007/BF02577838

Huang, W., & Sun, X. (2000). Adhesive properties of soy proteins modified by sodium dodecyl sulfate and sodium dodecylbenzene sulfonate. *Journal of the American Oil Chemists' Society*, *77*(7), 705–708. https://doi.org/10.1007/s11746-000-0113-6

Kasetaite, S., Ostrauskaite, J., Grazuleviciene, V., Svediene, J., & Bridziuviene, D. (2014). Camelina oil- and linseed oil-based polymers with bisphosphonate crosslinks. *Journal of Applied Polymer Science*, *131*(17). https://doi.org/10.1002/app.40683

Kumar, R., Choudhary, V., Mishra, S., Varma, I. K., & Mattiason, B. (2002). Adhesives and plastics based on soy protein products. *Industrial Crops and Products*, *16*(3), 155–172.

Li, N., Qi, G., Sun, X. S., Stamm, M. J., & Wang, D. (2011). Physicochemical Properties and Adhesion Performance of Canola Protein Modified with Sodium Bisulfite. *Journal of the American Oil Chemists' Society*, *89*(5), 897–908. https://doi.org/10.1007/s11746-011-1977-7

Li, N., Qi, G., Sun, X. S., Wang, D., Bean, S., & Blackwell, D. (2014). Isolation and Characterization of Protein Fractions Isolated from Camelina Meal. *Transactions of the ASABE*, *57*(2010), 169–178. https://doi.org/10.13031/trans.57.10455

Mekonnen, T., Mussone, P., & Bressler, D. (2014). Valorization of rendering industry wastes and co-products for industrial chemicals, materials and energy: review. *Critical Reviews in Biotechnology*, *8551*(May), 1–12. https://doi.org/10.3109/07388551.2014.928812

Messina, M., Gardner, C., & Barnes, S. (2002). Gaining insight into the health effects of soy but a long way still to go: commentary on the fourth International Symposium on the Role of Soy in Preventing and Treating Chronic Disease. *The Journal of Nutrition*, *132*(3), 547S–551S.

Mo, X., Wang, D., & Sun, X. S. (2011). Physicochemical properties of β and α'α subunits isolated from soybean β-conglycinin. *Journal of Agricultural and Food Chemistry*, *59*(4), 1217–22. https://doi.org/10.1021/jf102903b

Myers, D. J. (1993). Industrial applications for soy protein and potential for increased utilization. *Cereal Foods World (USA)*.

Nguyen, H. T., Silva, J. E., Podicheti, R., Macrander, J., Yang, W., Nazarenus, T. J., … Cahoon, E. B. (2013). Camelina seed transcriptome: a tool for meal and oil improvement and translational research. *Plant Biotechnology Journal*, *11*(6), 759–69. https://doi.org/10.1111/pbi.12068

Qi, G., & Sun, X. S. (2010). Soy Protein Adhesive Blends with Synthetic Latex on Wood Veneer. *Journal of the American Oil Chemists' Society*, *88*(2), 271–281. https://doi.org/10.1007/s11746-010-1666-y

Reddy, N., Jin, E., Chen, L., Jiang, X., & Yang, Y. (2012). Extraction, characterization of components, and potential thermoplastic applications of camelina meal grafted with vinyl monomers. *Journal of Agricultural and Food Chemistry*, *60*(19), 4872–9. https://doi.org/10.1021/jf300695k

Ren, X., & Soucek, M. (2014). Soya-Based Coatings and Adhesives. In *ACS Symposium Series* (pp. 207–254). https://doi.org/10.1021/bk-2014-1178.ch010

Song, F., Tang, D.-L., Wang, X.-L., & Wang, Y.-Z. (2011). Biodegradable soy protein isolate-based materials: a review. *Biomacromolecules*, *12*(10), 3369–80. https://doi.org/10.1021/bm200904x

Sun, X. S. (2011). Soy Protein Polymers and Adhesion Properties. *Journal of Biobased Materials and Bioenergy*, *5*(4), 409–432. https://doi.org/10.1166/jbmb.2011.1183

Wang, J.-M., Yang, X.-Q., Yin, S.-W., Zhang, Y., Tang, C.-H., Li, B.-S., … Guo, J. (2011). Structural rearrangement of ethanol-denatured soy proteins by high hydrostatic pressure treatment. *Journal of Agricultural and Food Chemistry*, *59*(13), 7324–32. https://doi.org/10.1021/jf201957r

Wang, Y., Mo, X., Sun, X. S., & Wang, D. (2007). Soy Protein Adhesion Enhanced by Glutaraldehyde Crosslink. *Journal ofApplied Polymer Science*, *104*, 130–136. https://doi.org/10.1002/app

Zhao, Y., Jiang, Q., Xu, H., Reddy, N., Xu, L., & Yang, Y. (2014). Cytocompatible and water-stable camelina protein films for tissue engineering. *Journal of Biomedical Materials Research. Part B, Applied Biomaterials*, *102*(4), 729–36. https://doi.org/10.1002/jbm.b.33053

Chapter 2 - Literature Review

2.1 Adhesion mechanism

Adhesion is the strength of the bonds forming between one material and another, which behaves as tendency of dissimilar particles and/or surfaces to cling to one another. The performance and durability of adhesive depended both adhesion and cohesion. The adhesion strength was explained by several models and theories, including mechanical interlocking, interfaces adsorption, chemical bonding, diffusion, and electron transfer (Wool & Sun, 2011).

Chemical bonding, interfacial absorption and interlocking are the major forces governing the adhesion performance. Chemical bondings are formed at the interface between the paint and the substrate; it is expected to be the strongest and most durable bonding, which is an important consideration when developing the water-resistant or solvent-resistant adhesives. However, under ambient condition, chemical bonding at the interface is not widely-existed (Guangyan Qi & Sun, 2010a).

The mechanical bonding theory describes how adhesives spread and wet the surface of the substrate, penetrate into the fibers cells through the capillary path, act like a mechanical anchor. At one time, adhesion was thought to occur only by the resin flowing and filling pores, holes, crevices and micro-voids on the substrate. When the resin was cured, the lock structure is held on mechanically. One way that surface roughness aids in adhesion is by increasing the total contact area between the paint and the adherend. If interfacial or intermolecular attraction is the basis for adhesion, increasing the actual area of contact will increase the total energy of surface interaction by a proportional amount. Thus, the mechanical interfacing theory generally teaches that roughening of surfaces is beneficial because it (1) gives "teeth" to the substrate and (2) increases the total effective area over which the forces of adhesion can develop. It explains why one of the most common surface treatments is abrasion or mechanical roughening. Though weaker than the chemical bonding, this kind of adhesion predominates, especially on surfaces such as wood, concrete, or even metal and plastic (G Qi, 2011).

The adsorption theory states that adhesion results from molecular contact between two materials and the surface forces that develop. Most adsorption forces are physical or electrostatic attraction between adhesive polymer and substrate through hydrogen bonding and van der Waals forces. The process of establishing continuous contact between a liquid paint film and the

substrate surface is known as "wetting. Good wetting results when the adhesive flows into the valleys and crevices on the substrate surface; poor wetting results when the adhesive bridges over the surface irregularities. Good wetting between adhesive and substrate should be established to obtain the good adhesive strength. For good wetting, the substrate must have a higher surface energy than the liquid paint film. Thus, the presence of contaminant on the substrate surface is undesirable because it becomes a weak boundary layer which can easily fail cohesively and thereby seriously weaken the entire adhesion system. Some other complementary mechanism including diffusive forces and electrostatic bond theory also prevail. The diffusive forces work like mechanical tethering at the interface. When the material from one surface penetrates into the adjacent surface, it is still bound to the origin phase. The electrostatic bonds occur between adhesive and substrate (G Qi, 2011; "Wikipedia," 2016).

Soy protein can be used as an adhesive because the protein molecules are able to disperse and unfold in solution. The unfolded molecules increase the contact area and adhesion to other surfaces. In addition, these molecules entangle with each other during the curing process to produce bond strength. However, this kind of bond is easily broken by moisture, which is the main disadvantage of the adhesive (Luo et al., 2015).

2.2 Soy protein structure

Soy protein is a typical storage protein that provides abundant and various kinds of amino acids during seed germination and protein synthesis which enable it to be appropriate precursor for high-performance biopolymers. Soy protein is globular protein, and thus the morphology of the protein under microscopy is ball-like. According to the purity of extractive, soy protein isolate (SPI) refers to the protein ingredient, which is higher than 90%, extracted from the soy meal. According to its sedimentation coefficients, there are 4 four major components: 2S, 7S (mostly β-conglycinin), 11S (mostly glycinin) and 15S. 7S, 11S and their different ratio determine the rheological properties of soy protein gel. The relative proportion of 11S to 7S ranges from 1:3 to 3:1 depending on the cultivar and growing conditions (Wool & Sun, 2011). 11S globulin is a hexamer consisting of an acidic and a basic polypeptide linked by a disulfide bond. 7S is a trimer with a molecular weight of 150 to 200 kDa that is composed of three major subunits: α, α', and β. Xiaoqun Mo has reported that the content of the αα′ and β subunits in beta-conglycinin is 42% and 36%, and the yield of acidic and basic subunits was 7.7 and 8.2 g, respectively, from 140 g of soy flour (Mo, Wang, & Sun, 2011b; Mo,

Zhong, Wang, & Sun, 2006). Soy protein was made up of 20 kinds of amino acids forming the primary, secondary, tertiary and quaternary structure.

For the primary structure, it contains about 25% acidic amino acids, 20% basic amino acids, and 20% hydrophobic amino acids (the amino acid distribution was shown in Table 2.1). Different soy protein classifications have also been characterized by their sedimentation constants (S stands for Svedberg Unit). The numerical coefficient is the characteristic sedimentation constant in water at 20 ºC. The content of 11S is around 52% and of 7S is 35%. The other minor fractions have been designated as 2S (8%) and 15S (5%). Two major fractions, known as 7S and 11S have been studied extensively. The 11S fraction has a molecular weight of about 100-200 KDa, and 7S had 200-400KDa. Both glycinin and conglycinin had similar secondary and tertiary structure: about 6% α-helix, 38% β-sheet, and 57 random coils. Many hydrophobic amino acids such as glycine, tyrosine, and tryptophan were folded and buried inside. Solubility of the protein is lowest at its isoelectric point. Thus, to extract these fractions, the isoelectric pH (PI) value is used to induce protein sediment. The PI value for soy protein is 4.5. For the conglycinin fraction, it is 4.8, and for glycinin it is 6.8 (Table 2.2) (X. S. Sun, 2011).

2.3 Camelina sativa and the storage proteins

Camelina sativa, also known as false flax, wild flax, linseed dodder, or German sesame, is an important and ancient oil plant that originated in Germany around 600 B.C. (Nguyen et al., 2013). Then, camelina nicely adapted to the climate of North America, Europe, and Asia. Compared with other oilseed crops, camelina is recognized as an easy-cultivated oilseed crop with some obvious advantages: drought-resistance, no pesticide needed, very fast growing, short crop cycle, early spring growth, winter types, good rusticity, and wide adaptability.

In general, camelina seed contains 36–47% oil in dry matter, which is twice of that of soybean (18–22%). The camelina was consisted of 30% to 40% oil, 30% protein, 10% carbohydrates, and 7% ash (Zhu, Wang, & Sun, 2016). The content of unsaturated fatty acids in camelina oil (CO) is about 90%, with an average of 5.8 double bonds per triglyceride (M. I. N. J. Kim, 2015). Both the unsaturated fatty acid content and the degree of unsaturation of CO are higher than that of soybean oil (84% and 4.6, respectively). These highly unsaturated structures make camelina oil attractive for the health benefit and producing high-performance oil derivatives. Furthermore, camelina is a non-food oilseed crop that does not compete with food production; therefore, it has been cultivated extensively in the USA as a low-input biofuel crop

during the past decade. Accordingly, the meal-cake of the oil-extraction residues which contained rich amount of protein and carbohydrate became available. According to Li's study, the four isolated protein fractions from cemalina meal were based on their different protein solubilities at different pH: albumins (water-soluble), globulins (5% NaCl-soluble), prolamins (70% ethanol-soluble), and glutelins (0.1 N NaOH-soluble). For camelina, the minimum solubility of albumin, globulin, and glutelin were found at pH 3.0, 3.0, and 4.5 to 5.0, respectively. Camelina proteins had 26% to 28% hydrophobic amino acids, which is lower than canola, soy, and sorghum pro- teins. Glutelins exhibited higher α-helix to β-sheet ratios (1.03 to 1.05) than the globulin fractions (0.91 to 1.00) and albumin (0.84); The amino acid distribution of the camelina protein was also shown in Table 2.3. In spite of the available information on storage protein fractions in camelina sativas, the protein modification and application is still under-investigated. By investigating the physicochemical properties and adhesion properties of the three fractions of camelina protein (albumin, globulin, and glutelin), Li et al found glutelin (65% db) was the major fraction in total camelina protein, followed by globulin (15%). glutelin had more compact protein structure and higher aggregation than globulin, which may contribute to glutelin's lower adhesion strength. Camelina displayed comparable water resistance at optimum curing temperature with sorghum protein or soy protein, which may be improved by hydrophobic enhancers. (Ningbo Li, Qi, Sun, Xu, & Wang, 2015)

2.4 Protein modification

2.4.1 Unfolding

The globular proteins are folded at their native state. In this state, the hydrophobic clusters exclude water and are tightly packed together and buried inside of the protein. However, the folded protein exhibited very limited intermolecular interaction. After the protein is unfolded or denatured, the buried hydrophobic groups are exposed toward the surface of the protein, which would promote protein–protein interactions and form hydrophobic clusters. Besides, protein unfolding resulted in the exposed functional groups such as amino groups, carboxyl groups and hydroxyl groups that increased protein's reactivity (Guangyan Qi, Li, Wang, & Sun, 2012).

There are many unfolding agents aiming to break protein's structures by destroying their secondary or tertiary structures. When reducing agents, such as sodium bisulfite, are used, protein's disulfide bond was broken down. As expected, sodium bisulfite-induced disulfide bond cleavage resulted in increased the surface hydrophobicity of modified glycinin. Hydrophobic

force is the main driving force for glycinin aggregation, and the balance between hydrophobic and electrostatic forces makes glycinin form chain-like aggregates with increased protein interaction. For other oilseed protein such as canola, camelina, sorghum, similar reducing effects were also reported to unfold their protein structures with significant increased shear strength for the plywood. However, the weakening effect of $NaHSO_3$ on adhesion performance was also observed on soy protein and canola protein adhesives. An excess of 1% (dry base) of sodium bisulfite modification to protein isolate is negative to the tensile strength of wood adhesion, especially at the wet conditions. $NaHSO_3$ can disrupt the S-S bond of protein with the formation of R-SH groups. During the reducing reaction, some sulfhydryls resulting from deoxidization are blocked as a sulfonate group ($RS-SO_3^-$); therefore, the negative effects of $NaHSO_3$ can be attributed to this extra negative $RS-SO_3^-$ group that bonded with water through the formation of a chemical bond in the protein adhesive, stimulating the hydrophilic behavior and causing the $RS-SO_3^-$ group to absorb more water and to disrupt the continuous adhesive which is detrimental to its wet shear strength(Ningbo Li et al., 2011, 2015).

Besides sodium bisulfite, other effective unfolding agents include SDS and urea target protein's hydrophobic interaction and hydrogen bonds. It is well known that hydrogen bond is the most important force to maintain the protein's secondary structure. Therefore, the addition of denaturing agents such as urea or guanidine-HCl would break down the hydrogen bond of proteins' secondary structure. Huang et al (W. Huang & Sun, 2000b) reported the effect of urea and guanidine-HCl modification to the adhesion strength of soy protein isolate for Walnut, cherry and pine wood. Significant increase was observed for the shear strength for all wood samples. In detail, guanidine-HCl is more effective than urea in denaturing proteins and giving SPI better adhesion. 3 M guanidine-HCl and 1M urea had the best adhesion strength at both wet and dry condition, and further increase of detergents resulted in reduced adhesion. Similarly, this indicated that too much unfolding was not beneficial to protein's adhesion property. The native protein is rather compact, while the denatured protein peptide became more flexible. Thus, they were more expanded in the water with a liable surface to penetrate some membrane or surface than the native proteins.

2.4.2 Protein stabilization

After protein was unfolded, protein adhesives became more hydrophobic and water resistant due to the exposed hydrophobic groups. Besides, the reactive functional groups of protein

molecules became more accessible. However, the water resistance of the modified protein-based adhesive was still low at the wet condition. (Friesen, Chang, & Nickerson, 2015; Rhim, Lee, & Hong, 2006; Usha, Sreeram, & Rajaram, 2012). The limited molecular weight and non-covalent bonding between subunits made protein polymers vulnerable to applied force and sensitive to the humidity (Shi & Dumont, 2014b). In the aquatic environment, the hydrophilic amino acids are affinitive to the water, and protein-protein interactions became weaker (De Graaf, Harmsen, Vereijken, & Mönikes, 2001a).

Applying some crosslinking agents is one of the most widely used and facile methods to stimulate protein's polymerization and stabilize their structures even in the wet conditions. Glutaraldehyde is an extensively used chemical approach for inactivating, stabilizing, or immobilizing proteins. It has been used to improve the water resistance of soy protein-based adhesives (Ying Wang et al., 2007) and mechanical properties of SPI-based edible films (González, Strumia, & Alvarez Igarzabal, 2011). Wang et al (Ying Wang et al., 2007) reported the significant effect of glutaraldehyde to improve SPI's adhesion strength at both dry and wet conditions. The wet strength of SPI adhesive for plywood is rather weak. Incorporation of only 20uM glutaraldehyde into the SPI dispersion would increase adhesion's tensile strength from 1.3 to 2.8 MPa after 48-hour water soaking. Protein's molecular weight and conformation change are the main reasons that crosslink agents improve to protein adhesive mechanical strength. Crosslink agents such as glutaraldehyde connect protein's free amino groups and carboxyl groups, resulting in reduced amino groups and increased hydrophobic groups. Besides, concentration of crosslink agents had significant effect on adhesion of modified protein. Mild conformation change resulted from crosslink could benefit adhesive performance. Higher glutaraldehyde concentration could induce more conformation and structure changes that might not be favorable for adhesive performance (M. I. N. J. Kim, 2015). Such over-crosslinked protein dispersion exhibited poor flow-ability and limited reactivity with wood surface. In this case, though the cohesion of protein adhesive increased, the interfacial bond decreased significantly. Though the application of glutaraldehyde is successful in SPI adhesives, the associated cytotoxicity and toxicity of glutaraldehyde was unfavorable. Therefore, some green and efficient crosslink agents were worth further investigation.

2.4.3 Hydrophobic enhancers

Due to protein's intrinsic characteristics, such as flexible and hydrophilic, blending some tough and hydrophobic components with proteins is a facile method to improve the water resistance of protein adhesives. Such hydrophobic enhancers include nanoparticles, free fatty acid, lignin, and phenolic compounds. Their enhancing effects were widely used by fabricating oil seed protein-based films, scaffold, coating to improve the hydrophobicity and mechanical strength. Our group have used undecylenic acid (UA), a hydrophobic long chain free fatty acid was copolymerized with SPI to prepare the adhesives with improved water resistance. UA was successfully grafted onto soy protein through the reaction between -COOH and $-NH_2$. As expected, the tensile strength of modified SPI-glued wood panel increased from 2.0 to 3.2MPa. During the reaction, denaturation of SPI 7S and 11S fraction occurred, which facilitate protein's reaction with UA. The non-water-soluble nature and long hydrophobic alkyl chains of UA prevented water penetration, which contributed to significant improvement in water resistance(H. Liu, Li, & Sun, 2015). The nanoparticle, another important popular functional ingredient, was also useful to enhance protein adhesives water resistance. In our groups, nano-clay was also added to SPI-based adhesive, and we found only small amount addition would significantly increase the water resistance of cured-wood (unpublished data).

Due to the highly cross-linked phenolic structure, lignin with rigid structure and hydrophobicity was widely used for materials application with increased water stability and mechanical strength. Xiao et al (Xiao et al., 2013) investigated the adhesion properties of lignin (SL or ESL) blended soy protein adhesives (SPA) based on soy protein isolates (SPI) or modified soy protein (MSP) respectively. In their study, the shear strength and water resistance of lignin (SL or ESL)-blended SPI on wood veneer joints were obviously improved. Moreover, the small molecules phenolic compound derived from lignin such as, rutin and epicatechin, also exhibited great potential to modify protein's structures with improved hydrophobicity and mechanical strength. Friesen et al (Friesen et al., 2015) incorporated phenolic compounds, rutin and epicatechin, into soy protein isolate films, and studied their mechanical, barrier and crosslinking properties. The addition of rutin significantly increased puncture strength (9.3 N) over SPI alone (6.4 N) whereas epicatechin had no effect. Tensile strengths of SPI films with rutin and epicatechin were similar (35.1 MPa and 22.1 MPa, respectively) and significantly stronger than films without added phenolics (9.3 MPa). SPI films without phenolics showed the

greatest flexibility, as measured by tensile elongation. The addition of epicatechin was found to increase water vapor permeability significantly to 2.3 g mm/ m^2 h kPa from 1.7 g mm/m^2 h kPa for SPI alone whereas rutin decreased water vapor permeability to 1.2 g mm/m^2 h kPa.

2.4.4 Lignin as a hydrophobic enhancer

Currently, lignin is the most abundant aromatic polymer on Earth, and this makes it an attractive material to be exploited as a feedstock alternative to petrol-based chemicals. In spite of the mentioned benefits of lignin, however, most of the lignin from industrial waste streams is still relegated to low value uses of combustion for the production of power and/or heat. Lignin's complex structure and limited reactivity greatly limited its use applied polymers. In order to get better understanding of lignin structures and increase its compatibility with other polymers, research on lignin modification has become a hot spot. This strengthening effect of functionalized lignin was widely utilized to improve the water resistance of hydrophilic biopolymers. Luo et al(Luo et al., 2015) developed a soy meal-based wood adhesive with improved water resistance by using kraft lignin. Huang et al investigated the effect of alkaline lignin and lignosulfonate to soy protein based composite for enhanced mechanical performance and aqueous absorption. They found that as a hydrophobic filler, the alkaline lignin increased the tensile strength, thermal stability and water resistance of soy protein (J. Huang, Zhang, & Chen, 2003b), while lignosulfonate contributed to soy protein's micro-phase separation and the formation of crosslinked structures.(J. Huang, Zhang, & Chen, 2003a)

2.4.5 Lignin functionalization

Chemical modification of lignin can be classified into two main categories: (1) Fragmentation or lignin depolymerization to use lignin as a carbon source or to cleave lignin structure into aromatic macromers. (2) Modification by creating new chemical active sites.
After such treatment, we may obtain some more reactive functional groups such as aldehyde, which make it accessible to further crosslink to form the co-polymers.

There are generally two widely-used approaches for lignin depolymerization: pyrolysis, oxidation and hydrotreating (hydrogenolysis, deoxygenation) (Xu, Arancon, Labidi, & Luque, 2014). However, the mechanism of depolymerization processes are often not well understood, and the associated harsh conditions, such as high hydrogen pressures, temperature > 400°C, are undesirable. Therefore, some chemical catalysis and reaction was applied to stimulate the depolymerization in a mild condition. Oxidative cracking of lignin is a good choice. Aromatic

aldehydes and carboxylic acids are formed as main products from the oxidative degradation of lignin. The catalytic system consisting of strong oxidative agents such TEMPO, HNO_3 and HCl could achieve selective oxidation of a range of lignin model compounds including some highly reactive ketones and acids (e.g. vanillin, vanillic and veratric acids) under mild reaction conditions after 24 h reaction. In order to induced even stronger oxidative conditions, ionic liquid such as copper sulfate, ferric chloride, zirconia acetate was also included to lower the reaction temperature (mostly < 100 °C). (Lange, Decina, & Crestini, 2013)

Similar to protein unfolding, lignin depolymerization is a facile and useful method to expose more functional groups and increase the reactivity. However, to further activate the inert lignin, grafting technique is another important approach. Hydroxyl groups, either aliphatic hydroxyl or phenolic hydroxyl, are the most abundant chemical groups for lignin that participate in chemical reactions; therefore, the functionalization of hydroxyl groups is a good strategy to develop multiple-functional lignin copolymers. Based on the chemical pathways, chemical modification including hydroxylkylation, amination, nitration, alkylation, amination, esterification, and phenolation. Hydroxypropylation, esterification and phenolation are the most promising pathways that required mild condition and few toxic chemical agents. Amination of lignin can be achieved through a Mannich reaction with amine and formaldehyde, and the resultant products can be used for the preparation of a cationic surfactant (with high surface activity) and as a filler to reinforce the properties of polymer/ lignin composites. Esterification is one of the easiest ways to modify the hydroxyl groups of lignin. Different esterifying agents, including acidic compounds, acid anhydrides and chloride acids, have been utilized for lignin esterification. This reaction can introduce more phenolic hydroxyl groups onto lignin and therefore improve its chemical reactivity for synthesizing new lignin-based phenol resins (Stewart, 2008). Since the lignin structure was similar to the polyphenol, it is a potential substitute for phenol in phenol-formaldehyde resin synthesis. Luo et al (Luo et al., 2015) synthesized the phenol formaldehyde resin based on sorghum lignin, which was then used to improve the mechanical and water resistance of soy meal-based adhesives. The synthesis products effectively improved the wet shear strength of the resultant plywood bonded by 200% from 0.35 to 1.05 MPa.

Figure 2-1 Extraction procedure of camelina protein fractions (Albumin, Glutelin, Globulin)

Defatted camelina meal flour

↓

Mixed with 30-fold distilled water and stirred 2 h, then centrifuged at 12,000 × g for 15 min → Supernatant → Degumming removed soluble polysaccharide / *Albumin* → Lyophilization

↓

Residues: mixed with 30-fold distilled water, adjusted pH to 12 with 2 N NaOH, stirred 2 h, then centrifuged at 12,000 × g for 15 min → Supernatant: adjusted pH to 4.5, and then centrifuged at 12,000× g for 15 min → Precipitate: *Glutelin 1* → Lyophilization

↓

Residues: mixed with 30-fold 5% NaCl solution, adjusted pH to 8, stirred 2 h, then centrifuged at 12,000 × g for 15 min → Precipitate: non-protein impurities

↓

Supernatant: adjusted pH to 3.0, and centrifuged at 12,000× g for 15 min

↓

Precipitates: *Globulin 1*

↓

Lyophilization

Table 2-1 Amino acids composition in percentage (%) of soy protein

Amino acids	Soy protein	Soy glycinin	Soy conglycinin
Tryptophan	—	0.75	0.30
Isoleucine	2.86	4.24	6.40
Tyrosine	2.57	2.81	3.60
Phenylalanine	3.92	3.85	7.40
Proline	5.73	6.85	4.30
Leucine	8.02	7.05	10.30
Valine	3.39	4.83	5.10
Lysine	5.88	4.44	7.00
Methionine	1.23	0.98	0.30
Cysteine	0.99	1.44	0.00
Alanine	6.05	5.16	3.70
Arginine	4.68	5.81	8.80
Threonine	4.05	3.91	2.80
Glycine	9.74	7.50	2.90
Serine	7.46	6.66	6.80
Histidine	5.00	1.89	1.70
Aspartate	11.55	11.88	14.10
Glutamate	16.89	19.97	20.50

Adapted from Sun, 2011. Expressed as percentages

Table 2-2 Amount and composition of ultracentrifuge fractions of water-extractable soybean proteins

Fraction	Percentage (%)	Component	Molecular Weight	Isoelectric Poinnt
2S		Trypsin inhibitors	8000-21,500	4.2-4.5
		Cytochrome c	12,000	
7S	37	Hemagglutinins	110,000	6
		Lipoxygenase	102,000	5.5
		b-Amylase	61,700	5.8
		7S Globulin	180,000-210,000	4.8
11S	31	11S Globulin	350,000	6.4
15S	11	---	600,000	

Adapted from (Lui, Litster, & White, 2007; Wolf, 1974).

Table 2-3 Amino acid compostion (% of total) of camelina protein fractions

	Amino acid	Albumin	Globulin	Glutelin
Essential	Histidine	2.84	3.04	3.04
	Isoleucine	4.7	4.96	5.01
	Leucine	8.14	9.14	8.93
	Lysine	5.88	4.36	5.05
	Methionine	1.85	1.68	2.27
	Phenylalanine	5.77	6.64	5.63
	Threonine	5.35	4.78	5.05
	Valine	5.75	6.09	5.77
	Total Essential	40.29	40.69	40.75
None-essential	Alanine	5.87	5.29	5.62
	Aspartate	11.45	11.19	9.7
	Glutamate	18.46	19.03	19.24
	Serine	6.41	5.91	6.02
	Arginine	7.71	8.16	8.53
	Glycine	6.24	5.95	6.12
	Tyrosine	3.58	3.79	4.02
	Ornithine	0	0	0
	Total non-essential	59.71	59.31	59.25

Adapted from (N Li et al., 2014)

2.5 Reference

De Graaf, L. A., Harmsen, P. F. H., Vereijken, J. M., & Mönikes, M. (2001). Requirements for non-food applications of pea proteins A Review. *Food / Nahrung*, *45*(6), 408–411. https://doi.org/10.1002/1521-3803(20011001)45:6<408::AID-FOOD408>3.0.CO;2-#

Friesen, K., Chang, C., & Nickerson, M. (2015). Incorporation of phenolic compounds, rutin and epicatechin, into soy protein isolate films: Mechanical, barrier and cross-linking properties. *Food Chemistry*, *172*, 18–23. https://doi.org/10.1016/j.foodchem.2014.08.128

González, A., Strumia, M. C., & Alvarez Igarzabal, C. I. (2011). Cross-linked soy protein as material for biodegradable films: Synthesis, characterization and biodegradation. *Journal of Food Engineering*, *106*(4), 331–338. https://doi.org/10.1016/j.jfoodeng.2011.05.030

Huang, J., Zhang, L., & Chen, F. (2003a). Effects of lignin as a filler on properties of soy protein plastics. I. Lignosulfonate. *Journal of Applied Polymer Science*, *88*(14), 3284–3290. https://doi.org/10.1002/app.12185

Huang, J., Zhang, L., & Chen, P. (2003b). Effects of Lignin as a Filler on Properties of Soy Protein Plastics . II . Alkaline Lignin. *J. Appl. Polym. Sci*, *88*(14), 3291–3297.

Huang, W., & Sun, X. (2000). Adhesive properties of soy proteins modified by urea and guanidine hydrochloride. *Journal of the American Oil Chemists' Society*. https://doi.org/10.1007/s11746-000-0016-6

Kim, M. I. N. J. (2015). *PHYSICOCHEMAL AND ADHESION PROPERTIES OF SOY PROTEIN BASED*. Kansas State University.

Lange, H., Decina, S., & Crestini, C. (2013). Oxidative upgrade of lignin - Recent routes reviewed. *European Polymer Journal*, *49*(6), 1151–1173. https://doi.org/10.1016/j.eurpolymj.2013.03.002

Li, N., Qi, G., Sun, X. S., Stamm, M. J., & Wang, D. (2011). Physicochemical Properties and Adhesion Performance of Canola Protein Modified with Sodium Bisulfite. *Journal of the American Oil Chemists' Society*, *89*(5), 897–908. https://doi.org/10.1007/s11746-011-1977-7

Li, N., Qi, G., Sun, X. S., Xu, F., & Wang, D. (2015). Adhesion properties of camelina protein fractions isolated with different methods. *Industrial Crops and Products*, *69*, 263–272. https://doi.org/10.1016/j.indcrop.2015.02.033

Liu, H., Li, C., & Sun, X. S. (2015). Improved water resistance in undecylenic acid (UA)-

modified soy protein isolate (SPI)-based adhesives. *Industrial Crops and Products*, *74*, 577–584. https://doi.org/10.1016/j.indcrop.2015.05.043

Luo, J., Luo, J., Yuan, C., Zhang, W., Li, J., Gao, Q., & Chen, H. (2015). An eco-friendly wood adhesive from soy protein and lignin: performance properties. *RSC Adv.*, *5*(122), 100849–100855. https://doi.org/10.1039/C5RA19232C

Mo, X., Wang, D., & Sun, X. S. (2011). Physicochemical properties of β and α'α subunits isolated from soybean β-conglycinin. *Journal of Agricultural and Food Chemistry*, *59*(4), 1217–1222. https://doi.org/10.1021/jf102903b

Mo, X., Zhong, Z., Wang, D., & Sun, X. (2006). Soybean glycinin subunits: Characterization of physicochemical and adhesion properties. *Journal of Agricultural and Food Chemistry*, *54*(20), 7589–93. https://doi.org/10.1021/jf060780g

Nguyen, H. T., Silva, J. E., Podicheti, R., Macrander, J., Yang, W., Nazarenus, T. J., … Cahoon, E. B. (2013). Camelina seed transcriptome: a tool for meal and oil improvement and translational research. *Plant Biotechnology Journal*, *11*(6), 759–69. https://doi.org/10.1111/pbi.12068

Qi, G. (2011). *Modified soy protein based adhesives and their physicochemical properties*. Kansas State University.

Qi, G., Li, N., Wang, D., & Sun, X. S. (2012). Physicochemical properties of soy protein adhesives obtained by in situ sodium bisulfite modification during acid precipitation. *JAOCS, Journal of the American Oil Chemists' Society*, *89*(2), 301–312. https://doi.org/10.1007/s11746-011-1909-6

Rhim, J. W., Lee, J. H., & Hong, S. I. (2006). Water resistance and mechanical properties of biopolymer (alginate and soy protein) coated paperboards. *LWT - Food Science and Technology*, *39*(7), 806–813. https://doi.org/10.1016/j.lwt.2005.05.008

Shi, W., & Dumont, M.-J. (2014). Review: bio-based films from zein, keratin, pea, and rapeseed protein feedstocks. *Journal of Materials Science*. https://doi.org/10.1007/s10853-013-7933-1

Song, F., Tang, D.-L., Wang, X.-L., & Wang, Y.-Z. (2011). Biodegradable soy protein isolate-based materials: a review. *Biomacromolecules*, *12*(10), 3369–80. https://doi.org/10.1021/bm200904x

Usha, R., Sreeram, K. J., & Rajaram, a. (2012). Stabilization of collagen with EDC/NHS in the

presence of l-lysine: A comprehensive study. *Colloids and Surfaces B: Biointerfaces*, *90*(1), 83–90. https://doi.org/10.1016/j.colsurfb.2011.10.002

Wang, Y., Mo, X., Sun, X. S., & Wang, D. (2007). Soy Protein Adhesion Enhanced by Glutaraldehyde Crosslink. *Journal ofApplied Polymer Science*, *104*, 130–136. https://doi.org/10.1002/app

Wikipedia. (2016).

Wool, R., & Sun, X. S. (2011). *Bio-based polymers and composites*. Academic Press.

Xiao, Z., Li, Y., Wu, X., Qi, G., Li, N., Zhang, K., … Sun, X. S. (2013). Utilization of sorghum lignin to improve adhesion strength of soy protein adhesives on wood veneer. *Industrial Crops and Products*, *50*, 501–509. https://doi.org/10.1016/j.indcrop.2013.07.057

Xu, C., Arancon, R. A. D., Labidi, J., & Luque, R. (2014). Lignin depolymerisation strategies: towards valuable chemicals and fuels. *Chemical Society Reviews*, *43*(22), 7485–500. https://doi.org/10.1039/c4cs00235k

Zhu, X., Wang, D., & Sun, X. S. (2016). Physico-chemical properties of camelina protein altered by sodium bisulfite and guanidine-HCl. *Industrial Crops and Products*, *83*, 453–461. https://doi.org/10.1016/j.indcrop.2015.12.085

Chapter 3 - Physico-chemical properties of camelina protein unfolded by sodium bisulfite and guanidine-HCl

3.1 Abstract

The objective of this research was to investigate the unfolding behaviors of camelina protein isolate (CPI) induced by sodium bisulfite ($NaHSO_3$) and guanidine-HCl (Gdm.Cl). Protein was extracted from defatted camelina meal through alkali solubilization and acid precipitation and modified with varying amount of $NaHSO_3$ (0-12% of the protein dry base) and Gdm.Cl (0-250% of the protein dry base). $NaHSO_3$ treatment broke the disulfide bonds of the CPI and increased free sulfhydryl content and surface hydrophobicity. As $NaHSO_3$ concentration increased, the viscosity, elastic modulus (G') and water resistant of $NaHSO_3$-modified camelina protein (SMCP) dispersion decreased, and the protein became aggregated due to high surface hydrophobicity. Gdm.Cl treatment broke the CPI's hydrogen bonds but decreased their surface hydrophobicity. Similarly, viscosity, G', and water resistant of Gdm.Cl-modified camelina protein (GMCP) dispersions decreased as Gdm.Cl increased and protein aggregation formed. The reducing effect of $NaHSO_3$ was greater than Gdm.Cl for CPI's protein-protein interaction and less obvious for the viscosity and water resistant. Gdm.Cl reduced CPI's decomposing temperature at high concentration, but no remarkable effect was observed for $NaHSO_3$ treatment. These findings on physicochemical changes of SMCPs and GMCPs may contribute to the application of camelina proteins in the biodegradable materials products.

3.2 Introduction

To date, the application of environment-friendly biopolymers from the natural sources has drawn much attentions to replace petroleum-based synthetic polymers such as phenol–formaldehyde (PF), urea–formaldehyde (UF), melamine–formaldehyde (MF) (X. S. Sun, 2011; Yixiang Wang, Cao, & Zhang, 2006). Soy protein, one of the most commonly investigated bio-based material, has exhibited its process-ability and biocompatibility in fabricating the biodegradable polymers with bulk and surface modification (Song et al., 2011; Teng, Luo, & Wang, 2012; J. Zhang, Jiang, Zhu, Jane, & Mungara, 2006). However, soy protein comprises a portion of humans' diets, thereby creating competition between utilization of soy protein for protein-based products or human food. Therefore, alternative bio-resources must be discovered.

Camelina sativa, an oilseed crop of easy availability, has been primarily used for biodiesel (Kasetaite et al., 2014). Recently, the crop has drawn increasing attention due to its abundance in high quality oil, namely the omega-3 and polyunsaturated fatty acids, which is potential sources for animal feedings and film manufacturing. Accordingly, the demand for biofuels and unsaturated camelina oil resulted in increased production of camelina meal (CM) as protein resources for value-added products (Reddy et al., 2012). CM, a by-product of camelina seed's oil extraction process, typically contains 10-15% residual oil, 40% crude protein, 5% minerals, and 10-12% crude fiber. Camelina protein (CP) is a mixture of 2S (albumin storage protein) and 12S fraction (cruciferin), which are linked by disulfide bonds (Nguyen et al., 2013). Li et al. (N Li et al., 2014) isolated four fractions of CP from the meal: albumins (water-soluble), globulins (5% NaCl-soluble), prolamins (70% ethanol-soluble), and glutelins (0.1 N NaOH-soluble). Acid-sedimentation could also be used to extract glutelin, the primary fractions, as soy protein for further processing. Similar to soy protein isolate (SPI), ongoing studies have investigated application of CM and its protein isolate for the biodegradable materials. Zhao et al.(Zhao et al., 2014)developed CP-based water-stable films with potential for tissue engineering in a cytocompatibility study. Reddy (Reddy et al., 2012) used vinyl-grafted CM for thermoplastic application. However, information about the extraction and modification of CP is still limited.

Studies have shown that controlling protein's unfolding degree was the most widely used method to modify protein's functional properties (Abtahi and Aminlari, 1997; Jiang et al., 2010; Kishore et al., 2012). Unfolded protein structures released protein's embedded functional groups and increased its reactivity, which is essential and requisite for further modifications. Modifiers, such as reducing agents and chaperone agents, have been used to unfold protein's secondary and tertiary structures and weaken the protein-protein interaction, consequently decreasing the protein's elasticity and viscosity of protein dispersion (Jana, Chaudhuri, & Deb, 2006; Guangyan Qi, Venkateshan, Mo, Zhang, & Sun, 2011; Rashid, Sharma, & Bano, 2005). However, this weakening effect on protein structures also decreased the water resistance of SPI gel and adhesive (W. Huang & Sun, 2000a; Ningbo Li et al., 2011; Guangyan Qi et al., 2012).

Sodium bisulfite ($NaHSO_3$) and guanidine-HCl (Gdm.Cl) are two effective unfolding agents. $NaHSO_3$, a strong reducing agent, unfolds protein's higher structures by breaking their intermolecular S-S to expose the buried hydrophobic groups of the globulin. In Sun and Qi's studies(Guangyan Qi et al., 2011), $NaHSO_3$ broke down protein's S-S and decreased the

viscosity of protein solution during in situ modification. $NaHSO_3$ also has function to increase the hydrophobicity of glycinin of SPI dispersion. Gdm.Cl, destroys protein's hydrogen bond to unfold structures (Kiefhaber & Baldwin, 1995; Zhong, Sun, Fang, & Ratto, 2001). Huang and Sun (W. Huang & Sun, 2000a) used Gdm.Cl to unfold SPI, and they observed that SPI structure was stabilized at low Gdm.Cl concentrations (0.5M and 1M) and was disrupted at higher concentrations (3M) by comparing their denaturing temperatures. Based on the previous studies on SPI, we speculated that, due to their different unfolding mechanisms, $NaHSO_3$ modified camelina protein (SMCP) and Gdm.Cl modified camelina protein (GMCP) would demonstrate unique behaviors. To the best of our knowledge, though there were many studies on the modification of SPI-based biodegradable materials, little was known for the physiochemical properties and structures of unfolded camelina protein isolate (CPI).

The unfolded protein structure resulted in 1) exposed protein's free functional groups such as free -SH, 2) stronger surface hydrophobicity for the water resistance, or 3) decreased viscosity of protein solution facilitating the protein's further processing. Thus, the objective of this study was to unfold CPIs by disrupting their H bond or S-S bond using $NaHSO_3$ or Gdm.Cl and comparing their unfolding behaviors. We confirmed the unfolding behaviors of camelina protein by free sulfhydryl group, surface hydrophobicity, and viscosity. We also characterized the physicochemical properties such as particle size, rheological properties, water resistance, and thermal properties.

3.3 Materials and Methods

3.3.1 Materials

Camelina meal (CM) with 15% lipids (db), 32.4% crude protein (db), and 11.0% moisture content (db) was provided by Field Brothers Inc. (Pendroy, MT, US). CM with particle size <0.5 mm was obtained by milling the CM using a cyclone sample mill (Udy Corp., Fort Collins, CO, USA). CM was then defatted with hexane at a solid/liquid ratio of 1:10 (w/v) for 2 h at room temperature in three cycles. The defatted camelina meal (DCM) was placed in a fume hood in a very thin layer ($\sim$2 mm) for 24 h to evaporate residual hexane. $NaHSO_3$, Gdm.Cl, Modified Lowry Protein Assay, hydrochloric acid (HCl), and sodium hydroxide (NaOH) were purchased from Fisher Scientific (Fair Lawn, N.J.).

3.3.2 Isolation of camelina protein

CPI was separated from DCM using the method described by Li et al. (N Li et al., 2014) with some modifications. DCM samples were mixed with distilled water at a solid/liquid ratio of 1:30 (w/v), stirred for 2 h, and then centrifuged to wash the soluble carbohydrate. Residues were collected and re-suspended in water at a solid/liquid ratio of 1:30 (w/v), adjusted to pH 12 using 2 N NaOH with continuous stirring for 2 h, and centrifuged. Supernatants were adjusted to pH 4.5 and centrifuged to precipitate protein fractions. Isolated CP was washed twice with distilled water, dissolved in distilled water with pH adjusted to 7.0, and lyophilized. The CPI contained approximately 83% protein, (Nitrogen was converted to protein using a factor of 6.25) as evaluated by Elemental Analyzer (PerkinElmer 2400 Series II CHNS/O).

3.3.3 Preparation of SMCP and GMCP dispersions

CPI was resolved in deionized water at a solid/liquid ratio of 1:10 (w/v). For SMCP, $NaHSO_3$ (0, 1, 3, 6, 9, 12% of CPI dry base) was added, namely SMCP-0, 1, 3, 6, 9, 12. For GMCP, Gdm.Cl (2, 5, 10, 50, 100, 250% of the CPI dry base) was added, namely GMCP-0, 2, 5, 10, 50, 250. The CPI dispersion was adjusted to pH 8.0 by adding 2 N NaOH, and the reaction was implemented with mild stirring at room temperature for 2 h. The reaction was terminated by adjusting pH to 4.5 for further characterization.

3.3.4 Determination of free sulfhydryl groups

SH groups of CPI, SMCP, and GMCP were determined using Ellman's reagent DTNB (5,5'-dithiobis-(2-nitrobenzoic acid)) according to the method described by Kazuko Shimada (Shimada & Cheftel, 1988), with some modification. Samples were dissolved in reaction buffer (0.1M sodium phosphate, pH 8.0, containing 1mM EDTA at pH 8) at a concentration of 0.25% (50 mg of protein/20 mL of buffer). Mixtures were gently stirred for 24 h at room temperature and then centrifuged at 20,000g for 15 min at 4 °C. Supernatant fractions were analyzed for SH group content, and 50µL of Ellman's Reagent Solution (4 mg of DTNB/mL of reaction buffer) was added to a 250µL aliquot of the protein supernatant with 2.5mL of reaction buffer. After the solution was rapidly mixed and allowed to stand at 20 °C for 15 min, absorbance was read at 412 nm. Buffers were used instead of protein solutions as a reagent blank. A molar extinction coefficient of 14,150 $M^{-1}cm^{-1}$ was used to calculate micromoles of SH/ g of protein.

3.3.5 Surface hydrophobicity

Surface hydrophobicity was determined using ANS (8-Anilinonaphthalene-1-sulfonic acid) as a fluorescence probe as described by Hu (Hu et al., 2013) with modification. Lyophilized CPI, SMCP, and GMCP samples in buffer (1 mg/ml in 0. 1 M phosphate buffer at pH 7.4) were centrifuged at 20,000g for 15 min at 4 °C. After determining the protein content of supernatant fraction using Lowry's method, each supernatant was diluted to 0.1mg/ml, and then 60 ul ANS solution (8.0 mM in 0.1 M phosphate buffer, pH 7.4) was added to 3 ml sample solution. Sample solutions were excited at 365 nm, and the relative fluorescence intensity (RFI) of emission spectra was recorded from 400 nm to 540 nm using a Hitachi F-7000 fluorescence spectrophotometer (Hitachi, Ltd., Tokyo, Japan) with a slit width of 10 nm.

3.3.6 Particle size

The SMCP and GMCP dispersion were prepared and stored at 4 °C overnight to ensure that the SMCP and GMCP samples were completely dissolved. Particle sizes of samples were measured by light scattering using Horiba Laser Scattering Particle Size Distribution Analyzer LA-910. Particle size was reported as volume distribution and volume-mean diameter.

3.3.7 Rheological properties

A Bohlin CVOR 150 rheometer (Malvern Instruments, Southborough, MA) was used to characterize viscoelastic properties of SMCP and GMCP dispersions. A parallel plate head was used with 20-mm plate diameter and a 500-um gap. A thin layer of silicon oil was spread over the circumference of the sample to prevent sample dehydration during testing All experiments were performed in triplicate at 1% strain (within its linear viscoelastic region). Apparent viscosity was sweep at 25 s^{-1} shear rate for 150s, mean values were calculated and reported. Frequency sweep analyses were performed for a frequency range of 0.1rad s^{-1} to 100 rad s^{-1}.

3.3.8 Water soaking test

SMCP and GMCP dispersion were prepared for the water soaking test. In a typical experiment, dispersion was uniformly brushed onto a glass panel and cured at 110 °C for 120 min. After cooling down to room temperature, the protein-covered glass panel was soaked in distilled water for 120 min, followed by 100 °C drying for 30 min. Protein lost was calculated as

$$Protein\ loss = \frac{W_i - W_f}{W_i - W_g} \times 100\% \qquad (1)$$

where W_g is the weight of the glass panel, W_i is the weight of the glass panel and protein after 110 °C curing, and W_f is the weight of the glass panel and protein after 100 °C drying.

3.3.9 Thermal gravimetric analysis

TGA of CPs was conducted with a Perkin-Elmer TGA 7 (Perkin-Elmer, Norwalk, CT, USA) in a nitrogen atmosphere. Approximately 5 mg of ground powder was weighed into a platinum cup and scanned from 45 to 700 °C at a heating rate of 10 °C /min. Derivative thermogratimetry curves. Maximum degradation temperature was calculated at the peak temperature of the derivative thermogratimetry curves.

3.4. Results and Discussion

3.4.1 Free sulfhydryl groups

SH groups that are on the surface of protein molecule and readily accessible to reaction with Ellman's reagent are referred as "free SH" groups (Kalapathy & Hettiarachchy, 1996; Tang, Ten, Wang, & Yang, 2006). $NaHSO_3$ is an agent known to unfold protein's structure by disrupting the intermolecular S-S bond; therefore, increasing SH concentration of SMCP denotes increasing unfolding degree. In Figure 3.1 (A), it was observed that free –SH content of SMCP increased significantly with $NaHSO_3$ content. Interestingly, free –SH content reached 17.20umol/g at SMCP-3, and remained stable around 18umol/g for SMCP-6, 9, 12, indicating that 3% $NaHSO_3$ was able to reduce the available S-S bonds of CPI. Kalapathy and Hettiarachchy (Kalapathy & Hettiarachchy, 1996)reported similar results when they modified SPI using $NaHSO_3$. They also observed increasing SH group content of SPI at in present of $NaHSO_3$, and the break of S-S also resulted in reduced viscosity of SPI dispersion. This phenomenon was in consistence with our studies for viscosity. However, compared to the free -SH content of SMCP-9, that of SMCP-12 dropped. possibly due to the shielding effect of excessive HSO_3^- to form the sulfonate group ($RS-SO_3^-$) (Ningbo Li et al., 2011). For GMCP, the content of free SH group also increased with the content of Gdm.Cl, indicating the unfolding effect to camelina protein structure. Unlike the thiol-exchange effect of $NaHSO_3$ to break protein's disulfide bond, Gdm.Cl was a reagent destroying the hydrogen bond of protein matrix, and then embedded free SH groups became accessible.

3.4.2 Surface hydrophobicity

Protein's hydrophobic groups at the side chain of amino acid are mostly buried at folded state, forming a compact hydrophobic core, while the surface was more hydrophilic. Therefore, we used the protein's surface hydrophobicity to describe protein's unfolding degree by detecting ANS binding capacity because ANS is accessible to surface hydrophobic groups and exhibited fluorescence properties. The intensity of ANS binding capacity increased as unfolding hydrophobic groups increased. The intensity of SMCP -0, 3, 6, 9 and GMCP -0, 10, 50, 250 were reported in Figure 3.2.

As expected, the RFI of SMCPs increased as $NaHSO_3$ content increased. No significant difference was observed between SMCP-3 and CPI, but RFI increased significantly for SMCP -6 and SMCP-9. As $NaHSO_3$ broke more S-S at high concentrations, CPI's structures were destroyed, and buried hydrophobic groups were exposed. This was in consistence with the findings discussed in free SH groups. Zhang and Sun (L. Zhang & Sun, 2008) obtained similar surface hydrophobicity trend of $NaHSO_3$-modified SPI by determining SDS-binding capacity, indicating that $NaHSO_3$ could unfold SPI and cause the increase of surface hydrophobicity.

However, a decrease of the RFI of GMCPs was observed. For GMCPs, no significant difference was observed between CPI and GMCP-10, but RFI decreased at GMCP-50, and increased again at GMCP-250. Many studies have described the "molten globule" state of proteins, thereby explaining the RFI quenching phenomenon for GMCP unfolding progress. Gdm.Cl unfolded the proteins in two ways. With low Gdm.Cl content, the protein turned into a molten globule state with destroyed tertiary structures but stabilized secondary structure with lower hydrophobicity than the folded protein. Proteins under the molten state presented pronounced secondary structure and considerable conformational mobility compared to native and fully unfolding state (Ohgushi and Wada, 1983). With high Gdm.Cl content, the secondary structure unfolded and the hydrophobic groups were exposed (Huang and Sun, 2000; Povarova et al., 2010). Similar denaturing progress on the cotton protein was observed by He at al (He, Uchimiya, & Cao, 2014) using Gdm.Cl, and corresponding collapsing effect on protein's hydrophobic domains was reported. Rashid et al. (Rashid et al., 2005) also found that the quenching phenomenon of Gdm.Cl denatured human placental cystatin (HPC) from the native protein up to 1.5M Gdm.Cl for emission fluorescence spectroscopy; proteins in the presence of more than 2M Gdm.Cl exhibited significant increase in surface hydrophobicity, suggesting the

breakdown of secondary structures. These findings are in consistent with our results suggested that with low concentration of Gdm.Cl, CPI was unfolded into the molten state with reduced surface hydrophobicity.

3.4.3 Particle size

The effect of $NaHSO_3$ and Gdm.Cl on volume-mean diameter of CPI dispersions is shown in Figure 3.3. (A) (B), with increasing $NaHSO_3$, SMCPs decreased from 10.21μm to 5.97 μm (from CPI to SMCP-3) and then increased to 21.48 μm (SMCP-12). The initial decrease of particle volume of SMCP was attributed to the disappearance of S-S. Similar dissociation phenomenon of protein particles was also reported for SPI as S-S-induced conformational rearrangement(Hu, Fan, et al., 2013). With the accumulation of hydrophobic groups, particle size increase from SMCP-3 to SMCP-6 and SMCP-12 due to hydrophobic interaction (Section 3.2) that connected the protein. For GMCPs, the volume median of GMCPs increased gradually at low Gdm.Cl content (0-10%). However, from GMCP-50 to GMCP-250, the volume median increased significantly from 42.91 μm to 159.93 μm due to the Gdm.Cl-induced CPI aggregation.

As shown in Figure 3.3. (C) (D), $NaHSO_3$ and Gdm.Cl had significant effects on particle size distribution of CPI dispersion corresponding to the SMCP and GMCP's volume medium. Non-treated CPI exhibited unimodal particle distribution with a peak appeared around 10 μm. Compared to the untreated CPI, single peak of GMCP-5 was right shifting. Then, bimodal curves appeared at 10 μm and 100 μm for GMCP-10. Further increase of Gdm.Cl content resulted in unimodal distribution and right-shifting of the peak distribution for GMCP-50, and GMCP-250, indicating their aggregation behaviors. For SMCP, a left-shifting peak was observed for SMCP-3, and then protein particles grew larger at SMCP-6, 9, 12.

3.4.4 Rheological properties

3.4.4.1 Viscosity

Viscosity, a significant rheological property, governs flow-ability behavior of protein dispersions and influences their handling, processing, and efficiency for further modification (Sun, 2011). Apparent viscosities of SMCP-0, 1, 3, 6, 9, 12 and GMCP-0, 5, 10, 50, 100, 250 are shown in Figure 3.4. In general, both SMCPs and GMCPs exhibited lower viscosity than the native CPI. Because S-S and hydrogen bond both help maintain the protein structures, unfolding

protein exhibited decreased viscosity when shearing(Guangyan Qi et al., 2012). As expected, the viscosity kept decreasing with increasing $NaHSO_3$ content for SMCPs. For GMCPs, the lowest viscosity was 130.53 cp for GMCP-5, and slowly increased to 151.59cp for GMCP-250. Unlike the continuous decreasing viscosity of SMCPs, protein aggregation caused the increase of GMCP's viscosities at high Gdm.Cl concentrations (GMCP-50, 100, 250). Furthermore, we observed that GMCPs were less viscous than SMCPs, indicating that hydrogen bond was more influential than disulfide bond on the shearing behavior in this hydro-protein system.

3.4.4.2 Frequency sweep

Chemical bonds between CPI molecules may be disrupted during the increasing shearing force. Thus, protein's rheological property varies due to their individual bonding. This variation could be used to evaluate the degree of intermolecular interaction. Figure 3.5 shows the effect of Gdm.Cl and $NaHSO_3$ treatments on the variation of storage modulus (G') for CPI dispersions (10%, w/v). G' increased linearly at a certain frequency region (0.5-5 rad/s) for all samples, followed by a sharp increase. Similar frequency-modulus files for SPI were reported (Hu et al., 2013; Tunick, 2011).

Tunick (Tunick, 2011) classified protein interaction into three major types: entangled networks (of biopolymers), cross-linked bonding, or physical (non-covalent linkages) bonding. Entangled networks are highly frequency dependent, suggesting weakest bonding. Cross-linking is a strong covalent bond with minimal frequency dependence. Physical bonding refers to non-covalent interactions that are intermediate between strong and weak bonds, including hydrogen bond and hydrophobic interaction. To better describe the G' variation of CPI dispersion, we used the following equation to characterize the frequency sweep.

$$\log G' = n \log \omega + K \qquad\qquad (2)$$

where n and K are constants with n being the degree of frequency dependence (Tunick, 2011).

Parameters of equation (2) were shown in Table 3.1 by fitting linear curves. The n values for GMCP and SMCP increased at higher $NaHSO_3$ or Gdm.Cl concentration, denoting the effectiveness of Gdm.Cl and $NaHSO_3$ in unfolding CPI structures and breaking the protein interaction. However, GMCP-250 was an exception, in which its n value decreased significantly, meaning the protein was less frequency dependent. This may be due to the strong protein aggregation at GMCP-250 during the unfolding process. By comparing n values of SMCPs and GMCPs, we found that SMCPs were generally more frequency dependent than GMCPs,

suggesting that NaHSO$_3$ may be more effective in breaking the protein-protein interaction. Because the covalent S-S bond is stronger than the non-covalent hydrogen bond, SMCP's intermolecular interaction were more reduced.

3.4.5 Water soaking test

Figure 3.6 shows the weight loss of SMCP -1, 3, 6, 9, 12 and GMCP-5, 10, 20, 50, 250. Weight loss during the water soaking test for cured SMCPs and GMCPs was primarily governed by the degree of protein interaction (Section 3.5.2). A high conjugation degree caused water-resistant protein, while loose structures stimulated increased protein loss (Guangyan Qi et al., 2012; Ying Wang et al., 2007). The weight loss of SMCPs and GMCPs increased as NaHSO$_3$ and Gdm.Cl content increased. At low salt concentration (<10%), a comparison of SMCP and GMCP weight loss revealed that, GMCPs were less dissolved in water than the SMCPs. This result was in consistent with previous protein interaction evaluation by frequency sweep: NaHSO$_3$ was more effective in unfolding protein structure and breaking their interaction, which resulted in high protein loss at high salt concentration. For SMCPs, excessive additions of NaHSO$_3$ into the protein system are detrimental to the water resistance of CPI because –SH resulting from deoxidization were blocked as a sulfonate group (RS-SO$_3^-$) in the presence of excessive HSO$_3^-$ during the NaHSO$_3$ reducing reaction, so the protein became more hydrophilic. Similar results were also reported by Li et al and Zhang and Sun (Ningbo Li et al., 2011; L. Zhang & Sun, 2008) for the investigation of water resistance of NaHSO$_3$-modified SPI. For GMCPs, the protein loss increased significantly due to electrostatic force and salt-in effect at 50% Gdm.Cl or higher.

3.4.6 Thermal gravimetric analysis

Figure 3.7 shows derivative thermogravimetry (DTG) curves of SMCP-0, 3, 6, 9 and GMCP-0, 10, 50, 250 as a function of temperature from 50 °C to 600 °C. CPI, SMCPs, and GMCPs exhibited their maximum degradation rate in the temperature region from 325 °C to 345 °C. SMCP peaks were overlapping before 340°C, suggesting that NaHSO$_3$ did not influence CPI's maximum degradation temperature, but it induced more weight loss after 340 °C. Comparatively, high Gdm-HCl concentrations decreased CPI's maximum degradation temperature; GMCP-50 and GMCP-250 peaks were left-shifting. DTG curves of SMCP and GMCP were in agreement with the studies for glutelin fraction of CPI by Li et al. (N Li et al., 2014).

3.4.7 Proposed mechanism to the SMCP and GMCP

The proposed mechanism of $NaHSO_3$ and Gdm.Cl induced unfolding to CPI were depicted in Figure 3.8. $NaHSO_3$ was a strong reducing agent to cleave the S-S bond between molecules by thiol-disulfide exchange reaction (Gilbert, 1995). Intermolecular S-S bonds of CPI were destroyed and peptide chains became more independent and less compact due to decreasing CPI's secondary and tertiary structures. Hydrophobic groups became exposed and induced CPI aggregation due to hydrophobic interaction; therefore, protein interactions became weaker.

Gdm.Cl unfolded the CPI into a molten state. CPI's tertiary structures were destroyed by formation of a hydrogen bond with $-NH_2$ from Gdm.Cl instead of an amine group from the peptide chain (Pace and Grimsley, 2005). Then the Gdm.Cl penetrated into the protein matrix, and its globular shape began to inflate. Therefore, particle size of the CPI increased, and CPI's surface hydrophobic decreased. During this progress, CPI's secondary structure was present, but the tertiary and quaternary structures exhibited reduced stability.

3.5. Conclusions

Both $NaHSO_3$ and Gdm.Cl treatment had significant effects on CPI's structural and physicochemical properties. $NaHSO_3$ cleaved the S-S and increased surface hydrophobicity, which was demonstrated by increasing free SH group content and ANS binding capacity. $NaHSO_3$ resulted in reduced viscosity and protein-protein interaction as well as an increase of particle size (10.21-21.48mm). Gdm.Cl broke the hydrogen bond among molecules but decreased CPI's surface hydrophobicity, leading to reduced viscosity and protein interaction as well as a significant increase of particle size (10.21-159.53 mm). The decreasing in protein interaction resulted in increased protein loss of SMCPs and GMCPs during water soaking. The reducing effect of $NaHSO_3$ was greater than Gdm.Cl for CPI's intermolecular interaction and less obvious for the viscosity and water resistant. Gdm.Cl reduced the decomposition temperature of CPI, but $NaHSO_3$ demonstrated no obvious reducing effect on the thermal properties of CPI. This information shed light on the structural conformation and bio-processing of camelina protein.

Figure 3-1Effect of NaHSO3 (A) and Gdm.Cl (B) treatment on the free SH group of CPI dispersions. Content of NaHSO3 and Gdm.Cl was the dry base of CPI.
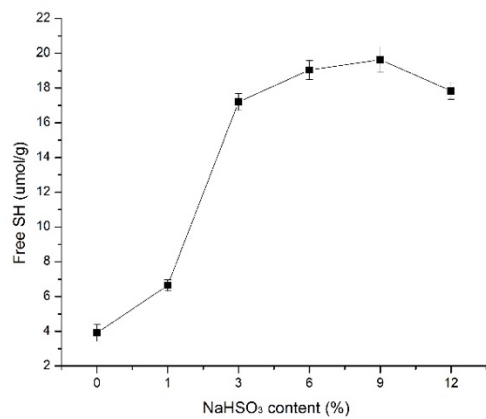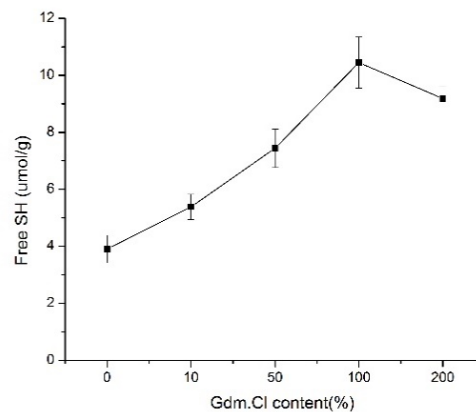
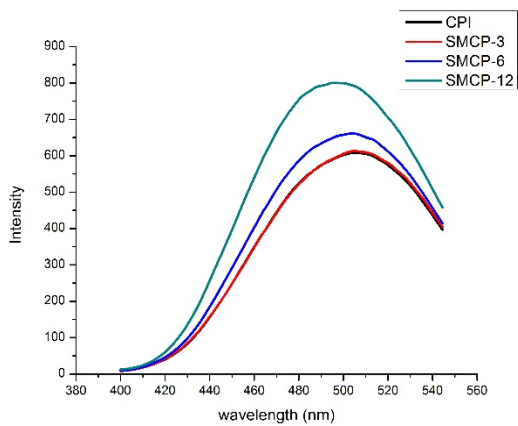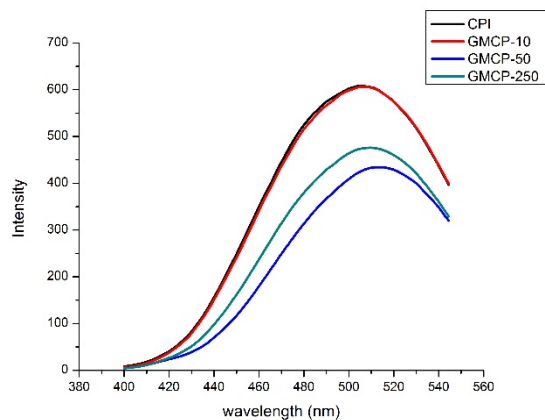(A)   (B)

Figure 3-2Effect of NaHSO3 (A) and Gdm.Cl (B) treatment on the surface hydrophobicity of CPI dispersions. Content of NaHSO3 and Gdm.Cl was the dry base of CPI.

(A)

(B)

Figure 3-3 Effect of NaHSO₃ and Gdm.Cl treatment on the volume medium and particle size distributions of CPI dispersions. (A) Volume medium of SMCP (B) Volume medium of GMCP (C) Particle size distribution of SMCP (D) Particle size distribution of GMCP. Content of NaHSO3 and Gdm.Cl was the dry base of CPI.

(A)

(B)

(C)

(D)

Figure 3-4 Effect of NaHSO3 and Gdm.Cl treatment on the viscosity of CPI dispersions.
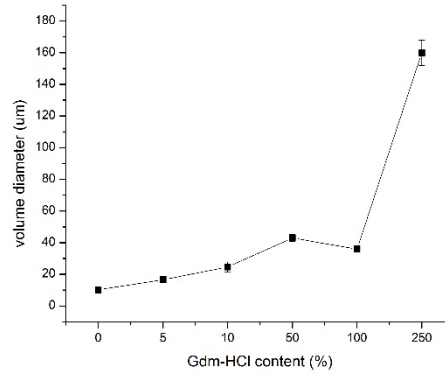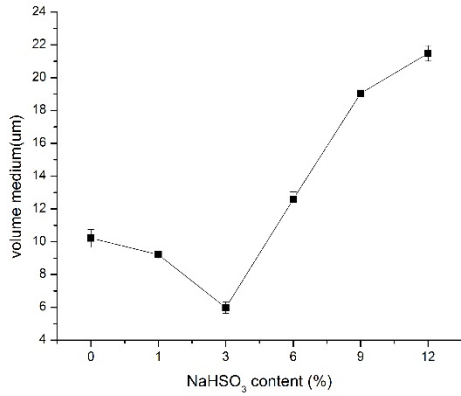
(A) Content of NaHSO3 and Gdm.Cl was the dry base of CPI
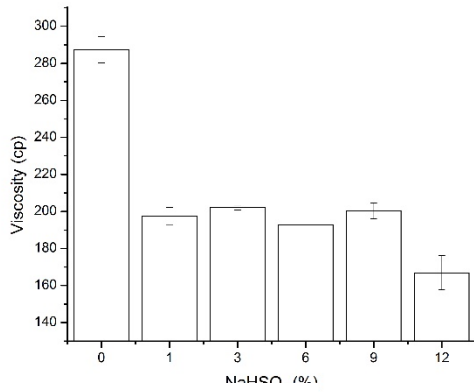
(A)
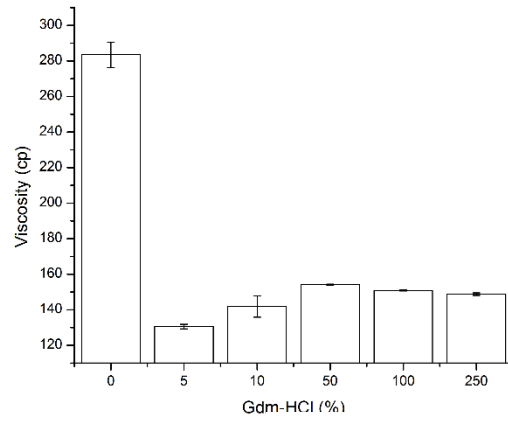
(B)

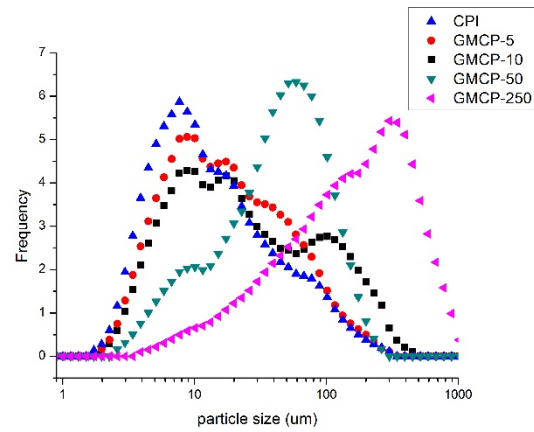**Figure 3-5 Effect of NaHSO₃ (A) and Gdm.Cl (B) treatment on the variation of storage modulus of CPI dispersions for the frequency sweep. Content of NaHSO₃ and Gdm.Cl was the dry base of CPI.**
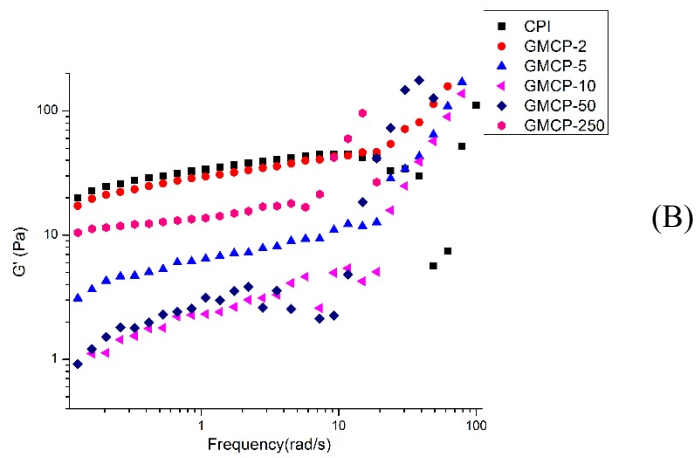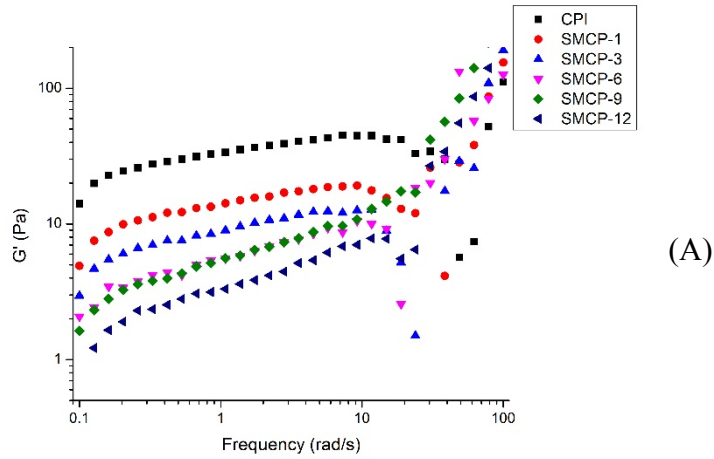
Figure 3-6 Effect of NaHSO$_3$ (A) and Gdm.Cl (B) treatment on the weight loss of 10% cured CPI after water soaking. Content of NaHSO3 and Gdm.Cl was the dry base of CPI.
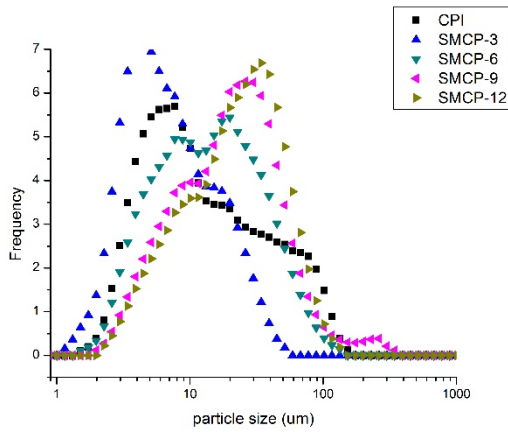

(A)

(B)
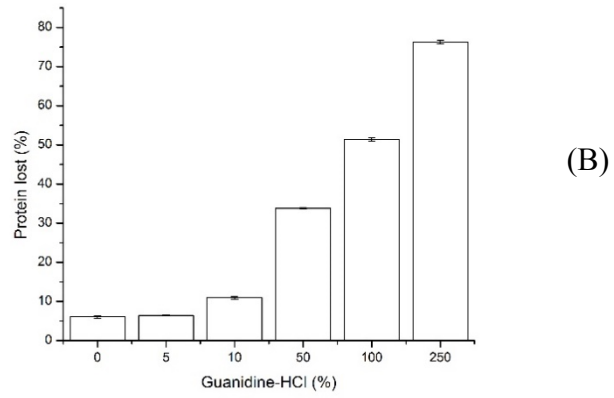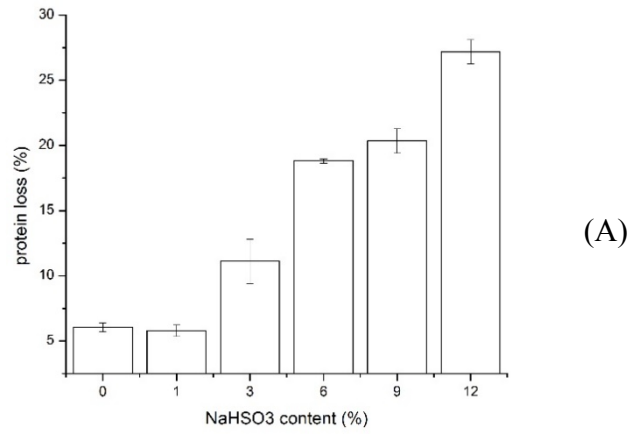
Figure 3-7 Derivative thermogratimetry curves of SMCP (A) and GMCP (B). Content of NaHSO3 and Gdm.Cl was the dry base of CPI.
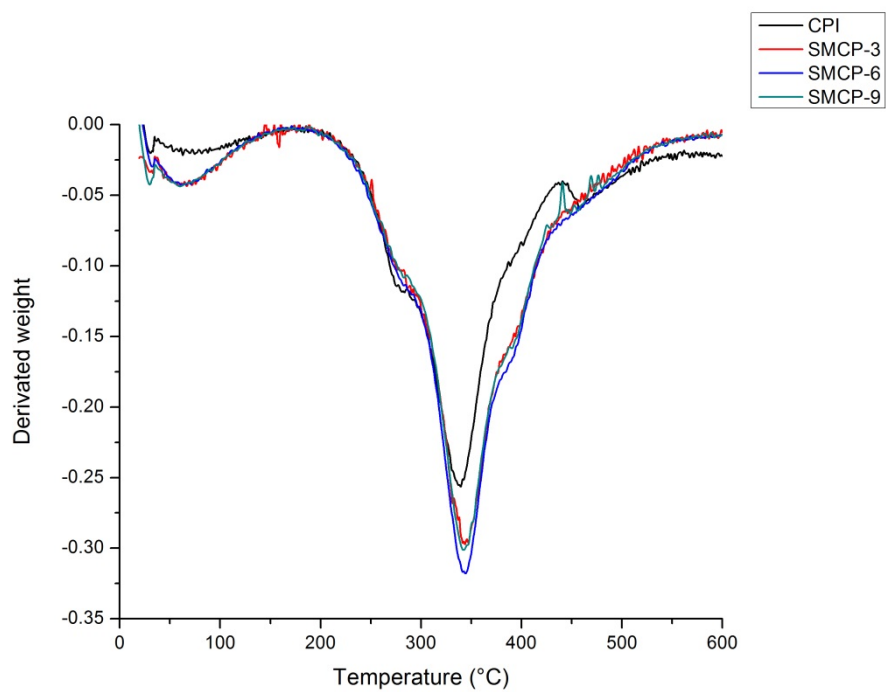
(A)
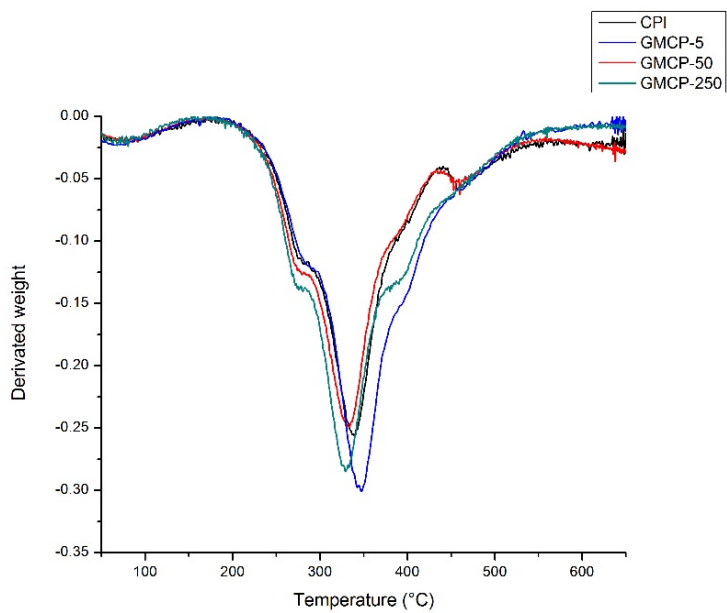
(B)

Figure 3-8 Proposed mechanism for the unfolding process of CPI by NaHSO₃ and Gdm.Cl

Camelina protein

NaHSO₃
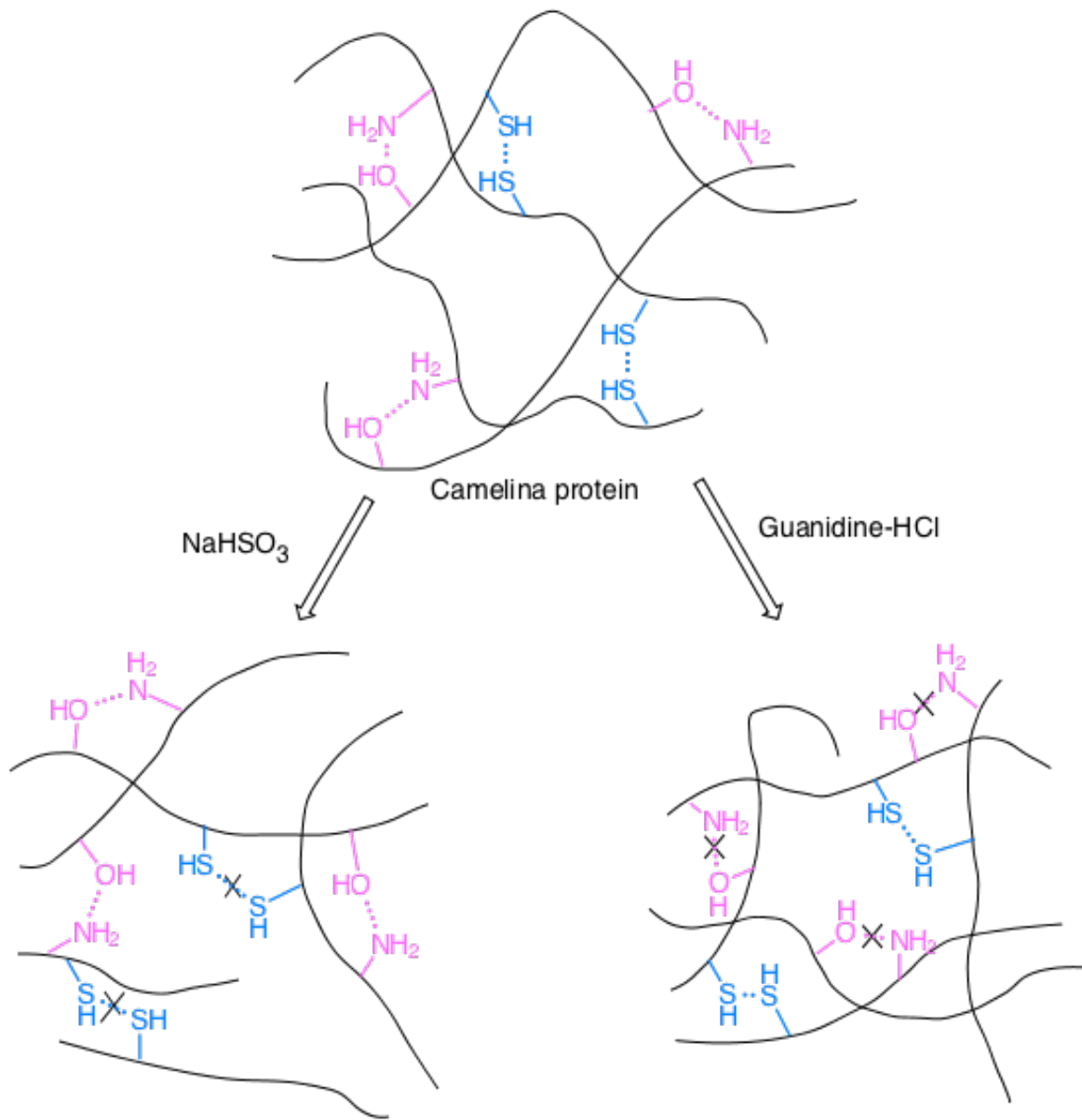
Guanidine-HCl

Table 3-1 Rheological properties of NaHSO$_3$ and Gdm.Cl treated CPI dispersions for frequency sweep at 0.1 to 100 rad/s.

NaHSO$_3$ content (%)	Fitting slope	R^2
0	0.15	0.997
1	0.17	0.990
3	0.19	0.973
6	0.26	0.973
9	0.31	0.995
12	0.33	0.987

Guanidine-HCl content (%)	Fitting slope	R^2
0	0.15	0.997
2	0.18	0.994
5	0.22	0.978
10	0.24	0.989
50	0.29	0.980
250	0.14	0.963

3.6. References

Abtahi, S., & Aminlari, M. (1997). Effect of Sodium Sulfite, Sodium Bisulfite, Cysteine, and pH on Protein Solubility and Sodium Dodecyl Sulfate−Polyacrylamide Gel Electrophoresis of Soybean Milk Base. *Journal of Agricultural and Food Chemistry*, *45*, 4768–4772. https://doi.org/10.1021/jf970035r

C. Nick Pace, Gerald R. Grimsley, J. M. S. (2005). Denaturation of Proteins by Urea and Guanidine Hydrochloride. In *Protein Science Encyclopedia* (pp. 45–47). Wiley-VCH Verlag GmbH & Co. KGaA. https://doi.org/10.1002/9783527610754

Custódio, J., Broughton, J., & Cruz, H. (2009). A review of factors influencing the durability of structural bonded timber joints. *International Journal of Adhesion and Adhesives*. https://doi.org/10.1016/j.ijadhadh.2008.03.002

Gilbert, H. F. (1995). Thiol/disulfide exchange equilibria and disulfidebond stability. *Methods in Enzymology*, *251*, 8–28. https://doi.org/http://dx.doi.org/10.1016/0076-6879(95)51107-5

Guo, C., & Irudayaraj, J. (2011). Fluorescent Ag clusters via a protein-directed approach as a Hg(II) ion sensor. *Analytical Chemistry*, *83*, 2883–2889. https://doi.org/10.1021/ac1032403

H. Christensen, R. H. P. (1991). molten globule intermediates and protein folding. *European Biophysics Journal*, *19*(5), 221–229.

He, Z., Uchimiya, M., & Cao, H. (2014). Intrinsic Fluorescence Excitation–Emission Matrix Spectral Features of Cottonseed Protein Fractions and the Effects of Denaturants. *Journal of the American Oil Chemists' Society*, *91*(9), 1489–1497. https://doi.org/10.1007/s11746-014-2495-1

Hu, H., Fan, X., Zhou, Z., Xu, X., Fan, G., Wang, L., … Zhu, L. (2013). Acid-induced gelation behavior of soybean protein isolate with high intensity ultrasonic pre-treatments. *Ultrasonics Sonochemistry*, *20*(1), 187–195. https://doi.org/10.1016/j.ultsonch.2012.07.011

Hu, H., Wu, J., Li-Chan, E. C. Y., Zhu, L., Zhang, F., Xu, X., … Pan, S. (2013). Effects of ultrasound on structural and physical properties of soy protein isolate (SPI) dispersions. *Food Hydrocolloids*, *30*(2), 647–655. https://doi.org/10.1016/j.foodhyd.2012.08.001

Huang, W., & Sun, X. (2000a). Adhesive properties of soy proteins modified by sodium dodecyl sulfate and sodium dodecylbenzene sulfonate. *Journal of the American Oil Chemists' Society*, *77*(7), 705–708. https://doi.org/10.1007/s11746-000-0113-6

Huang, W., & Sun, X. (2000b). Adhesive properties of soy proteins modified by urea and

guanidine hydrochloride. *Journal of the American Oil Chemists' Society*.
https://doi.org/10.1007/s11746-000-0016-6

Jana, S., Chaudhuri, T. K., & Deb, J. K. (2006). Effects of guanidine hydrochloride on the
conformation and enzyme activity of streptomycin adenylyltransferase monitored by
circular dichroism and fluorescence spectroscopy. *Biochemistry (Moscow)*, *71*(11), 1230–
1237. https://doi.org/10.1134/S0006297906110083

Jiang, J., Xiong, Y. L., & Chen, J. (2010). pH Shifting alters solubility characteristics and
thermal stability of soy protein isolate and its globulin fractions in different pH, salt
concentration, and temperature conditions. *Journal of Agricultural and Food Chemistry*,
58(13), 8035–42. https://doi.org/10.1021/jf101045b

Kalapathy, U., & Hettiarachchy, N. (1996). Alkali-modified soy proteins: effect of salts and
disulfide bond cleavage on adhesion and viscosity. *Journal of the American Oil CHemists'
Society*, *73*(8), 1063–1066. Retrieved from
http://link.springer.com/article/10.1007/BF02523417

Kasetaite, S., Ostrauskaite, J., Grazuleviciene, V., Svediene, J., & Bridziuviene, D. (2014).
Camelina oil- and linseed oil-based polymers with bisphosphonate crosslinks. *Journal of
Applied Polymer Science*, *131*(17). https://doi.org/10.1002/app.40683

Kiefhaber, T., & Baldwin, R. L. (1995). Kinetics of hydrogen bond breakage in the process of
unfolding of ribonuclease A measured by pulsed hydrogen exchange. *Proceedings of the
National Academy of Sciences*, *92*(7), 2657–2661. https://doi.org/10.1073/pnas.92.7.2657

Kishore, D., Kundu, S., & Kayastha, A. M. (2012). Thermal, Chemical and pH Induced
Denaturation of a Multimeric β-Galactosidase Reveals Multiple Unfolding Pathways. *PLoS
ONE*, *7*(11), e50380. https://doi.org/10.1371/journal.pone.0050380

Li, N., Qi, G., Sun, X. S., Stamm, M. J., & Wang, D. (2011). Physicochemical Properties and
Adhesion Performance of Canola Protein Modified with Sodium Bisulfite. *Journal of the
American Oil Chemists' Society*, *89*(5), 897–908. https://doi.org/10.1007/s11746-011-1977-
7

Li, N., Qi, G., Sun, X. S., Wang, D., Bean, S., & Blackwell, D. (2014). Isolation and
Characterization of Protein Fractions Isolated from Camelina Meal. *Transactions of the
ASABE*, *57*(2010), 169–178. https://doi.org/10.13031/trans.57.10455

Nguyen, H. T., Silva, J. E., Podicheti, R., Macrander, J., Yang, W., Nazarenus, T. J., … Cahoon,

E. B. (2013). Camelina seed transcriptome: a tool for meal and oil improvement and translational research. *Plant Biotechnology Journal*, *11*(6), 759–69. https://doi.org/10.1111/pbi.12068

Ohgushi, M., & Wada, A. (1983). "Molten-globule state": a compact form of globular proteins with mobile side-chains. *FEBS Letters*, *164*(1), 21–24. https://doi.org/10.1016/0014-5793(83)80010-6

Povarova, O. I., Kuznetsova, I. M., & Turoverov, K. K. (2010). Differences in the pathways of proteins unfolding induced by urea and guanidine hydrochloride: molten globule state and aggregates. *PloS One*, *5*(11), e15035. https://doi.org/10.1371/journal.pone.0015035

Qi, G., Li, N., Wang, D., & Sun, X. S. (2012). Physicochemical properties of soy protein adhesives obtained by in situ sodium bisulfite modification during acid precipitation. *JAOCS, Journal of the American Oil Chemists' Society*, *89*(2), 301–312. https://doi.org/10.1007/s11746-011-1909-6

Qi, G., Venkateshan, K., Mo, X., Zhang, L., & Sun, X. S. (2011). Physicochemical properties of soy protein: effects of subunit composition. *Journal of Agricultural and Food Chemistry*, *59*(18), 9958–64. https://doi.org/10.1021/jf201077b

Rashid, F., Sharma, S., & Bano, B. (2005). Comparison of Guanidine Hydrochloride (GdnHCl) and Urea Denaturation on Inactivation and Unfolding of Human Placental Cystatin (HPC). *The Protein Journal*, *24*(5), 283–292. https://doi.org/10.1007/s10930-005-6749-5

Reddy, N., Jin, E., Chen, L., Jiang, X., & Yang, Y. (2012). Extraction, characterization of components, and potential thermoplastic applications of camelina meal grafted with vinyl monomers. *Journal of Agricultural and Food Chemistry*, *60*(19), 4872–9. https://doi.org/10.1021/jf300695k

Shimada, K., & Cheftel, J. C. (1988). Determination of sulfhydryl groups and disulfide bonds in heat-induced gels of soy protein isolate. *Journal of Agricultural and Food Chemistry*, *36*(1), 147–153. https://doi.org/10.1021/jf00079a038

Song, F., Tang, D.-L., Wang, X.-L., & Wang, Y.-Z. (2011). Biodegradable soy protein isolate-based materials: a review. *Biomacromolecules*, *12*(10), 3369–80. https://doi.org/10.1021/bm200904x

Sun, X. S. (2011). Soy Protein Polymers and Adhesion Properties. *Journal of Biobased Materials and Bioenergy*, *5*(4), 409–432. https://doi.org/10.1166/jbmb.2011.1183

Tang, C.-H., Ten, Z., Wang, X.-S., & Yang, X.-Q. (2006). Physicochemical and functional properties of hemp (Cannabis sativa L.) protein isolate. *Journal of Agricultural and Food Chemistry*, *54*(23), 8945–50. https://doi.org/10.1021/jf0619176

Teng, Z., Luo, Y., & Wang, Q. (2012). Nanoparticles synthesized from soy protein: preparation, characterization, and application for nutraceutical encapsulation. *Journal of Agricultural and Food Chemistry*, *60*(10), 2712–20. https://doi.org/10.1021/jf205238x

Tunick, M. H. (2011). Small-strain dynamic rheology of food protein networks. *Journal of Agricultural and Food Chemistry*, *59*(5), 1481–6. https://doi.org/10.1021/jf1016237

Wang, Y., Cao, X., & Zhang, L. (2006). Effects of cellulose whiskers on properties of soy protein thermoplastics. *Macromolecular Bioscience*, *6*(7), 524–31. https://doi.org/10.1002/mabi.200600034

Wang, Y., Mo, X., Sun, X. S., & Wang, D. (2007). Soy Protein Adhesion Enhanced by Glutaraldehyde Crosslink. *Journal ofApplied Polymer Science*, *104*, 130–136. https://doi.org/10.1002/app

Wang, Y., Wang, D., & Sun, X. S. (2005). Thermal properties and adhesiveness of soy protein modified with cationic detergent. *Journal of the American Oil Chemists' Society*, *82*(5), 357–363. https://doi.org/10.1007/s11746-005-1078-1

Zhang, J., Jiang, L., Zhu, L., Jane, J.-L., & Mungara, P. (2006). Morphology and properties of soy protein and polylactide blends. *Biomacromolecules*, *7*(5), 1551–61. https://doi.org/10.1021/bm050888p

Zhang, L., & Sun, X. S. (2008). Effect of sodium bisulfite on properties of soybean glycinin. *Journal of Agricultural and Food Chemistry*, *56*(23), 11192–7. https://doi.org/10.1021/jf801137y

Zhao, Y., Jiang, Q., Xu, H., Reddy, N., Xu, L., & Yang, Y. (2014). Cytocompatible and water-stable camelina protein films for tissue engineering. *Journal of Biomedical Materials Research. Part B, Applied Biomaterials*, *102*(4), 729–36. https://doi.org/10.1002/jbm.b.33053

Zhong, Z., Sun, X. S., Fang, X., & Ratto, J. O. A. (2001). Adhesion strength of sodium dodecyl sulfate-modfied soy protein to fiberboard, *15*(12), 1417–1427.

Chapter 4 - EDC cross-linked camelina protein with ultrasound pretreatment: Microstructural, rheological, and aqueous behaviors

4.1 Abstract

A nonedible camelina protein (CP) was extracted from the defatted camelina sativa meal, a biodiesel residue after oil extraction. However, the protein was difficult to develop into useful polymeric materials due to its limited polymerization and poor water stability. This paper discusses the effect of crosslink reaction with ultrasound pretreatment to the structural, rheological, physiochemical properties, and water resistance of camelina protein isolate (CPI). Camelina protein was extracted from defatted camelina meal by alkali solubilization and acid precipitation and then treated by high intensity ultrasound. Both CPI and ultrasound-modified CPI (UCPI) were cross-linked by Ethyl-3-(3-dimethyl-aminopropyl-1-carbodiimide) (EDC) and N-hydroxysuccinimide (NHS) as a catalyst. The cross-linked CPI exhibited increased molecular weight and particle size due to the coupling effect of free amino groups and carboxyl groups. Microstructures of modified CPI also became rigid and condensed. CPI's increased intermolecular protein interaction resulted in its higher elastic modulus, viscosity and water resistance. The crosslink degree of EDC modification was higher for UCPI than CPI, leading to UCPI's stronger aggregation behaviors and more compact protein structures. The elastic modulus, viscosity, and water resistance of UCPI increased accordingly. Ultrasound pre-treatment stimulated the effect of EDC induced cross-linking reaction to camelina protein, which could be potentially used as inexpensive and green biopolymers.

4.2. Introduction

To date, the limited fuel resources and corresponding environmental concerns caused by the petroleum manufacturing have urged us to develop alternative bio-based materials (X. S. Sun, 2011). Compared with other natural polymers, plant proteins, exhibiting a wide range of functional properties due to the diversity of their amino acids and structures, was potentially utilized for bio-based resins or composites. One example is legume proteins (Cheng, Sun, & Zhao, 2014; Chien, Makridakis, & Shah, 2012; Usha et al., 2012), for instance, modified soybean protein (SP) has been used for bio-based materials such as, edible films, adhesives, and coatings (Song et al., 2011; Teng et al., 2012; J. Zhang et al., 2006). Other legume proteins such as canola, zein, and pea protein were also developed for similar purposes (De Graaf, Harmsen, Vereijken, & Mönikes, 2001b; H. X. Guo & Shi, 2009; S. Kim, Sessa, & Lawton, 2004; C. Li, Huang, Peng, Shan, & Xue, 2014; Ningbo Li et al., 2015; Shi & Dumont, 2014a; C. Wang, Wu, & Bernard, 2014). However, these proteins comprise a portion of humans' diets, thereby creating competition between utilization for protein-based products or human food. Thus, alternative proteins from nonedible sources were expected.

Camelina sativa is a widely grown dryland oilseed crop in the North America and Europe, and it was mostly utilized as biodiesel sources in the past few decades(Nguyen et al., 2013). Recently, camelina oil has drawn increasing attention due to its abundance in polyunsaturated fatty acids, favored by food and health products (Kasetaite et al., 2014; Peiretti & Meineri, 2007). Accordingly, the demand for biofuels and unsaturated camelina oil resulted in increased production of camelina meal (CM) as protein resources for value-added products. After oil extraction, CM typically contains 40% crude protein, which is a mixture of 2S (albumin storage protein) and 12S fraction (cruciferin)(N Li et al., 2014). However, it was reported that some potential toxic compound such as mustard and glucosinolates in the meal are antinutritional chemicals that restrained its food uses(Matthäus & Zubr, 2000). As a result, defatted camelina meal (DCM), the byproduct of camelina oil extraction with high value protein, was largely underutilized. Thus, while modifications of some edible protein-based biopolymers, such as soy, have been fully investigated, studies on the processing and functional properties of non-edible camelina protein were still in the start-up stage.

Currently, there are only limited studies on the extraction and modification of CP for polymeric materials. Li et al investigated the isolation and adhesion properties of camelina

protein from the defatted meal (Ningbo Li et al., 2015). Zhao et al developed CP-based film and discussed the cysteine-induced denaturation to its physiochemical properties (Zhao et al., 2014). Our previous study also reported different CPI properties unfolded by $NaHSO_3$ and guanidine-HCl (Zhu et al., 2016). Regardless the isolation, unfolding, or grafting treatment, we observed two major concerns for its further use as biodegradable polymers: lack of mechanical strength and poor water resistance. These are also the common drawbacks for most pristine protein-based polymers. The limited molecular weight and non-covalent bonding between subunits made protein polymers vulnerable to the applied force such as shearing and pressure, especially when exposed to the water(Shi & Dumont, 2014b). In the aquatic environment, protein-protein interactions became weaker (De Graaf et al., 2001a).

In order to resolve these problems, crosslink reaction could be induced by some coupling reagents to increase the intermolecular protein interaction, stabilize the protein network, and increase the water resistance (Song et al., 2011). Traditionally, some chemical and enzymatic cross-linkers such as glutaraldehyde, formaldehyde, transglutaminase (TGase) were extensively used for inactivating, stabilizing, or immobilizing pristine proteins. They have been used to improve the mechanical properties and water resistance of protein-based adhesives, gels, and edible films (González et al., 2011; Ying Wang et al., 2007; Yang, Liu, & Tang, 2013). However, glutaraldehyde's associated toxicity and TGase's decreased enzyme activity at different ambient chemical environment were undesirable.

Therefore, a popular zero-length cross-linker, Ethyl-3-(3-dimethyl-aminopropyl-1-carbodiimide) (EDC) and N-hydroxysuccinimide (NHS) as a catalyst, became increasingly utilized. It stimulates the amide bond formation by activating the carboxylic acid group of aspartic side chain and glutamic acid residues followed by amino group induced aminolysis (from lysine residues) of the O-isoacylurea intermediates (Usha et al., 2012). The reaction is efficient, mild, low toxic, and no unexpected protein denaturation occurred (Nam, Kimura, & Kishida, 2008; S. N. Park, Park, Kim, Song, & Suh, 2002). Its high solubility in water and reaction efficiency was another advantage. Many studies have reported that proteins such as zein, soy, collagen were fabricated into scaffolds, gels, or films by EDC crosslink (Barkay-Olami & Zilberman, 2015; Hou et al., 2015; S. Kim et al., 2004; Ren & Soucek, 2014).

Interestingly, many previous studies showed that unfolding is important to protein's reactivity and further crosslink. Therefore, scientists applied heating, high pressure, or some

unfolding reagents to denature the ordered protein structure and disassociate protein subunits before crosslink (Puppo et al., 2004; J M S Renkema, Gruppen, & van Vliet, 2002; van Vliet, Martin, & Bos, 2002). The ultrasound technique, a green and effective approach to unfold pristine protein's structures, was widely used in the food and material industry. After ultrasound modification, proteins exhibit increased free sulfydryl groups, free amino groups and surface hydrophobic groups for coupling and stabilizations (Chen, Chen, Ren, & Zhao, 2011; Hu, Fan, et al., 2013; O'Donnell, Tiwari, Bourke, & Cullen, 2010; Xue, Li, Zhu, Wang, & Pan, 2013). Therefore, we speculated that ultrasound modification stimulated the crosslink effect of EDC to camelina protein isolate (CPI).

To the best of our knowledge, while camelina protein exhibits its bio-availability and prospective values, little is known about the crosslink effect to CPI's structural and aqueous behaviors at both pristine and unfolded state. Thus, the objective of this study was to 1) crosslink CPI and ultrasound-pretreated CPI (UCPI) by EDC treatment, and 2) characterize the effect of EDC/NHS modification to the physicochemical characteristics, rheological properties, water resistant, and structural properties of CPI and UCPI; with the hope to increase the intermolecular bonding and water-resistance of CPI and explore camelina protein's future development as green biopolymers.

4.3. Materials and methods

4.3.1 Materials

Defatted camelina meal (DCM) with 32.4% crude protein (db), and 11.0% moisture content (db) was provided by Field Brothers Inc. (Pendroy, MT, US). N-(3-Dimethylaminopropyl)-N'-ethylcarbodiimide hydrochloride (EDC), N-Hydroxysuccinimide (NHS), ninhydrin reagent, SDS Gel Preparation Kit, hydrochloric acid (HCl), and sodium hydroxide (NaOH) were purchased from Sigma-Aldrich (St. Louis, MO, USA).

4.3.2 Isolation of camelina protein

CPI was separated from DCM using the method described by Li et al, with some modifications (N Li et al., 2014). DCM samples were mixed with distilled water at a solid/liquid ratio of 1:30 (w/v), stirred for 2 h, and then centrifuged. Residues were collected and re-suspended in water at a solid/liquid ratio of 1:30 (w/v), adjusted to pH 12 using 2 N NaOH with continuous stirring for 2 h, and centrifuged. Supernatants were adjusted to pH 4.5 and centrifuged to precipitate protein fractions. Isolated CP was washed twice with distilled water,

re-dissolved in distilled water with pH adjusted to 7.0, and lyophilized. The CPI contained approximately 83% protein, as evaluated by Elemental Analyzer (PerkinElmer 2400 Series II CHNS/O).

4.3.3 High-intensity ultrasound treatment

CPI dispersion (2.5%, w/v) was prepared by adding CPI powder into distilled water with pH adjusting to 8 and gently stirring at ambient temperature for 4 h. An ultrasound processor model VCF 1500 (SONICS & MATERIALS INC, Newtown, CT,USA) was used to sonicate 100mL of CPI dispersions in 200mL flat bottom conical flasks which were immersed in an ice-water bath. Samples were treated at 20 kHz at 375W for 20 min (pulse duration of on-time 1 min and off-time 1 min). After ultrasound treatment, samples were lyophilized and then stored at 4 °C refrigerator in air tight containers until used.

4.3.4 Preparation of CPI and UCPI dispersions

CPI and UCPI were dissolved in deionized water at a solid/liquid ratio of 1:20 (w/v) with pH adjusting to 8, and gently stirred for 1 h. EDC and NHS was added in the ratio of EDC (mmol)/ NHS (mmol)/protein (g) = 0:0:1; 0.1:0.1:1; 0.25:0.25:1; 0.4:0.4:1, namely CPI-0, 01, 0.25, 0.4 or UCPI-0, 0.1 0.25, 0.4. The protein dispersions were adjusted to pH 8 again and conditioned 30 min, followed by the oil bath at 75 °C for 20 min to stimulate the crosslink reaction. After that, CPI and UCPI dispersions were gently stirred and cooled at room temperature for 6 hours before further characterizations.

4.3.5 Qualitative analysis of free amino group

Based on the reaction between the amino group and ninhydrin, the concentration of the amino group can be tested by the changes in absorbance at 570 nm. A 1 ml ninhydrin reagent solution was mixed with each sample (2 ml, 10mg/ml protein solution). Samples were then placed into a boiling water bath for 10 min and cooled to room temperature. A 5 ml of 95% ethanol was added to each sample. Sample absorbance at 570 nm was measured and compared with the standard curve to determine the concentration of the amino group (glycine solution was used to make the standard curve Y = 0.0859x − 0.0004, R2 = 0.9988; Y: concentration of amino group; x: absorbance) (Moore, Spackman, & Stein, 1958; Sarin, Kent, Tam, & Merrifield, 1981). Crosslink degree (CD) was calculated using the equation:

$$CD = \frac{A_0 - A_t}{A_0} \times 100\% \tag{1}$$

A_0: free amino groups of heated CPI or UCPI solution (no crosslink reagent)

A_t: free amino groups of EDC/NHS modified CPI or UCPI solution

4.3.6 SDS-PAGE

SDS-PAGE was performed on a 4% stacking gel and 12% separating gel with a discontinuous buffer system, as described by Laemmli (LAEMMLI, 1970). EDC/NHS modified CPI and UCPI samples (5 mg/mL in buffer containing 2% SDS, 25% glycerol, and 0.01% bromphenol blue) were incubated for 1 h at room temperature, then heated at 95 °C for 5 min and cooled in the ice bath for 3 min. Aliquots (15 mL) of the prepared samples were loaded onto the gels. Electrophoresis was performed at 40mA and 150V for 120 min. The gel was stained in 0.25% Coomassie brilliant blue R- 250 and destained in a solution containing 10% acetic acid and 40% methanol.

4.3.7 Particle size

The EDC/NHS modified CPI and UCPI dispersion were prepared and stored at 4 °C overnight to ensure their complete dissolving. Particle sizes of samples were measured by light scattering using Horiba Laser Scattering Particle Size Distribution Analyzer LA-910. Particle size was reported as volume-mean diameter.

4.3.8 Rheological properties

A Bohlin CVOR 150 rheometer (Malvern Instruments, Southborough, MA) was used to characterize viscoelastic properties of CPI and UCPI dispersions. A parallel plate head was used with 20-mm plate diameter and a 500-um gap. A thin layer of silicon oil was spread over the circumference of the sample to prevent sample dehydration during testing.

4.3.8.1 Temperature Sweep

Measurements were performed at a constant strain percentage of 0.01%, which was within the linear region, and at an angular frequency of 1 Hz. EDC/NHS modified CPI and UCPI dispersions (10%, w/v) were prepared in distilled water. To mimic the crosslink reaction, samples were heated from 25 to 75 °C at a heating rate of 2 °C /min, kept at 75 °C for 20 min, and cooled down to 25 °C at a cooling rate of 2 °C /min.

4.3.8.2 Frequency sweep analyses

After temperature sweep, frequency sweep analyses were performed for a frequency range of 0.1 rad s^{-1} to 100 rad s^{-1}.

4.3.8.3 Apparent viscosity

Apparent viscosity was sweep at 25 s^{-1} shear rate for 150 s. Mean values were calculated and reported. All experiments were performed in triplicate.

4.3.9 Water soaking test

CPI and UCPI dispersions were prepared for the water soaking test. In a typical experiment, dispersion was uniformly brushed onto an aluminum lids and cured at 110 °C for 2 hours. After recovering to room temperature, the protein-covered container was soaked in distilled water for 20 hours, followed by 100 °C drying for 30 min. Protein lost could be calculated as

$$Protein\ loss = \frac{W_i - W_f}{W_i - W_g} \times 100\%$$ (2)

where W_g is the weight of the aluminum lids, W_i is the weight of the aluminum lids and protein after 110 °C curing, and W_f is the weight of the aluminum lids and protein after 100 °C drying.

4.3.10 Scanning electron microscopy (SEM)

The morphology of the samples were observed with a SEM (Hitachi S-3500N scanning electron microscope) at an accelerating voltage of 10 kV. Before using the SEM, samples were dried and coated with gold/palladium an argon atmosphere using a Balzers evaporator (model SCD 050, Baltec Lichtenstein, Austria).

4.4. Results and discussion

4.4.1 Free amino acid test

The levels of free amino groups of CPIs and UCPIs were determined (Table 4.1). The amount of CPI's free amino groups increased from 1.27 to 1.54 mmol/ml after ultrasound treatment. It was also possible that the strong cavitation force during ultrasound treatment broke protein's secondary and tertiary structures, and the buried amino groups became exposed and accessible. Similar result was reported that high intense ultrasound treatment partially unfolded soy protein, and thus increased free sulfhydryl groups and surface hydrophobicity (Hu, Li-Chan, Wan, Tian, & Pan, 2013).

Heat treatment also led to a significant increase of the free amino group content of CPI (1.27 to 1.94 mmol/ml) and UCPI (1.54 to 1.89 mmol/ml), because heating is an effective method to denature the pristine protein and expose the buried functional groups (Jacoba M S

Renkema & van Vliet, 2002; J M S Renkema et al., 2002; Roesch & Corredig, 2005). While EDC/NHS content increased, the amount of free amino groups kept decreasing due to the coupling effect and finally stayed at 1.18 mmol/ml for CPI-0.4 and 1.02 mmol/ml for UCPI-0.4. In addition, the crosslink degree of UCPI-0.25, 0.4 were higher than CPI-0.25, 0.4, because ultrasound treatment created increased free amino groups for EDC/NHS-induced crosslink reaction.

4.4.2 SDS-PAGE

Molecular weight distribution of modified CPI and UCPI were shown in Figure 4.1. There are four major bands for CPI distributing at molecular weight 14 KDa, 17KDa, 30KDa, and 50 KDa, which was in agreement with Li's results (Ningbo Li et al., 2015). Expectedly, as the EDC/NHS content increased, the band intensities became weaker for both CPI and UCPI, suggesting that all the four subunits were cross-linked to form high-molecular weight aggregates. As a result, the particle size of CPI and UCPI increased.

In the presence of 0.25 and 0.4 mmol/g EDC/NHS, the intensities of high-molecular weight subunits (30KDa, and 50KDa) were weaker than the low molecular weight fractions (14 KDa and 17 KDa) for both CPI and UCPI. Similar results were also observed by Wang when he treated soy protein by glutaradehyde, and found that more β-conglycinin subunits (76, 70, 57 KDa) were crosslinked than glycinin (31-45, 18-20 KDa) (Ying Wang et al., 2007). The reason for this phenomenon could be that the amino acids, such as lysine and aspartic acid that contained highly content of amine groups and carboxyl groups, were mainly found in the high molecular weight subunits. Little difference was found between the profiles of CPIs and UCPIs, suggesting that the ultrasound pretreatment did not change the CPI molecular weight distributions during the crosslink reaction. Similar results were also reported by Hu (Hu, Li-Chan, et al., 2013) and Karki (Karki et al., 2009) who investigated the effect of ultrasound treatment on soy protein isolate.

4.4.3 Particle size

Particle size is an index to reflect the protein aggregation behavior, which affects the protein's other functional properties. The particle size of EDC/NHS modified CPI and UCPI dispersions were shown in Figure 4.2. The diameters of CPI increased significantly with the addition of EDC/NHS for CPI (from 11.59 um to 51.62 um) and UCPI (from 7.68 um to 89.15 um). As previously discussed, EDC/NHS stimulated the formation of amide bond between

subunits (Table 1), protein particles turned into large aggregates with reduced solubility. Such crosslink-induced particle size growth of proteins was reported by Hariyadi that they crosslinked the ovalbumin by Ca^{2+}, and Ba^{2+}(Hariyadi, Hendradi, Purwanti, Fadil, & Ramadani, 2014). Yang also reported the increase of SPI dispersion's particle size crosslinked by transglutaminase (Yang et al., 2013).

Moreover, we found that the particle size of UCPI-0, 0.1, 0.25 were smaller than CPI-0, 0.1, 0.25, but the diameter of UCPI-0.4 (89.15μm) was obviously larger than CPI-0.4 (51.62um). As the protein matrix was unfolded by the ultrasound pretreatment, more binding sites became accessible for the following crosslink processing. At low EDC/NHS concentration, UCPI was partially cross-linked and exhibited reduced aggregation than CPI; when EDC/NHS concentration was high (0.4mmol/g), and UCPI formed larger aggregates than CPI.

Together with results of section 4.4.1 and 4.4.2, we propose the crosslink progress of CPI and UCPI molecules (Fig 4.3). After heat denaturation, CPI had a diameter of 11.59 μm, and amide bonds formed between free amino groups and carboxyl groups in presence of EDC/NHS, resulting in increased molecular weight and particle size (diameter: 51.62 μm). On the other hand, the ultrasound pretreatment dissociated CPI into smaller particles (7.68 μm) with increased exposed free amino groups leading to enhanced crosslink efficiency of EDC/NHS. Therefore, UCPI molecules were more cross-linked and aggregated with a larger particle size at UCPI-0.4.

4.4.4. Rheological properties

4.4.4.1 Temperature sweep

Fig 4.4 shows the elastic modulus (G') of CPI and UCPI dispersions as a function of temperature. The physical properties of protein products such as edible films, fibers, powders, scaffolds, and sponges are closely related to the rheological properties of protein solution. G' reflects the stiffness and compactness of the protein structure, so G' is often used to characterize protein's mechanical properties and intermolecular interaction. In the absence of EDC/NHS, G' of CPI-0 was relatively stable during the entire temperature circle (lower than 60 Pa), while G' of UCPI-0 increased to 118 Pa at the final cooling step. After ultrasound treatment, free radicals were created by the caviation phenomenon ($H_2O \rightarrow H + OH$), and such free radicals were highly oxidized reactive superoxide that induced polymerization (H. Park, Park, & Shalaby, 2011; Rokita, Rosiak, & Ulanski, 2009). Thus, the cross-linked UCPI exhibited higher G' than CPI.

At high EDC/NHS content such as 0.25 and 0.4 mmol/g, G' of all CPI and UCPI kept increasing during the entire temperature sweep. As temperature increased, G' increased obviously around 700s, indicating the onset of protein aggregation. Then, a mild increase region of G' was observed at the temperature holding stage, followed by a sharp increase at the cooling stage, which suggested the formation and stabilization of protein network. The final G' of CPI-0.4 was 1015 Pa higher than 548.9 Pa of 0.25-CPI, indicating the increased protein network at higher EDC/NHS. UCPI samples exhibited similar trends, and all their G' values were higher than the G' of CPI at the same EDC/NHS concentration.

4.4.4.2 Frequency sweep

The typical frequency sweep plots for EDC/NHS modified CPI and UCPI are shown in Figure 4.5. Chemical bonds between protein molecules may be disrupted during the increasing shearing force, which resulted in polymers' different rheological properties due to their individual bonding. For all CPI and UCPI samples, G' increased linearly at the frequency region from 0.1 to 10 rad/s, followed by a sharp increase, indicating the breakdown of protein network at high frequency (Tunick, 2011). In the absence of heating, the G' value of UCPI was lower than that of CPI due to the weakening intermolecular protein interaction caused by unfolding treatment.

The final G' values of EDC/NHS modified CPIs and UCPIs were: UCPI-0.4 > CPI-0.4 > UCPI-0.25 > CPI-0.25 > UCPI-0 > CPI-0. Thus, the frequency sweep further confirmed that ultrasound pre-treatment stimulated the crosslink effect of EDC/NHS, which resulted in stronger intermolecular protein interaction, higher compressive resistance, and increased the mechanical properties of CPIs and UCPIs.

4.4.4.3 Viscosity

Viscosity, an important rheological property, governs the flowing behaviors of protein dispersion. Apparent viscosities of EDC/NHS modified CPI and UCPI dispersions are shown in Figure 4.6. The viscosity of CPI and UCPI increased with the EDC/NHS content. For CPIs, it increased from 80 (CPI-0) to 115 (CPI-0.4) gradually. For UCPIs, viscosity was low at lower EDC/NHS (Figure 4.6); however, the viscosity of UCPI-0.25 increased to 80cp, and then a drastic increase at 0.4 mmol/g EDC/NHS concentration. Therefore, EDC/NHS modification increased the viscosity of camelina protein dispersion, and this effect was more obvious to UCPI than CPI.

4.4.5 Water resistance

4.4.5.1 Protein lost

In order to investigate the water resistance of modified CPIs and UCPIs, the protein loss of cured protein films were determined after water soaking (Figure 4.7). Proteins with compact structure and stronger crosslink were more water resistant, while protein's weak intermolecular interaction resulted in the higher amount of weight lost in water. The protein lost decreased with the increasing EDC/NHS content for both CPIs (from 20 to 13%) and UCPIs (from 17 to 6%). Moreover, less protein lost was observed for UCPIs than CPIs, suggesting that ultrasound induced unfolding promoted crosslink, and then lead to high water resistance. This result was in good agreement with our previous discussion.

4.4.5.2 Morphology

In Figure 4.8, the aggregated CPI and UCPI fractions were loosely connected to each other. However, by introducing the EDC/NHS, the crosslink effect made protein fractions dense, compact, and uniform. After water soaking, we observed porous structure of CPI-0, 0.1 (Figure 4.9). Due to the hydrophilic property of protein surface, water was dragged gradually into the core of protein matrix during water soaking and the protein molecules became swollen. After the water evaporation during lyophilization, porous network formed. As the EDC/NHS content increased, the structure of CPI was becoming more cross-linked and less water-permeated. Consequently, more intact protein structures were observed at higher EDC/NHS content (CPI-0.4). For UCPIs, the increased crosslink effect induced by ultrasound pretreatment was also observed in the SEM image. The porous protein network of UCPI-0, 0.1 were more condensed and cross-lined than CPI-0, 0.1.

The macroscopic image of soaked CPIs and UCPIs are shown (Figure 4.10). Generally, both CPIs and UCPIs modified at different EDC/NHS concentration exhibited corresponding morphology to SEM profile. Protein structure of non-crosslinked CPI and UCPI was destroyed into pieces, while increasing EDC/NHS content stabilized the structure of CPI and UCPI while keeping the protein film intact in the water.

4.5. Conclusion

EDC/NHS was effective in stabilizing the structure of camelina protein. The molecular weight and particle size of CPI increased due to the crosslink effect; thus, stronger intermolecular interaction, higher elastic modulus (G'), and apparent viscosity were observed.

EDC/NHS modification further increased CPI's water resistance by forming a compact and aggregated microstructure. Moreover, ultrasound pretreatment increased the crosslink effect by breaking CPI into small particles with increased free amino groups. Therefore, UCPI had better water resistance and mechanical properties than CPI. Overall, the EDC/NHS-induced crosslink reaction could be considered as a powerful method to increase the protein's elastic modulus and water resistance together with the ultrasound-induced unfolding pretreatment.

Lane 1-4: CPI-0, 0.1, 0.25, 0.4; Lane Figure 4-1 Non-reducing SDS-PAGE patterns of camelina protein fractions.
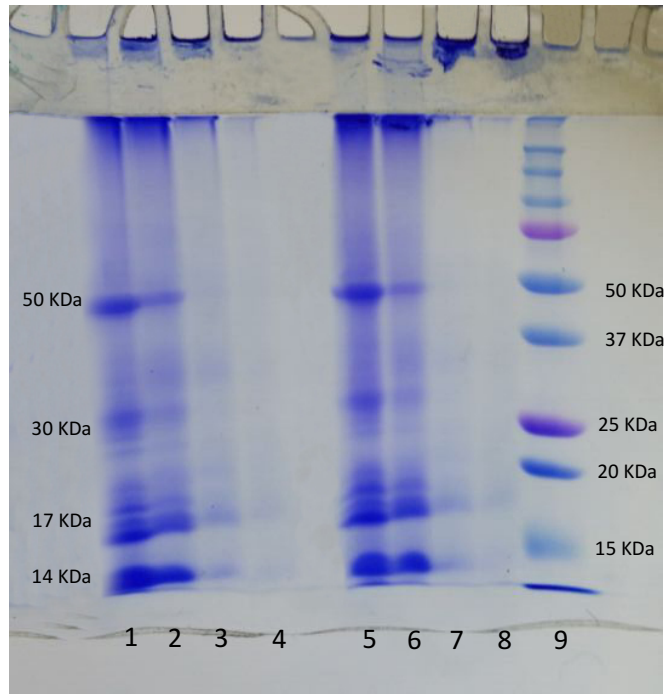
5-8: UCPI-0, 0.1, 0.25, 0.4; Lane 9: marker

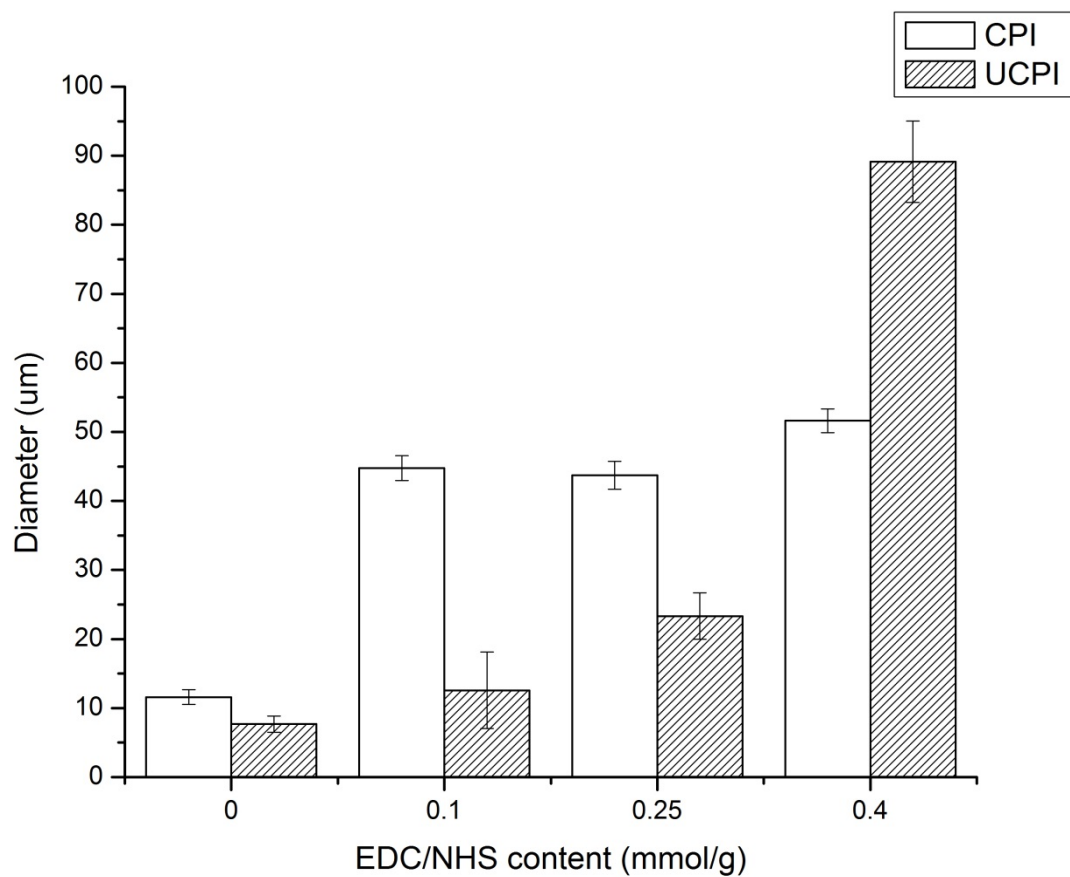**Figure 4-2 Particle size of CPI and UCPI dispersions**

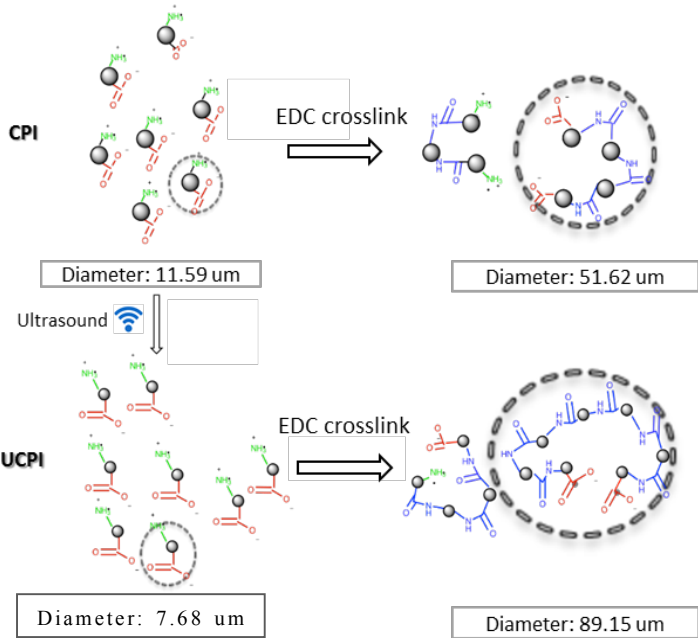**Figure 4-3 Shematic representation of the CPI crosslinking progress**

Figure 4-4 The effect of temperature on elastic modulus (G') of CPI and UCPI dispersions.
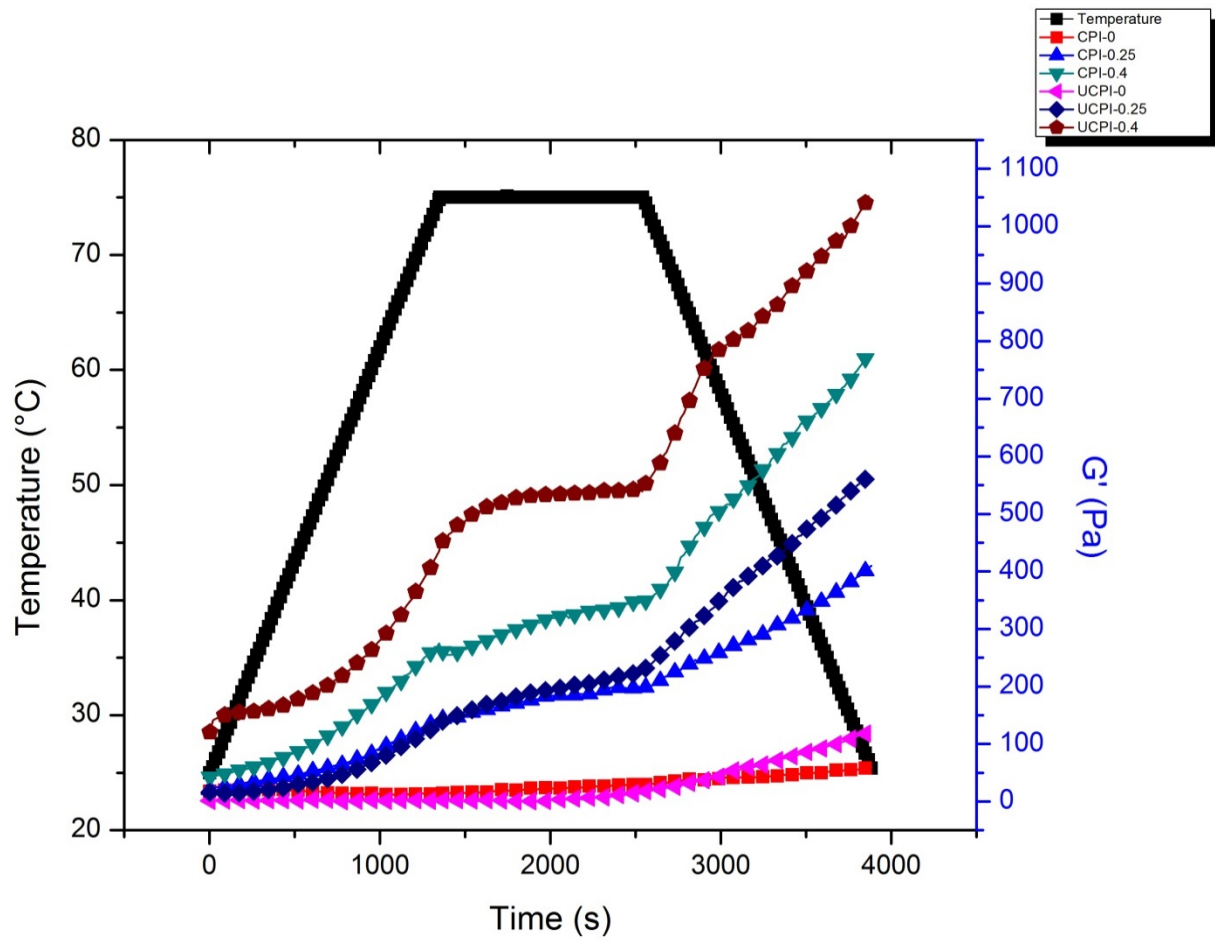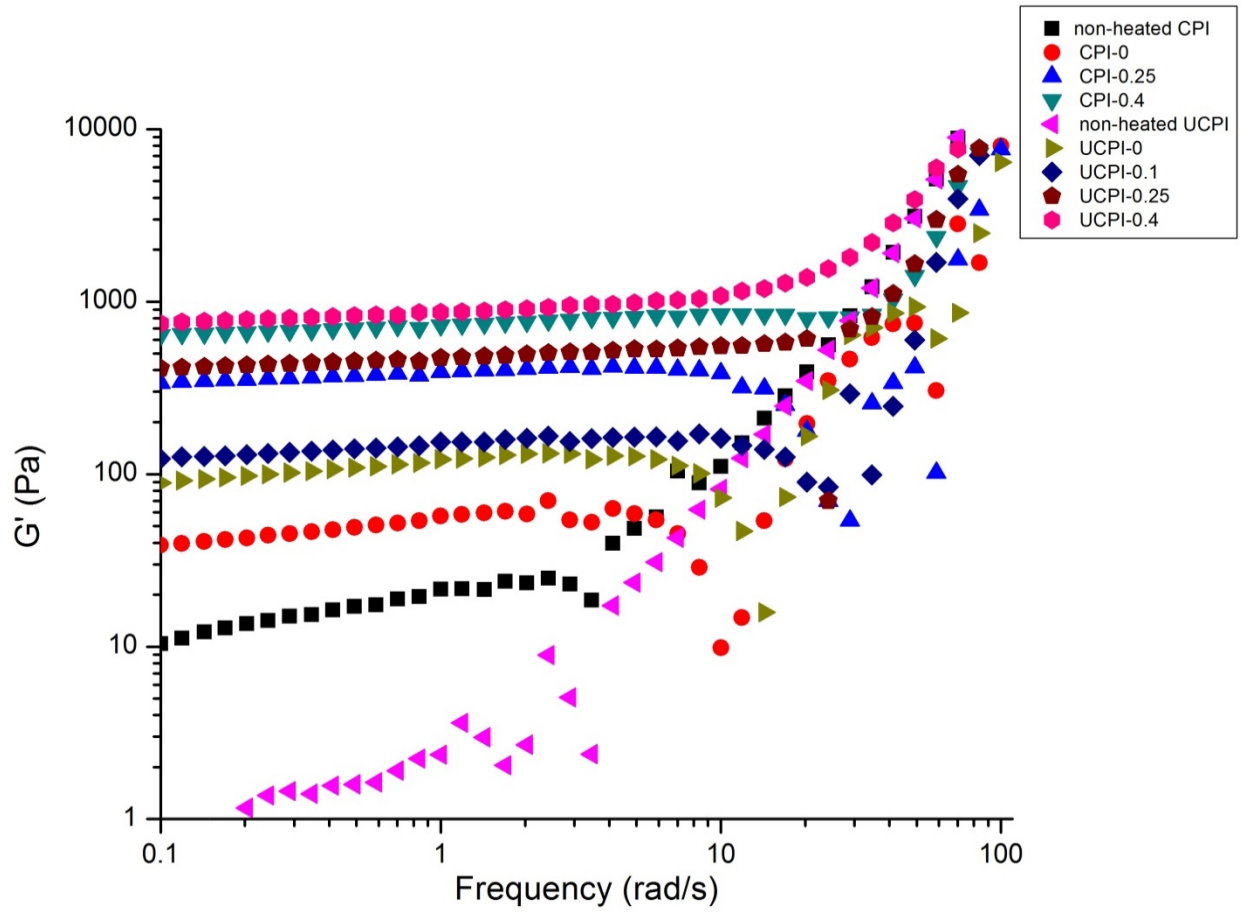
Figure 4-6 Apparent viscosity of CPI and UCPI dispersions
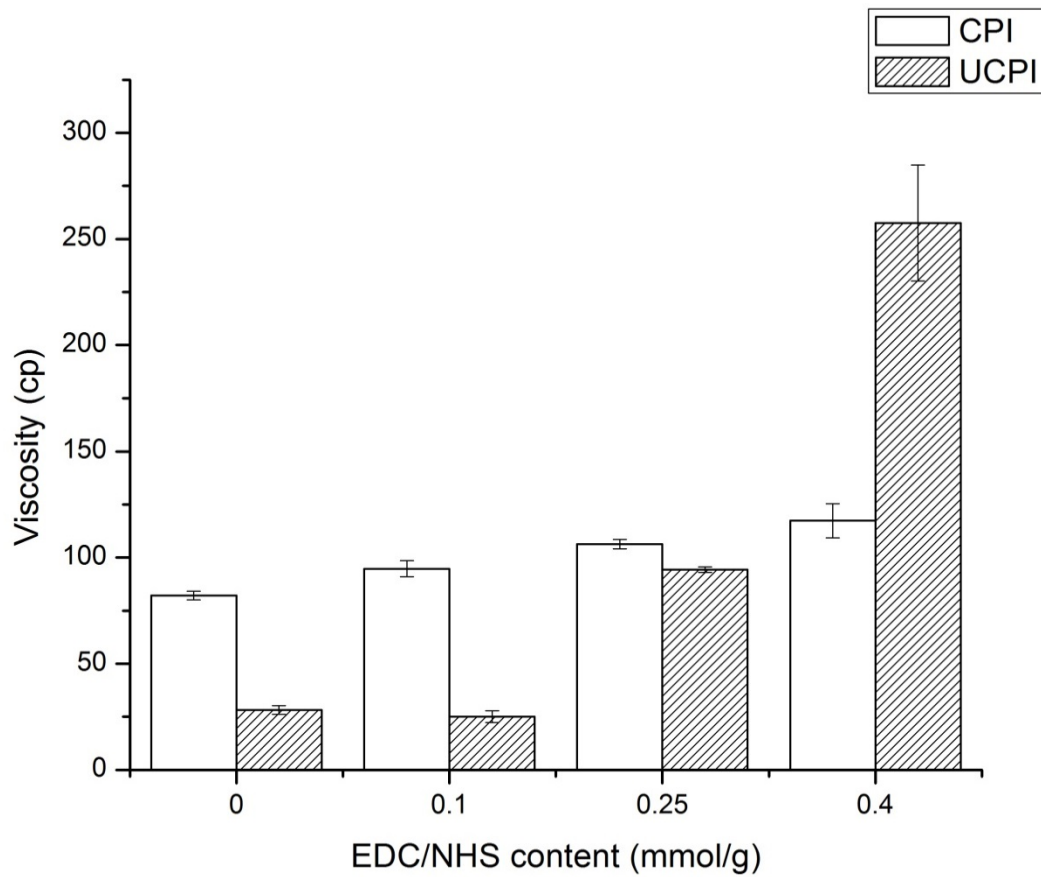
Figure 4-7 Weight loss of cured CPI and UCPI dispersions after water soaking

Figure 4-8 SEM image of cured CPI and UCPI dispersions. (A) CPI-0, (B) CPI-0.1, (C) CPI-0.25, (D) CPI-0.4; (E) UCPI-0, (F) UCPI-0.1, (G) UCPI-0.25, (H) UCPI-0.4

Figure 4-9 SEM image of cured CPI and UCPI dispersions after water soaking. (A) CPI-0, (B) CPI-0.1, (C) CPI-0.25, (D) CPI-0.4; (E) UCPI-0, (F) UCPI-0.1, (G) UCPI-0.25, (H) UCPI-0.4
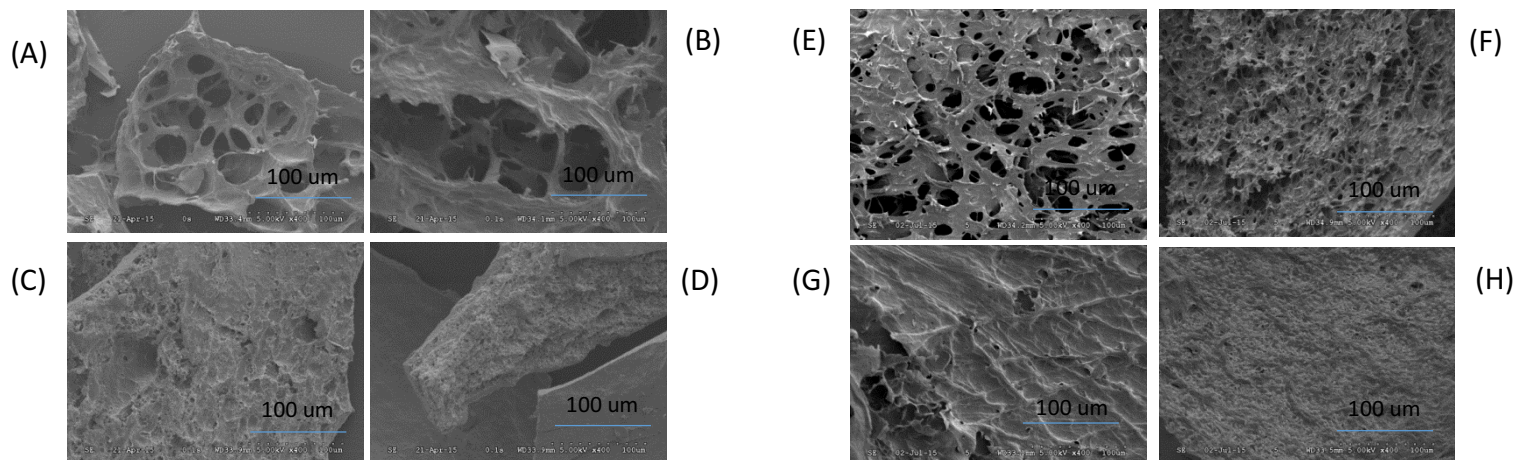
Figure 4-10 Macroscopic view of cured CPI and UCPI dispersions after water soaking

CPI-0

CPI-0.1

CPI-0.25

CPI-0.4

UCPI-0

UCPI-0.1

UCPI-0.25

UCPI-0.4

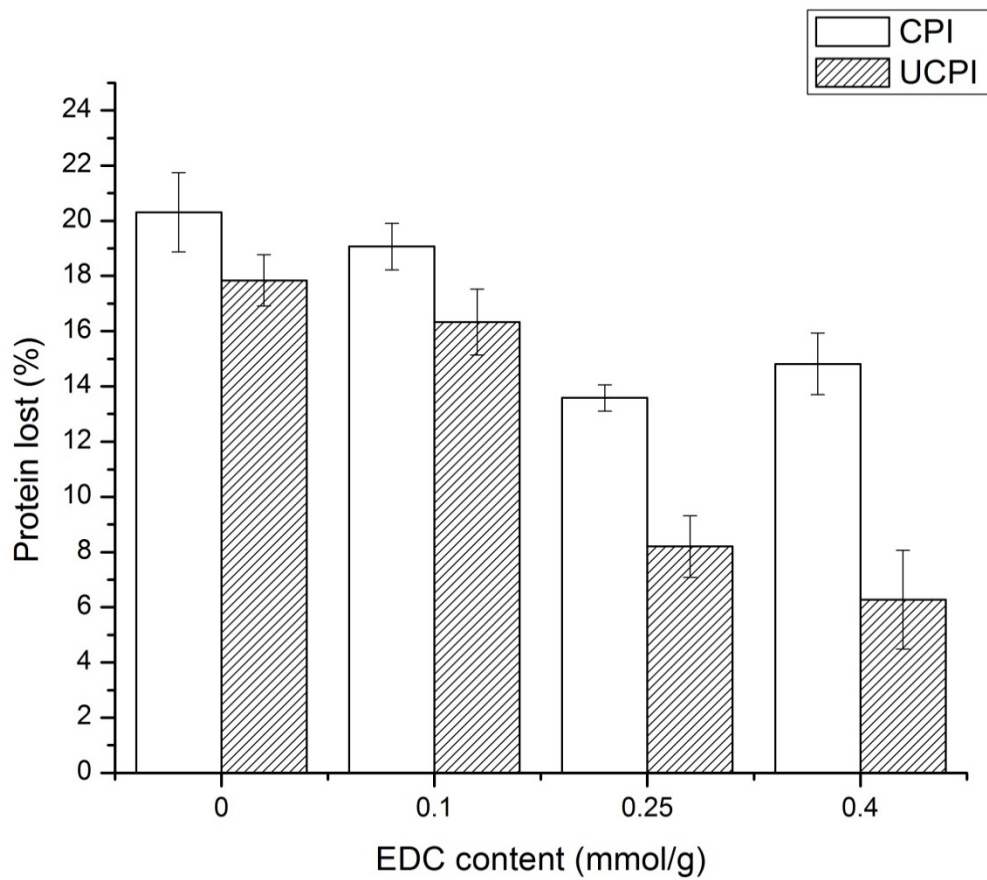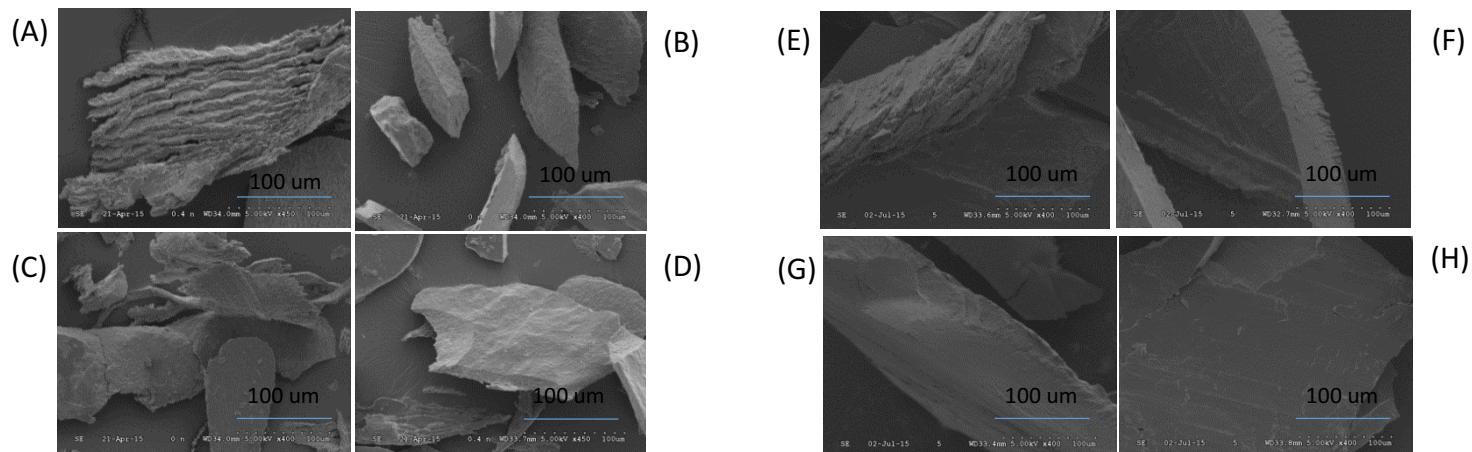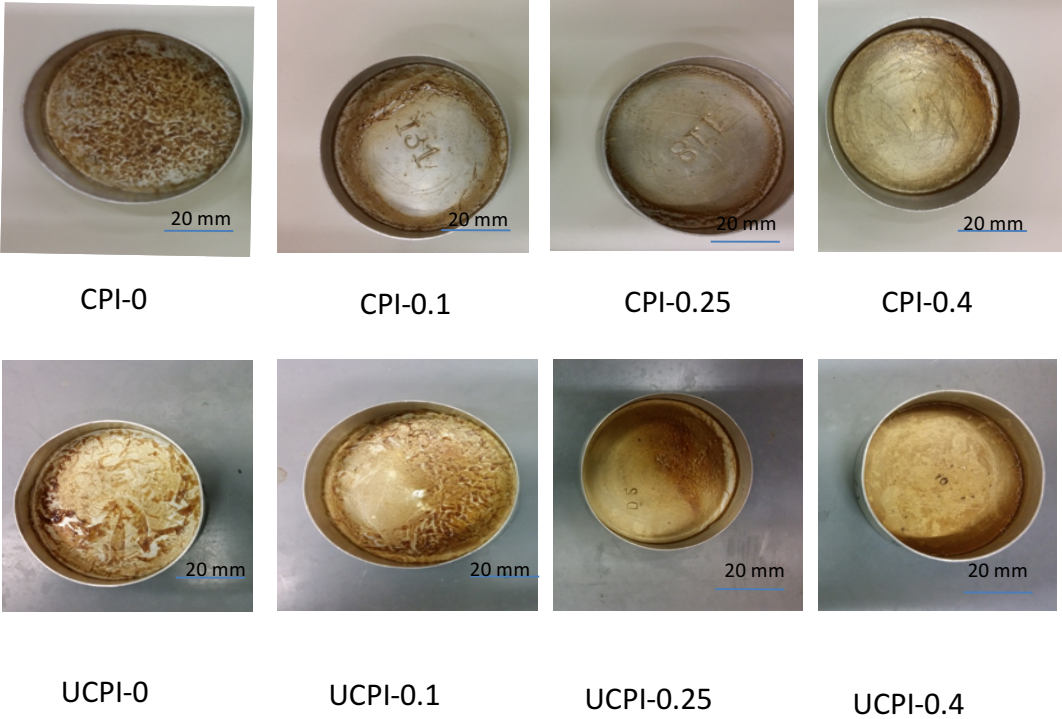**Table 4-1 Free amino group content and crosslink degree of CPIs and UCPIs modified by various EDC/NHS concentrations**

EDC content (mmol/g)	CPI		UCPI	
	Free amino acid content (mmol/ml)	Crosslink degree (%)	Free amino acid content (mmol/ml)	Crosslink degree (%)
[a]0	1.27±(0.01)	--	1.54±(0.03)	--
[b]0	1.94±(0.02)	0	1.89±(0.02)	0
[b]0.1	1.54±(0.02)	19.69	1.60±(0.05)	14.82
[b]0.25	1.30±(0.03)	32.44	1.21±(0.03)	35.68
[b]0.4	1.18±(0.05)	38.41	1.02±(0.01)	45.29

a: non-heated CPI and UCPI solution; b: heated EDC/NHS modified CPI and UCPI solution.

4.6 Reference

Barkay-Olami, H., & Zilberman, M. (2015). Novel porous soy protein-based blend structures for biomedical applications: Microstructure, mechanical, and physical properties. *Journal of Biomedical Materials Research Part B: Applied Biomaterials*. https://doi.org/10.1002/jbm.b.33459

Chen, L., Chen, J., Ren, J., & Zhao, M. (2011). Effects of ultrasound pretreatment on the enzymatic hydrolysis of soy protein isolates and on the emulsifying properties of hydrolysates. *Journal of Agricultural and Food Chemistry*, *59*(6), 2600–2609. https://doi.org/10.1021/jf103771x

Cheng, C., Sun, S., & Zhao, C. (2014). Progress in heparin and heparin-like/mimicking polymer-functionalized biomedical membranes. *J. Mater. Chem. B*, *2*, 7649–7672. https://doi.org/10.1039/C4TB01390E

Chien, K. B., Makridakis, E., & Shah, R. N. (2012). Three Dimensional Printing of Soy Protein Scaffolds for Tissue Regeneration. *Tissue Engineering Part C: Methods*. https://doi.org/10.1089/ten.TEC.2012.0383

Custódio, J., Broughton, J., & Cruz, H. (2009). A review of factors influencing the durability of structural bonded timber joints. *International Journal of Adhesion and Adhesives*. https://doi.org/10.1016/j.ijadhadh.2008.03.002

De Graaf, L. A., Harmsen, P. F. H., Vereijken, J. M., & Mönikes, M. (2001a). Requirements for non-food applications of pea proteins A Review. *Food / Nahrung*, *45*(6), 408–411. https://doi.org/10.1002/1521-3803(20011001)45:6<408::AID-FOOD408>3.0.CO;2-#

Feng, J., Xiong, Y. L., & Mikel, W. B. (2003). Textural Properties of Pork Frankfurters Containing Thermally/Enzymatically Modified Soy Proteins. *Journal of Food Science*, *68*(4), 1220–1224. https://doi.org/10.1111/j.1365-2621.2003.tb09628.x

González, A., Strumia, M. C., & Alvarez Igarzabal, C. I. (2011). Cross-linked soy protein as material for biodegradable films: Synthesis, characterization and biodegradation. *Journal of Food Engineering*, *106*(4), 331–338. https://doi.org/10.1016/j.jfoodeng.2011.05.030

Guo, H. X., & Shi, Y. P. (2009). A novel zein-based dry coating tablet design for zero-order release. *International Journal of Pharmaceutics*, *370*(1–2), 81–6. https://doi.org/10.1016/j.ijpharm.2008.11.026

Hariyadi, D. M., Hendradi, E., Purwanti, T., Fadil, F. D. G. P., & Ramadani, C. N. (2014). Effect of cross linking agent and polymer on the characteristics of ovalbumin loaded alginate microspheres. *International Journal of Pharmacy and Pharmaceutical Sciences*, *6*(4), 469–474.

Hou, J.-J., Guo, J., Wang, J.-M., He, X.-T., Yuan, Y., Yin, S.-W., & Yang, X.-Q. (2015). Edible double-network gels based on soy protein and sugar beet pectin with hierarchical microstructure. *Food Hydrocolloids*. https://doi.org/10.1016/j.foodhyd.2015.04.012

Hu, H., Fan, X., Zhou, Z., Xu, X., Fan, G., Wang, L., … Zhu, L. (2013). Acid-induced gelation behavior of soybean protein isolate with high intensity ultrasonic pre-treatments. *Ultrasonics Sonochemistry*, *20*(1), 187–195. https://doi.org/10.1016/j.ultsonch.2012.07.011

Hu, H., Li-Chan, E. C. Y., Wan, L., Tian, M., & Pan, S. (2013). The effect of high intensity ultrasonic pre-treatment on the properties of soybean protein isolate gel induced by calcium sulfate. *Food Hydrocolloids*, *32*(2), 303–311. https://doi.org/10.1016/j.foodhyd.2013.01.016

Karki, B., Lamsal, B., Grewell, D., Pometto III, A., van Leeuwen, J., Khanal, S., & Jung, S. (2009). Functional Properties of Soy Protein Isolates Produced from Ultrasonicated Defatted Soy Flakes. *Journal of the American Oil Chemists' Society*, *86*(10), 1021–1028. https://doi.org/10.1007/s11746-009-1433-0

Kasetaite, S., Ostrauskaite, J., Grazuleviciene, V., Svediene, J., & Bridziuviene, D. (2014). Camelina oil- and linseed oil-based polymers with bisphosphonate crosslinks. *Journal of Applied Polymer Science*, *131*(17). https://doi.org/10.1002/app.40683

Kim, S., Sessa, D. J., & Lawton, J. W. (2004). Characterization of zein modified with a mild cross-linking agent. *Industrial Crops and Products*, *20*, 291–300. https://doi.org/10.1016/j.indcrop.2003.10.013

LAEMMLI, U. K. (1970). Cleavage of Structural Proteins during the Assembly of the Head of Bacteriophage T4. *Nature*, *227*(5259), 680–685. Retrieved from http://dx.doi.org/10.1038/227680a0

Li, C., Huang, X., Peng, Q., Shan, Y., & Xue, F. (2014). Physicochemical properties of peanut protein isolate-glucomannan conjugates prepared by ultrasonic treatment. *Ultrasonics Sonochemistry*, *21*(5), 1722–7. https://doi.org/10.1016/j.ultsonch.2014.03.018

Li, N., Qi, G., Sun, X. S., Wang, D., Bean, S., & Blackwell, D. (2014). Isolation and Characterization of Protein Fractions Isolated from Camelina Meal. *Transactions of the*

ASABE, *57*(2010), 169–178. https://doi.org/10.13031/trans.57.10455

Li, N., Qi, G., Sun, X. S., Xu, F., & Wang, D. (2015). Adhesion properties of camelina protein fractions isolated with different methods. *Industrial Crops and Products*, *69*, 263–272. https://doi.org/10.1016/j.indcrop.2015.02.033

Matthäus, B., & Zubr, J. (2000). Variability of specific components in Camelina sativa oilseed cakes. *Industrial Crops and Products*, *12*(1), 9–18. https://doi.org/http://dx.doi.org/10.1016/S0926-6690(99)00040-0

Moore, S., Spackman, D. H., & Stein, W. H. (1958). Chromatography of Amino Acids on Sulfonated Polystyrene Resins. An Improved System. *Analytical Chemistry*, *30*(7), 1185–1190. https://doi.org/10.1021/ac60139a005

Nam, K., Kimura, T., & Kishida, A. (2008). Controlling coupling reaction of EDC and NHS for preparation of collagen gels using ethanol/water co-solvents. *Macromolecular Bioscience*, *8*, 32–37. https://doi.org/10.1002/mabi.200700206

Nguyen, H. T., Silva, J. E., Podicheti, R., Macrander, J., Yang, W., Nazarenus, T. J., … Cahoon, E. B. (2013). Camelina seed transcriptome: a tool for meal and oil improvement and translational research. *Plant Biotechnology Journal*, *11*(6), 759–69. https://doi.org/10.1111/pbi.12068

O'Donnell, C. P., Tiwari, B. K., Bourke, P., & Cullen, P. J. (2010). Effect of ultrasonic processing on food enzymes of industrial importance. *Trends in Food Science & Technology*, *21*(7), 358–367. https://doi.org/10.1016/j.tifs.2010.04.007

Park, H., Park, K., & Shalaby, W. S. W. (2011). Biodegradable hydrogels for drug delivery. *International Journal of Pharmaceutics*. CRC Press.

Park, S. N., Park, J. C., Kim, H. O., Song, M. J., & Suh, H. (2002). Characterization of porous collagen/hyaluronic acid scaffold modified by 1-ethyl-3-(3-dimethylaminopropyl)carbodiimide cross-linking. *Biomaterials*, *23*(4), 1205–1212. https://doi.org/10.1016/S0142-9612(01)00235-6

Peiretti, P. G., & Meineri, G. (2007). Fatty acids, chemical composition and organic matter digestibility of seeds and vegetative parts of false flax (Camelina sativa L.) after different lengths of growth. *Animal Feed Science and Technology*, *133*(3–4), 341–350. https://doi.org/10.1016/j.anifeedsci.2006.05.001

Puppo, C., Chapleau, N., Speroni, F., De Lamballerie-Anton, M., Michel, F., Añón, C., & Anton,

M. (2004). Physicochemical modifications of high-pressure-treated soybean protein isolates. *Journal of Agricultural and Food Chemistry*, *52*(6), 1564–71. https://doi.org/10.1021/jf034813t

Ren, X., & Soucek, M. (2014). Soya-Based Coatings and Adhesives. In *ACS Symposium Series* (pp. 207–254). https://doi.org/10.1021/bk-2014-1178.ch010

Renkema, J. M. S., Gruppen, H., & van Vliet, T. (2002). Influence of pH and ionic strength on heat-induced formation and rheological properties of soy protein gels in relation to denaturation and their protein compositions. *Journal of Agricultural and Food Chemistry*, *50*, 6064–6071. https://doi.org/10.1021/jf020061b

Renkema, J. M. S., & van Vliet, T. (2002). Heat-induced gel formation by soy proteins at neutral pH. *Journal of Agricultural and Food Chemistry*, *50*(6), 1569–73. Retrieved from http://www.ncbi.nlm.nih.gov/pubmed/11879038

Roesch, R. R., & Corredig, M. (2005). Heat-induced soy-whey proteins interactions: Formation of soluble and insoluble protein complexes. *Journal of Agricultural and Food Chemistry*, *53*, 3476–3482 ST–Heat–induced soy–whey proteins int. https://doi.org/10.1021/jf048870d

Rokita, B., Rosiak, J. M., & Ulanski, P. (2009). Ultrasound-induced cross-linking and formation of macroscopic covalent hydrogels in aqueous polymer and monomer solutions. *Macromolecules*, *42*(9), 3269–3274. https://doi.org/10.1021/ma802565p

Sarin, V. K., Kent, S. B. H., Tam, J. P., & Merrifield, R. B. (1981). Quantitative monitoring of solid-phase peptide synthesis by the ninhydrin reaction. *Analytical Biochemistry*, *117*(1), 147–157. https://doi.org/http://dx.doi.org/10.1016/0003-2697(81)90704-1

Shi, W., & Dumont, M.-J. (2014a). Processing and physical properties of canola protein isolate-based films. *Industrial Crops and Products*, *52*, 269–277. https://doi.org/10.1016/j.indcrop.2013.10.037

Shi, W., & Dumont, M.-J. (2014b). Review: bio-based films from zein, keratin, pea, and rapeseed protein feedstocks. *Journal of Materials Science*. https://doi.org/10.1007/s10853-013-7933-1

Song, F., Tang, D.-L., Wang, X.-L., & Wang, Y.-Z. (2011). Biodegradable soy protein isolate-based materials: a review. *Biomacromolecules*, *12*(10), 3369–80. https://doi.org/10.1021/bm200904x

Sun, X. S. (2011). Soy Protein Polymers and Adhesion Properties. *Journal of Biobased*

Materials and Bioenergy, *5*(4), 409–432. https://doi.org/10.1166/jbmb.2011.1183

Teng, Z., Luo, Y., & Wang, Q. (2012). Nanoparticles synthesized from soy protein: preparation, characterization, and application for nutraceutical encapsulation. *Journal of Agricultural and Food Chemistry*, *60*(10), 2712–20. https://doi.org/10.1021/jf205238x

Tunick, M. H. (2011). Small-strain dynamic rheology of food protein networks. *Journal of Agricultural and Food Chemistry*, *59*(5), 1481–6. https://doi.org/10.1021/jf1016237

Usha, R., Sreeram, K. J., & Rajaram, a. (2012). Stabilization of collagen with EDC/NHS in the presence of l-lysine: A comprehensive study. *Colloids and Surfaces B: Biointerfaces*, *90*(1), 83–90. https://doi.org/10.1016/j.colsurfb.2011.10.002

van Vliet, T., Martin, A. H., & Bos, M. A. (2002). Gelation and interfacial behaviour of vegetable proteins. *Current Opinion in Colloid & Interface Science*, *7*, 462–468. https://doi.org/10.1016/s1359-0294(02)00078-x

Wang, C., Wu, J., & Bernard, G. M. (2014). Preparation and characterization of canola protein isolate–poly(glycidyl methacrylate) conjugates: A bio-based adhesive. *Industrial Crops and Products*, *57*, 124–131. https://doi.org/10.1016/j.indcrop.2014.03.024

Wang, Y., Mo, X., Sun, X. S., & Wang, D. (2007). Soy Protein Adhesion Enhanced by Glutaraldehyde Crosslink. *Journal ofApplied Polymer Science*, *104*, 130–136. https://doi.org/10.1002/app

Xue, F., Li, C., Zhu, X., Wang, L., & Pan, S. (2013). Comparative studies on the physicochemical properties of soy protein isolate-maltodextrin and soy protein isolate-gum acacia conjugate prepared through Maillard reaction. *Food Research International*, *51*(2), 490–495. https://doi.org/10.1016/j.foodres.2013.01.012

Yang, M., Liu, F., & Tang, C. H. (2013). Properties and microstructure of transglutaminase-set soy protein-stabilized emulsion gels. *Food Research International*, *52*(1), 409–418. https://doi.org/10.1016/j.foodres.2011.11.012

Zhang, J., Jiang, L., Zhu, L., Jane, J.-L., & Mungara, P. (2006). Morphology and properties of soy protein and polylactide blends. *Biomacromolecules*, *7*(5), 1551–61. https://doi.org/10.1021/bm050888p

Zhao, Y., Jiang, Q., Xu, H., Reddy, N., Xu, L., & Yang, Y. (2014). Cytocompatible and water-stable camelina protein films for tissue engineering. *Journal of Biomedical Materials Research. Part B, Applied Biomaterials*, *102*(4), 729–36.

https://doi.org/10.1002/jbm.b.33053

Zhu, X., Wang, D., & Sun, X. S. (2016). Physico-chemical properties of camelina protein altered by sodium bisulfite and guanidine-HCl. *Industrial Crops and Products*, *83*, 453–461. https://doi.org/10.1016/j.indcrop.2015.12.085

Chapter 5 - A Bio-Based Wood Adhesive from Camelina Protein (a Biodiesel Residue) and De-Polymerized Lignin with Improved Water Resistance

5.1 ABSTRACT

The aim of this study was to improve water resistance of camelina protein (CP) for wood adhesives with de-polymerized lignin. Kraft lignin was de-polymerized by H_2O_2-induced oxidation in the presence of ultrasound irradiation to reduce lignin's particle size, thermal stability, and increased the hydroxyl group. Coupled with de-polymerized lignin, camelina protein exhibited increased hydrophobicity. Fluorescence spectroscopy analysis revealed that the oxidation treatment of lignin further stimulated the hydrophobization effect of the protein-lignin copolymer due to the increased reactivity of depolymerized lignin to camelina protein. Accordingly, the water resistance of CP-lignin adhesives was significantly improved. When copolymerized with ultrasound-induced oxidized lignin, the camelina protein had increased wet shear adhesion strength from 0.28 MPa to 1.43 MPa, with wood panels passing the three-cycle water soaking test. The CP resin, with depolymerized lignin as an economical, green, and bio-based hydrophobic enhancer, provided an alternative to the petroleum-based and other edible protein-based adhesive such as soy protein.

5.2 INTRODUCTION

Plant proteins, such as soybean protein, have been modified and commercially available for biobased adhesive and coatings. However, soybean proteins are also important human diets worldwide; therefore, the competition between the food and non-food uses of edible proteins urged us to find other alternative nonedible protein sources. Camelina is an easy-growing oilseed crop on dry land; in the past few decades, it has drawn increasing attention due to its abundance in polyunsaturated fatty acids, which were known for the aviation fuels and health benefits. Accordingly, the ever-accumulating interests for camelina oil is generating increasing desired amounts of camelina meal (CM) that contains 40% crude protein. However, some potential antinutritional toxic compounds in camelina restricted the food uses of the protein extracted from CM. Therefore, camelina protein (CP) becomes a suitable non-edible protein sources for bio-based products, such as adhesives.

Plant proteins had similar amino acids profiles; however, they have different amino acids sequences that make the protein different from each other. Therefore, the modification method good for soybean protein does not necessarily suitable for camelina protein. As a relatively new protein sources, there are only limited studies on the modification and application of CP. We previously elucidated the unfolding behaviors of CP by disrupting hydrogen bond and disulfide bonds.(Zhu et al., 2016) By utilizing the cysteine-induced denaturation, Zhao et al(Zhao et al., 2014) developed the CP-based film with improved physicochemical properties for cell culture. Reddy et al(Reddy et al., 2012) grafted camelina with vinyl monomers to modify the thermoplastic properties. However, similar to other plant protein polymers, there are two major concerns regarding to CP's adhesive application: 1) low mechanical strength, which is due to the weak protein-protein interaction and 2) poor water resistance caused by protein's hydrophilic nature. In order to resolve these problems, scientists usually applied classic protein modification techniques such as unfolding, crosslink, and side group grafting to increase the protein's hydrophobicity, crosslink degree, and reactivity.(X. S. Sun, 2011) Regarding to plant protein-based wood adhesives such as soy, adding proper hydrophobic additives seems to be most effective and convenient to increase the adhesion properties of the cured protein resins, especially in the aqueous conditions.(H. Liu et al., 2015; Ren & Soucek, 2014) Those hydrophobic materials such as polyvinyl acetate,(Guangyan Qi & Sun, 2010a) polyamidoamine-

epichlorohydrin,(Gui, Wang, Wu, Zhu, & Liu, 2013) and polyurethane,(D. Liu, Tian, Zhang, & Chang, 2008; Zheng, Zhang, & Cheng, 2013) would stabilize the protein structure during the curing progress, and contribute to the water resistance of adhesives. Besides the previously mentioned chemicals, to date, there are growing interests in developing bio-based hydrophobic enhancers for polymer fabrication. Lignin, a most abundant and underutilized biopolymer, exhibited its potential in improving the mechanical and thermal and hydrophobic properties. From the chemist's point of view, lignin's abundant aromatic structures, phenolic hydroxyls, and tough structures should be appropriate copolymers to modify protein's hydrophobicity, reactivity, and mechanical properties.

In spite of the appealing performance, lignin's inert nature limits its reactivity and solubility and hinders its further applications; thus, functionalization treatment is necessary. De-polymerization techniques, including pyrolysis, oxidation, enzymatic and ionic liquids treatment, are effective to break down lignin's heterogeneous structures, release the functional groups, and increase the reactivity.(Aracri, Díaz Blanco, & Tzanov, 2014; Mancera et al., 2010; Xu et al., 2014) Oxidative de-polymerization of lignin at mild and solvent –free reaction conditions should be considered because of eco-friendly and practicality. Hydrogen peroxide (H_2O_2) was widely used to induce such de-polymerization. Tortora et al utilized H_2O_2-oxidation to prepare lignin-based microcapsules for drug delivery while many others used this approach to prepare soluble lignin fragment with reactive moiety.(Crestini, Pro, Neri, & Saladino, 2005; Wi et al., 2015; Xu et al., 2014) For a higher oxidation efficiency of H_2O_2, ultrasound (US) technique, a green and efficient means, was utilized to increase free radicals that accelerated the oxidation.(Napoly et al., 2015) In addition, the cavitation force generated by US could also fragment lignin substrates into nano-particles.(Gilca, Popa, & Crestini, 2015)

In recent years, development of lignin-based biopolymer became attractive. However, to the best of our knowledge, little is known about the interaction between plant proteins and depolymerized lignin. Therefore, we speculate that H_2O_2-induced de-polymerization to lignin stimulates its reactivity and miscibility with plant protein and thus increases the water resistance of protein-based wood adhesives.

Our aim was to develop an eco-friendly wood adhesive from the low-value nonedible camelina proteins and improve its water resistance by copolymerizing it with functionalized

lignin. Lignin was depolymerized by (ultrasound-assisted) H_2O_2 oxidation. The modified lignin was analyzed by Dynamic Light Scattering (DLS), Transmission electron microscopy (TEM), (Fourier transform infrared spectroscopy) FTIR, and (Thermogravimetric analysis) TGA to exam the de-polymerization effect. After copolymerization, the resultant adhesives were characterized for the hydrophobicity, rheological properties, and wood adhesion strength. Once optimized, this approach provides a green and facile way to stimulate lignin and protein interaction and adds marketable values to camelina meals and lignin.

5.3 MATERIALS AND METHODS

5.3.1 Materials

Defatted camelina meal (DCM) with 32.4% crude protein (db), and 11% moisture content (db) was provided by Field Brothers Inc. (Pendroy, MT, US). Lignin (alkali), Poly (ethylene glycol) diglycidyl ether (PEGDE Mn 500), hydrochloric acid (HCl), and sodium hydroxide (NaOH) were purchased from Sigma-Aldrich (St. Louis, MO, USA). Hydrogen peroxide was purchased from Fisher Scientific (Fair Lawn, NJ, USA). Yellow pine wood veneers with dimensions of 305.50 mm × 305.50 mm × 3.26 mm (width × length × thickness) were provided by Veneer One (Oceanside, NY).

5.3.2 Isolation of camelina protein

CPI was separated from DCM using the method described by Li et al, with some modifications.(N Li et al., 2014) The specific).

5.3.3 Lignin de-polymerization

To prepare the oxidized lignin (OL) solution, 2 g lignin substrate was dispersed into 100 mL distilled water, with pH adjusting to 10.5 by NaOH solution (3M) and gently stirring for 30 min. Then, 1 mL hydrogen peroxide was added. After conditioned for 10 min, the solution was heated at 50 °C for 16 h to induce the oxidation reaction. To prepare the ultrasound-induced oxidized lignin (UL) solution, an ultrasound processor model VCF 1500 (SONICS & MATERIALS INC, Newtown, CT, USA) was used to sonicate the lignin dispersion instead of heating treatment to induce the oxidation. Sample solutions were treated at 20 kHz, 480W for 60 min (pulse duration of on-time 5 sec and off-time 5 sec). The resultant OL solution and UL solution had a pH at 7.2,

and they were further used for the adhesive preparation and particle size characterization. Their lyophilized samples were used for IR and TGA test.

5.3.4 Characterization of de-polymerized lignin

5.3.4.1Particle Size

The particle size of lignin was characterized both in Dynamic Light Scattering (DLS) and TEM (transmission electron microscope). Native lignin, OL, and UL solution (2% w/v) were prepared to measure their volume distribution and volume-mean diameters by DLS (Horiba Laser Scattering Particle Size Distribution Analyzer LA-910). A Philips CM 100 (FEI Company, Hillsboro, OR) TEM was used to study the microstructure of native lignin, OL, and UL. All samples were diluted to 0.2% with deionized water and absorbed onto Formvar/carbon-coated 200-mesh copper grids (Electron Microscopy Science, Fort Washington, PA). Morphology properties of each sample were recorded while the TEM was operating at an accelerating voltage of 100 kV.

5.3.4.2 FTIR and Thermogravimetric analysis (TGA)

FTIR spectra of native lignin, OL and UL samples were acquired with a PerkinElmer Spectrum 400 FT-IR/FT-NIR Spectrometer (Waltham, MA) over the 4000–400 cm^{-1} region at a resolution of 4 cm^{-1}. The TGA (PerkinElmer, Norwalk, CT) test was also carried out in a nitrogen-rich environment, which provided an inert atmosphere during pyrolysis. The samples were heated from 50 to 700 °C at a heating rate of 20 °C /min.

5.3.4.3 Preparation of CP-lignin based adhesives

CP powder (1:10 w/v) was dissolved in DI, lignin solution, OL solution, and UL solution respectively, and gently stirred for 1h at pH 7.2. Then PEGDE was added at 2% v/v (percent was based on the content of DI water), and the resultant dispersion was heated at 85 °C for 30 min to stimulate the copolymerization. After cooling to room temperature, the adhesive was used for wood test and also lyophilized for the fluorescence test. In summary, five different formulations for CP-based adhesives were shown in Table 5.1 (percent lignin was based on the dry weight of CP).

5.3.5 Surface hydrophobicity

Surface hydrophobicity was measured using the 1-anilino-8-naphthalenesulfonate (ANS) as the fluorescence probe as previously reported with modification.(Zhu et al., 2016) P-CP, P-CPL, P-CPOL, and P-CPUL dispersions (see Table 1 for sample description) were prepared in phosphate buffer solution (0.2 M, pH 7.5) at 2mg/ml. After centrifuging to remove any insoluble matters, 60 ul ANS solution (8.0 mM in 0.1 M phosphate buffer, pH 7.4) was added to 3 ml sample solution. Sample solutions were excited at 365 nm, and the relative fluorescence intensity (RFI) of emission spectra was recorded from 400 nm to 600 nm using a Hitachi F-7000 fluorescence spectrophotometer (Hitachi, Ltd., Tokyo, Japan) with a slit width of 10 nm.

5.3.6 Rheological properties

A Bohlin CVOR 150 rheometer (Malvern Instruments, Southborough, MA) was used to characterize viscoelastic properties of adhesives. A parallel plate head was used with 20- mm plate diameter and a 500-um gap. A thin layer of silicon oil was spread over the circumference of the sample to prevent sample dehydration during testing. All experiments were performed in triplicate at 1% strain (within its linear viscoelastic region). The dynamic viscosity measurements were tested in the shear rate range of 0.5–50 s^{-1}. Frequency sweep analyses were performed for a frequency range of 0.1 rad s^{-1} to 100 rad s^{-1}. The testing temperature was 23 °C.

5.3.7 Preparation of three layer wood

The $300 \times 300 \times 3.5$mm dimension yellow pine were preconditioned in a 27 °C, 30% RH chamber at least one week before wood adhesion test. The three veneers were layered up in a way that grain line of the middle panel was perpendicular to the grain lines up in a way that grain of the top and bottom panels. Around 20-22g/ft^2 wet basis) adhesives were brushed on the two faces of the middle veneer panel only. The assembled wood specimen was standing for 15 min before hot press. The hot press conditions were 150 °C, 10min at 1.03 MPa. The bonded three layer wood specimens were conditioned in a chamber at 23 C and 50% RH for two days. Then, they were cut into small 10 pieces (82.6×25.6 mm) and 4 large pieces with dimension of 50×127 mm for three-cycle water soaking test.

5.3.8 Shear strength measurement and water resistance

Five small wood specimens were soaked in water for 24 h at 23 °C to test the wet adhesion strength, while five specimens were used for dry adhesion strength. Both dry strength and wet strength were tested with an Instron Tester (Model 4465, Canton, MA) according to ASTM Standard Method D906-98("ASTM Standard Method D906-98," n.d.) at a crosshead speed of 1.6 mm/min. Adhesion strength was recorded as stress at the maximum load. Four large wood panels were used for three-cycle water soaking test. In each cycle, the wood specimen were soaked at 23 °C for 4h and then dry at 50 °C with well air circulation for 19 h. After drying, the wood specimen was scored according to the delamination length. The score was rated from zero to ten (zero means no delamination, five means delamination within 2 inch, and ten means completely veneer separation. Any individual value higher than 5 was considered as failed.

5.4 Results and discussion

5.4.1 Chemical reaction pathways

The proposed chemical reaction pathways of lignin and protein were presented in Schemes I, II, and III. Scheme I illustrated the oxidation reaction of kraft lignin in the presence of H_2O_2. This reaction would increase the lignin's surface area and -OH groups, and reduce particle size. Scheme II) described reinforced intermolecular interaction between camelina protein and depolymerized lignin. Initially, the pristine lignin exhibited low reactivity and miscibility with camelina protein due to its hydrophobic nature. It is hypothesized that after the oxidation treatment, the reduced particle size and increased functional group of depolymerized lignin would stimulate its conjugation with camelina protein in the presence of PEGDE; then, the stabilized copolymer would obtain increased cohesion and hydrophobicity, which further enhances its adhesion strength especially at the wet condition. Scheme III presents the interaction between the wood and copolymer adhesives. The newly-appeared -OH groups at the surface of oxidized-lignin molecules would react with the functional group (mostly –OH and -COOH) at wood surface, which contributes to the interfacial adhesion strength between the wood and adhesives. In brief, the camelina protein and oxidized lignin copolymer is expected to increase hydrophobicity and enhance cohesion and interfacial adhesion strength; consequently, the water resistance of its adhesive would be improved.

5.4.2 Particle size and morphology

Particle size is an important parameter to reveal the effect of de-polymerization on lignin, which further influences lignin's reactivity and compatibility with proteins. The effect of oxidation treatments on volume-mean diameter (D_{43}) of lignin and their distribution profiles were shown in Figure 5.1. The heat-induced oxidation reaction reduced the particle size (D_{43}) of lignin significantly from 26 um to 3.90 μm, and further reduced to 2.59 μm with ultrasound treatment. Three major possible reactions pathways (Scheme I)(Gidh, Talreja, Vinzant, Williford, & Mikell, 2006; Soria, McDonald, & Shook, 2008; Y.-G. Sun et al., 2015) have been proposed about the fragmentation effect on lignin structures by H_2O_2-induced oxidation. By de-alkylation, the C-C and C-O bonds of lignin were first cleaved. Then hydroxylation and oxidation reaction further increased the amphipathic property of lignin by introducing hydroxyl groups. As a consequent, the depolymerized lignin obtained reduced the particle size of the depolymerized lignin was reduced and thus increased reactivity. Ultrasound treatment led to further particle fragmentation through a physical "cavitation" phenomenon. Locally high pressure and temperature generated free radicals with high energy in the solution, and thus lignin decomposed. Napoly et al also reported and explained the cavitation mechanism of ultrasound-driven particle size reduction of kraft lignin.(Napoly et al., 2015)

To obtain more morphological details of the depolymerized lignin particles, TEM were used to observe the microstructure of OL and UL in comparison with the native lignin. In consensus with the particle size distribution profiles, native lignin turned into smaller particles (OL and UL) after oxidation reaction (Figure 5.2). Native lignin was a big chunk-like particle with no porous or fibrous structures, which was due to lignin's highly cross-linked structures. Unlike the other biopolymers, such as proteins or gums, whose structures are highly dependent on intermolecular non-covalent bonds,(X. S. Sun, 2011) lignin's phenyl rings are covalently bonded by C-C or C-O. Lignin's condensed structure results in the limited surface area and chemically inert nature. After oxidative de-polymerization, the lignin particle was fragmented into small pieces like a shattered rock. The average dimension of the newly formed OL was about 2 μm, which was in consistent to DLS results. When applying the ultrasound to induce the oxidation reaction, in addition to the H_2O_2-induced de-alkylation effect, the cavitation force further reduced the particle size of lignin by disrupting its intermolecular hydrogen bond, and thus UL exhibited more fragmented morphology than OL.

5.4.3 FTIR

FTIR analysis was used to qualitatively examine the changes for lignin's functional groups. In Figure 5.3 (a), a broad peak was observed ranging from 3050-3500 cm^{-1}, which was assigned to the stretching vibration of hydroxyl group (both aromatic and aliphatic hydroxyl group) for both pristine and modified lignin, and this peak for OL and UL was stronger respectively than the native lignin. This was due to the increased hydroxyl groups generated by de-alkylation and hydroxylation. There are also two peaks at 2864cm^{-1} and 2937 cm^{-1}, assigned to the methoxyl group linked with C-H band. Thus, the band intensity slightly decreased for OL and UL at 2864 cm^{-1} indicating the removal of methoxyls from lignin's aromatic ring. In addition, band around 1700 cm^{-1} was assigned to native lignin's C=O stretching of acetyl group; however, it significantly reduced for both OL and UL (Figure 5.3 (a)). This C=O group consumption may be due to the re-polymerization effect of lignin fragments by H_2O_2-induced oxidation. Such phenomenon was also reported by other studies on lignin's oxidative de-polymerization.(Gilca et al., 2015; Y. Liu et al., 2014)

In Figure 5.3 (b), more distinct difference in band shapes can be observed in the fingerprint region. The band intensities increased for OL and UL at 1590 cm^{-1} and 1510, which denoted the C=C stretching of the aromatic ring. Bands at 1260 cm^{-1} and 1330 cm-1 are the C-O stretch in lignin for guaiacyl groups and syringyl groups respectively. For OL and UL, the band intensity at 1268 cm^{-1} decreased significantly, while they were relatively stable at 1215 cm^{-1}. This result indicates that H_2O_2-induced oxidation had more obvious effects on decomposing guiacyl structures than on syringyl moiety.(Kardos, Jean-ge, Goux-henry, Andrioletti, & Draye, 2015; Tortora et al., 2014) Thus, by examining the IR spectra, we observed lignin's three oxidation pathways in the presence of H_2O_2: hydroxylation, de-alkylation, and oxidative coupling (Scheme I).

5.4.4 Thermogravimetric analysis (TGA)

Derivative thermogravimetry (DTG) curves of native lignin, OL and UL were shown in Figure 5.4. Native lignin exhibited one big thermal derivated weight loss peak ranging from 250 °C to 500 °C, whose maximum degradation rate was at 385 °C. Interestingly, after the oxidation and ultrasound treatment, besides the peak at 385 °C, there was a new peak for the DTG curves of OL and UL at about 310 °C. These differences can be explained by the varied stability of lignin

chemical bonds. There are three major chemical bonds for lignin's complex structures: lateral chain, C-C bonds, and aromatic rings. Due to their different chemical stability, they exhibited different decomposition temperatures: the laternal chain decomposed at around 245 °C, C-C bond decomposed at around 310 °C, and the aromatic ring with most stability decomposed from 350 to 410 °C.(Savy & Piccolo, 2014) Thus, the broad peak of native lignin's DTG curve was the mixture of these three bonds decomposition. For OL and UL, the newly appeared peak at 310 °C was assigned to the C-C bond degradation, and we can still find the aromatic ring degradation peak at about 385 °C. As the oxidation and ultrasound broke down and unfold the rigid structure for OL and UL, and thus, their C-C bond became more exposed than the native lignin for the heat decomposition.

5.4.5 Fluorescence

The hydrophobicity of CP-lignin was evaluated by detecting the ANS binding capacity. Lignin, with large amount of aromatic groups, contributed to CP's hydrophobicity, which can be determined by the fluorescence intensity (FI) in the presence of ANS(Zhu et al., 2016). As expected, all the CP-lignin copolymers exhibited increased FI than the P-CP (Figure 5.5). In addition, the FI of depolymerized lignin-based copolymer (P-CPOL, P-CPUL) was higher than the P-CPL, suggesting that the de-polymerized lignin was more crosslinked with CP than the native lignin. As previously discussed, lignin was functionalized by the oxidation reaction with increased reactivity and decreased particle size, which facilitated the protein-lignin interaction. Compared to heat-induced oxidation, ultrasound treatment stimulated the de-polymerization effect by further reducing lignin's particle size (Section 3.2). Accordingly, highest FI was obtained by P-CPUL.

5.4.6 Rheological properties

5.4.6.1 Frequency sweep

Figure 5.6 (a) shows the storage modulus (G') for different CP-lignin copolymers as a function of frequency sweep. For all the CP-lignin dispersions, G' increased linearly at a frequency region ranging from 0.1-3 PaS, followed by a sharp increase, and this sharp frequency increase is defined as critical frequency (f_c). Polymer structure became broken at f_c.(Zhu et al., 2016) Due to different degree of protein-lignin polymerization, their G' exhibited different frequency dependence, and thus different f_c. Polymers with strong intermolecular interaction

exhibited less frequency dependent and high f_c frequency than the one with weak interaction.(Tunick, 2011) In order to better describe the protein polymer's G' variation, in Table 5.2, we recorded the f_c and the G' modulus at f_c (M_{fc}).

CP exhibited weakest protein interaction, whose structure was broken at 1.00 PaS with G' of 5.52 Pa. After the addition of PEGDE, the structure of CP was stabilized, and the f_c of P-CP increased to 2.03 PaS. However, the f_c for P-CPL decreased to 1.19 PaS, indicating that the lignin incorporation destabilized P-CP's network. As a highly crosslinked macromolecule, lignin's small surface-volume ratio leading to its inert nature and low reactivity with bio-macromolecules. Only a small amount of lignin would be copolymerized with CP, and most unreacted lignin particles would weaken the protein polymerization due to the steric hindrance effect. This weakening effect did not appear for P-CPOL and P-CPUL, whose f_c was 2.42 and 3.46 PaS, respectively, and the M_{fc} for P-CPUL is 29.0 Pa higher than 22.1 Pa of P-CPOL. Thus, the increased functionality and surface-volume ratio of de-polymerized lignin (OL and UL) induced their stronger interaction with camelina protein than the native lignin. This effect also contributed to the adhesion properties of protein-lignin dispersions.

5.4.6.2 Dynamic viscoelastic measurement

Viscosity is an important physical property that influences the flowing behavior of wood adhesives. For all CP-lignin dispersions, their apparent viscosity decreased as the shear rate increased (In Figure 5.6b), which suggested the shear thinning behaviors of camelina protein and the CP-lignin copolymer. The unmodified CP exhibited a maximum viscosity at 16.00 PaS. In the presence of PEGDE, P-CP exhibited increased viscosity due to its reduced aqueous mobility. With the copolymerization of lignin (OL and UL), the viscosity of CP-based adhesives increased significantly. Expectedly, maximum viscosity of P-CPUL increased to 73.95 PaS, obviously higher than 59.62 PaS for P-CPOL.

5.4.7 Adhesion Properties of Camelina Protein

Similar to other plant proteins, CP molecules were unfolded in the solution, and their free side groups from the unfolded polypeptide, such as amino groups, carboxyl groups, and hydroxyl groups, formed strong chemical bond with the available hydroxyl groups on the wood surface under hot press condition. This process generated interfacial adhesion between the wood surface

and protein adhesives; in addition, the protein molecules were also cross-linked and entangled with each other, thus providing cohesion strength to the adhesives.

Figure 5.7 shows the dry shear strength and wet shear strength (refers to water resistance) of the CP based adhesives polymerized with different lignin. The dry shear strength of the unmodified camelina protein was 1.68 Pa. In the presence of PEGDE alone (P-CP), the adhesion strength increased to 2.13 MPa, followed by a small decrease to 1.87 MPa for P-CPL. This is in consistence with the results of frequency sweep that pointed the weakening effect of pristine lignin particles to the CP molecular interaction. When the lignin was de-polymerized, the dry shear strength for P-CPOL and P-CPUL increased to 2.28 and 2.35 MPa respectively.

Regarding to the wet strength, similar to soy protein, CP-based adhesives are not water-resistant as their adhesion strength decreased drastically after water soaking. The unmodified CP had the lowest wet adhesion strength at 0.28 MPa. In the addition of PEGDE crosslink agent, camelina protein structure was cross-linked, and its wet shear strength increased significantly to 0.84 MPa for P-CP. The addition of lignin induced further increased water-resistance of P-CPL to 0.95. Though the unmodified lignin interfered with protein's crosslink effect (Section 3.5.1) and reduced the dry shear strength of adhesives, it increased the wet strength of CP adhesives as a hydrophobic enhancer. This strengthening effect of native lignin was widely utilized to improve the water resistance of hydrophilic biopolymers. Luo et al (Luo et al., 2015) developed a soy meal-based wood adhesive with improved water resistance by using kraft lignin. Huang et al investigated the effect of alkaline lignin and lignosulfonate to soy protein based composite for enhanced mechanical performance and aqueous absorption. They found that as a hydrophobic filler, the alkaline lignin increased the tensile strength, thermal stability and water resistance of soy protein, (J. Huang et al., 2003b) while lignosulfonate contributed to soy protein's micro-phase separation and the formation of crosslinked structures. (J. Huang et al., 2003a)

Instead of simply mixing the lignin and protein, functionalized lignin further increased protein's water resistance. In this research, the wet shear strength of P-CPOL and P-CPUL reached 1.35 and 1.43 MPa, which could be used for industrial purpose (>1.0 MPa).(Efhamisisi et al., 2016) For the three-cycle water soaking test, while a proportional CP, P-CP and P-CPL failed, all the specimen of P-CPOL and PCPUL passed (Table 5.3). As we hypothesized in Schemes II and III, compared to native lignin, the de-polymerized lignin (PL and UL) contains

newly-formed hydroxyl groups that are able to form stronger hydrogen bond and covalent bond with the polar groups of camelina protein, which increased the cohesion of the adhesives. In addition, these hydroxyl groups increased the adhesion strength by stimulating the interfacial bonding between the wood surface and protein adhesives(Grossman, Nwabunma, Dufresne, Thomas, & Pothan, 2013) (Details in Scheme II and III).

5.5 Conclusion

Camelina protein copolymerized with oxidized kraft lignin improved water resistance of wood adhesives. In order to stimulate the protein-lignin interaction, lignin was de-polymerized by H_2O_2-induced oxidation under elevated temperature (50 ℃) and ultrasound irradiation, respectively. The modified lignin exhibited increased hydroxyl groups and reduced particle size. The oxidation induced by ultrasound irradiation treatment was more effective to induce the decomposition of lignin structure and increase its reactivity. Accordingly, the adhesive derived from camelina protein co-polymerized with oxidized kraft lignin induced by ultrasound irradiation (P-CPUL) had the strongest intermolecular interaction and highest water resistance. The non-edible camelina protein copolymerized with oxidized kraft lignin has potential for industrial adhesive applications, which would benefit camelina oil based energy industry as well as paper industry.

Scheme 1 Kraft lignin oxidation pathways in present of H2O2 at alkali condition
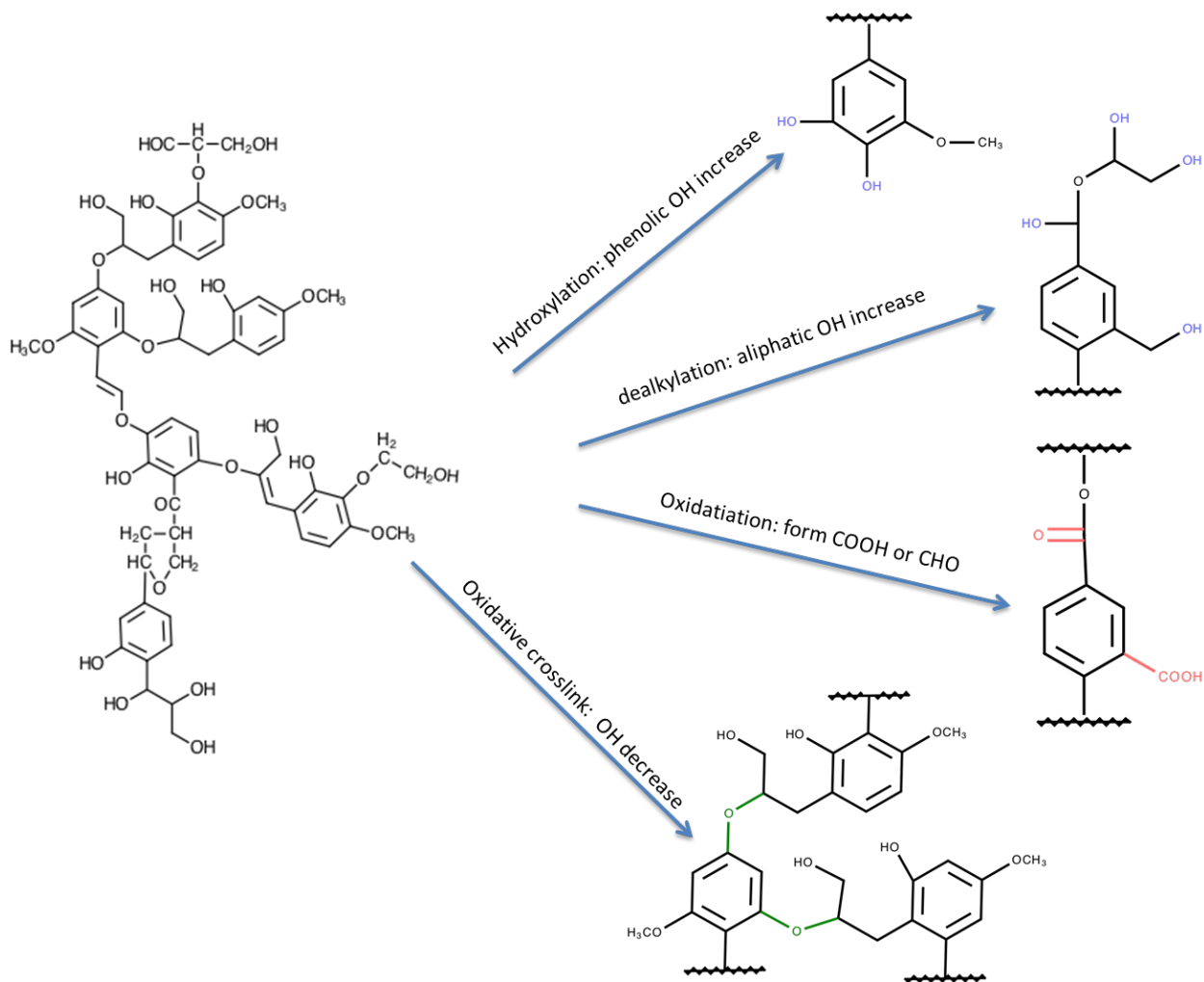
Scheme 2 Reaction between the protein and (oxidized) lignin
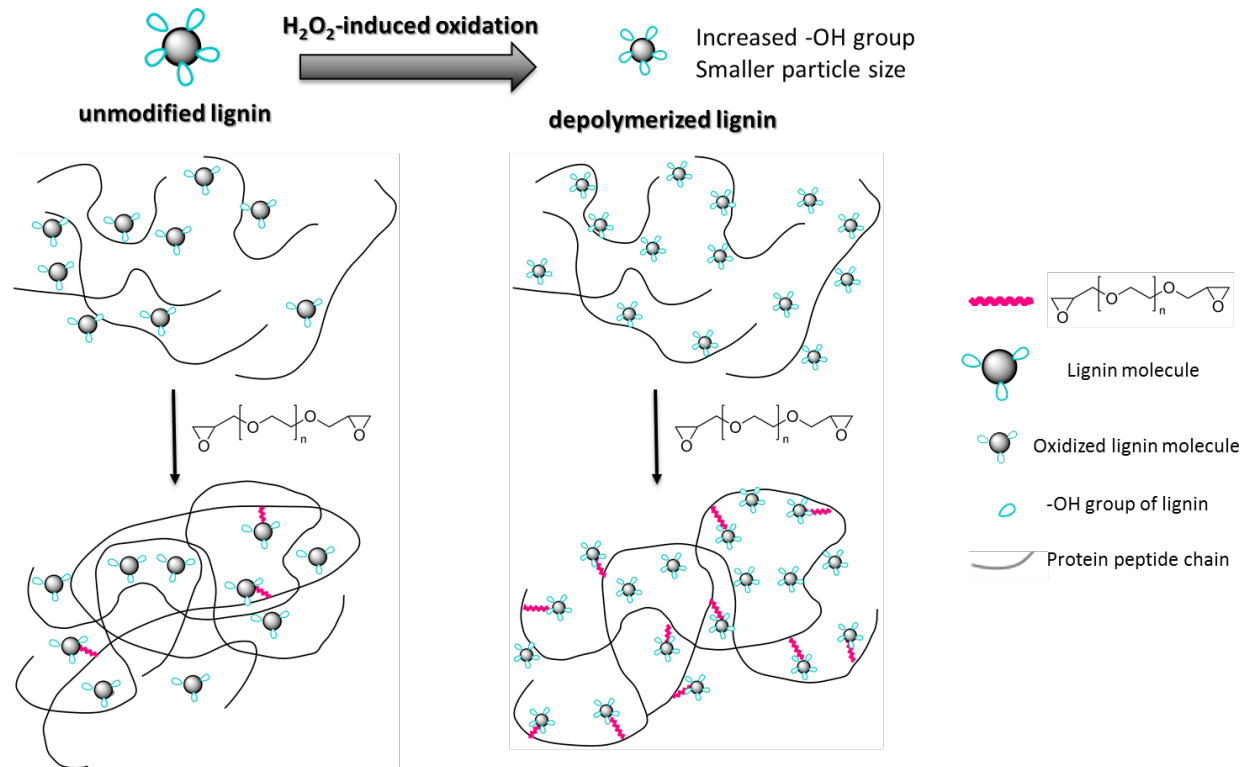
Scheme 3 protein-lignin adhesives bonding between wood panels
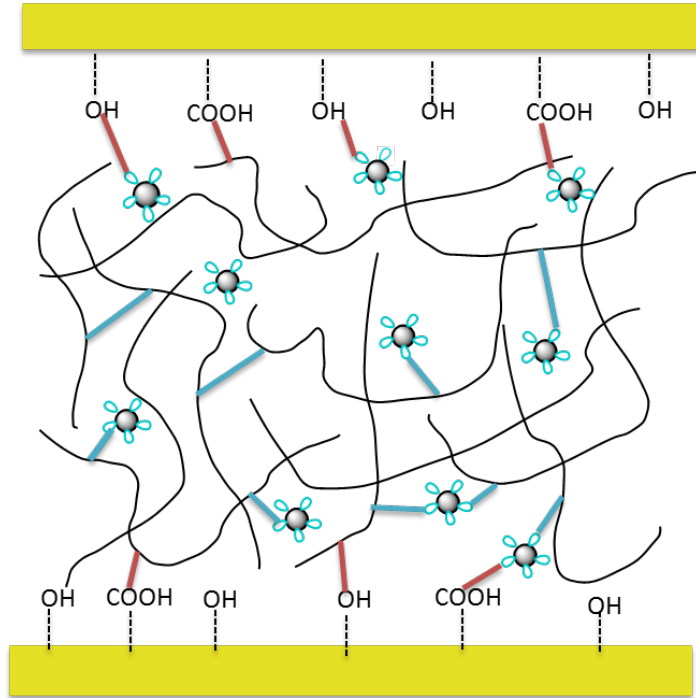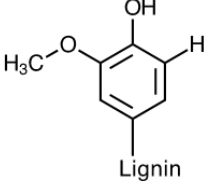

Wood surface

Interfacial bonding for adhesion

Intermolecular bonding for cohesion

Lignin

Protein peptide chain

Figure 5-1 Particle size distribution of lignin, oxidized lignin (OL), ultrasound-induced oxidized lignin (UL).
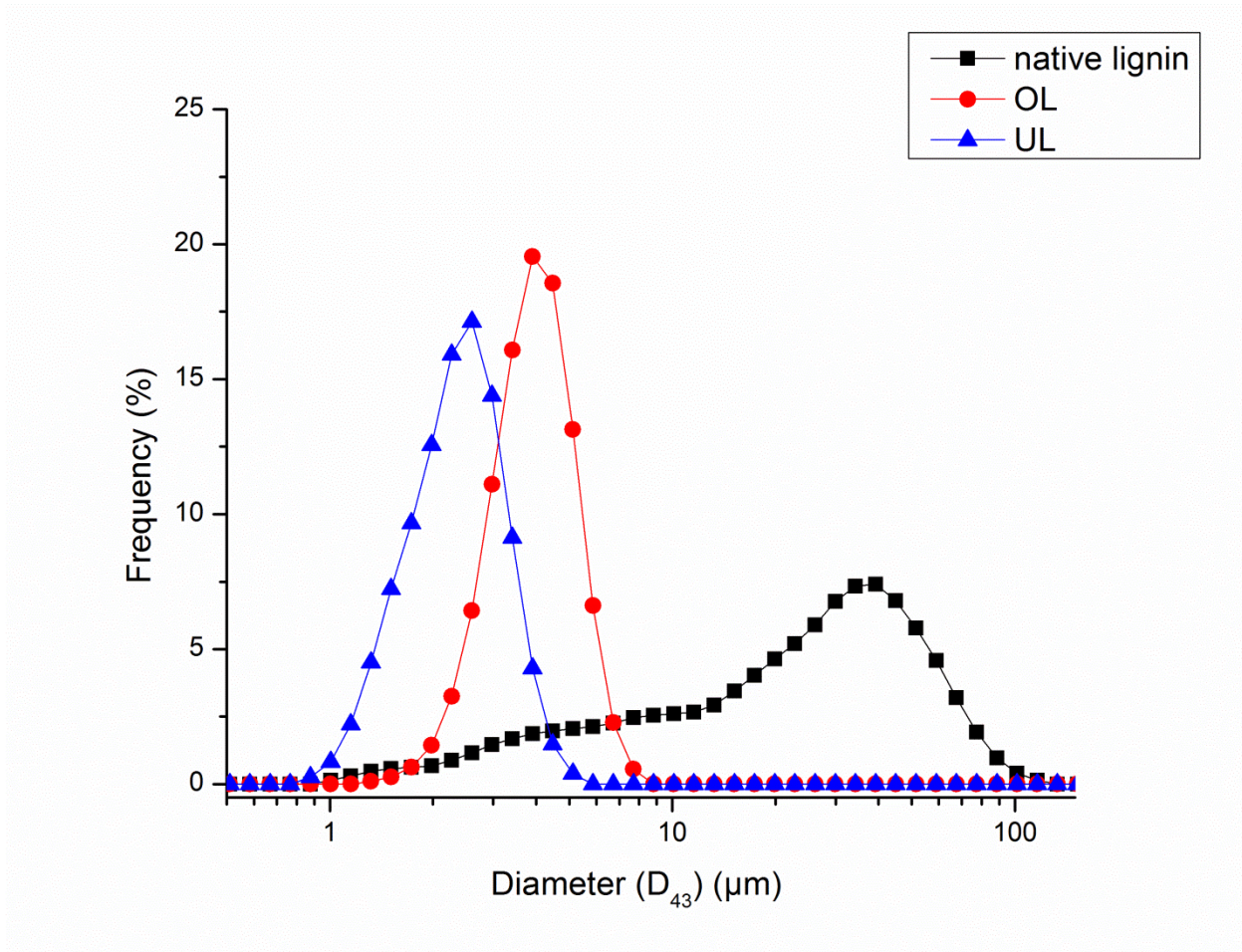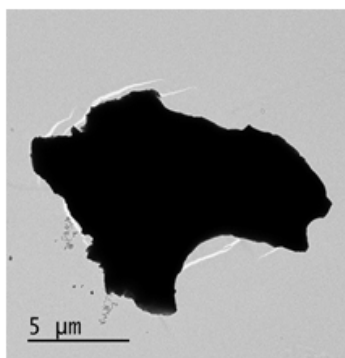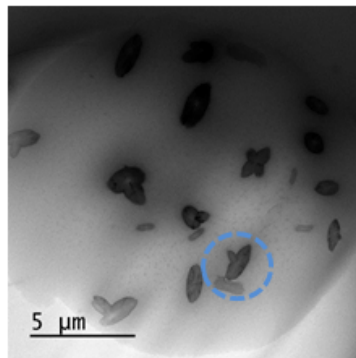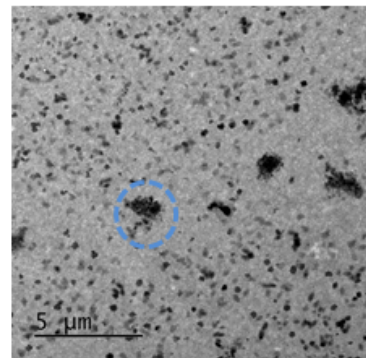
Figure 5-2 TEM images of lignin, oxidized lignin (OL), ultrasound-induced oxidized lignin (UL) (2) Native lignin, (b) oxidized-lignin (OL), (c) ultrasound-induced oxidized lignin (UL) (d) zoom-in morphology of OL, (e) zoom-in morphology of UL.
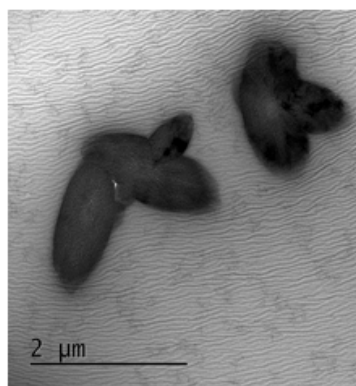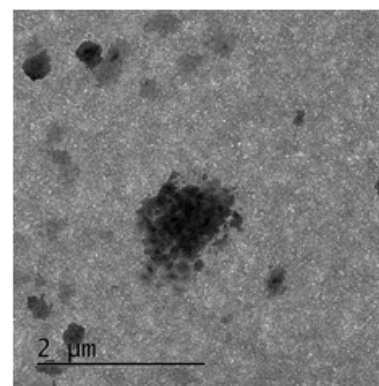

(a) Native lignin   (b) O-lignin   (c) UO-lignin

(d) O-lignin   (e) UO-lignin

Figure 5-3 FTIR spectra of lignin, oxidized lignin (OL), ultrasound-induced oxidized lignin (UL): (a) between 4,000 and 400 cm^{-1}; (b) between 1,000 and 1,800 cm^{-1} (the fingerprint region).
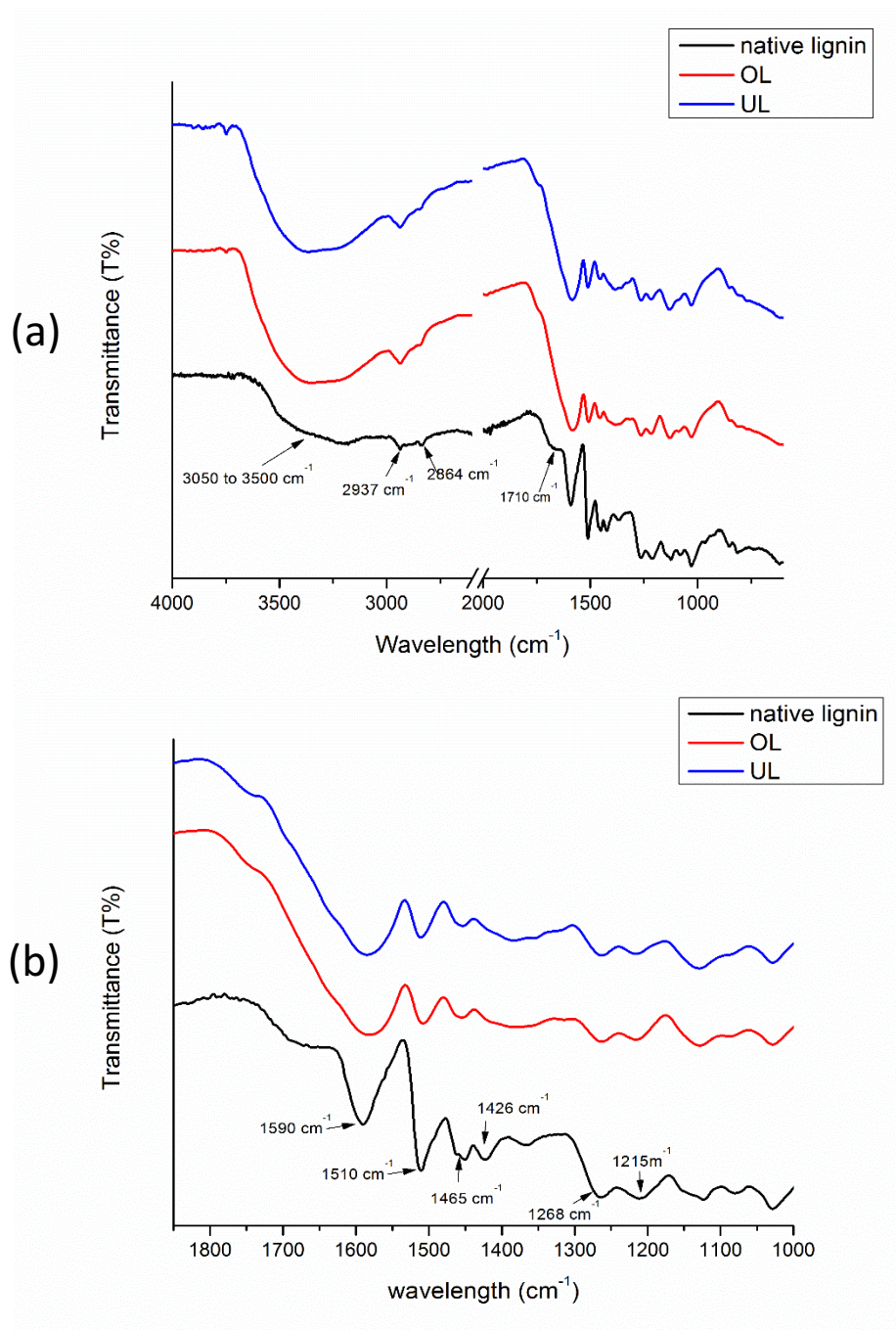
Figure 5-4 Derivative thermogratimetry (DTG) curves of lignin, oxidized lignin (OL), ultrasound-induced oxidized lignin (UL).
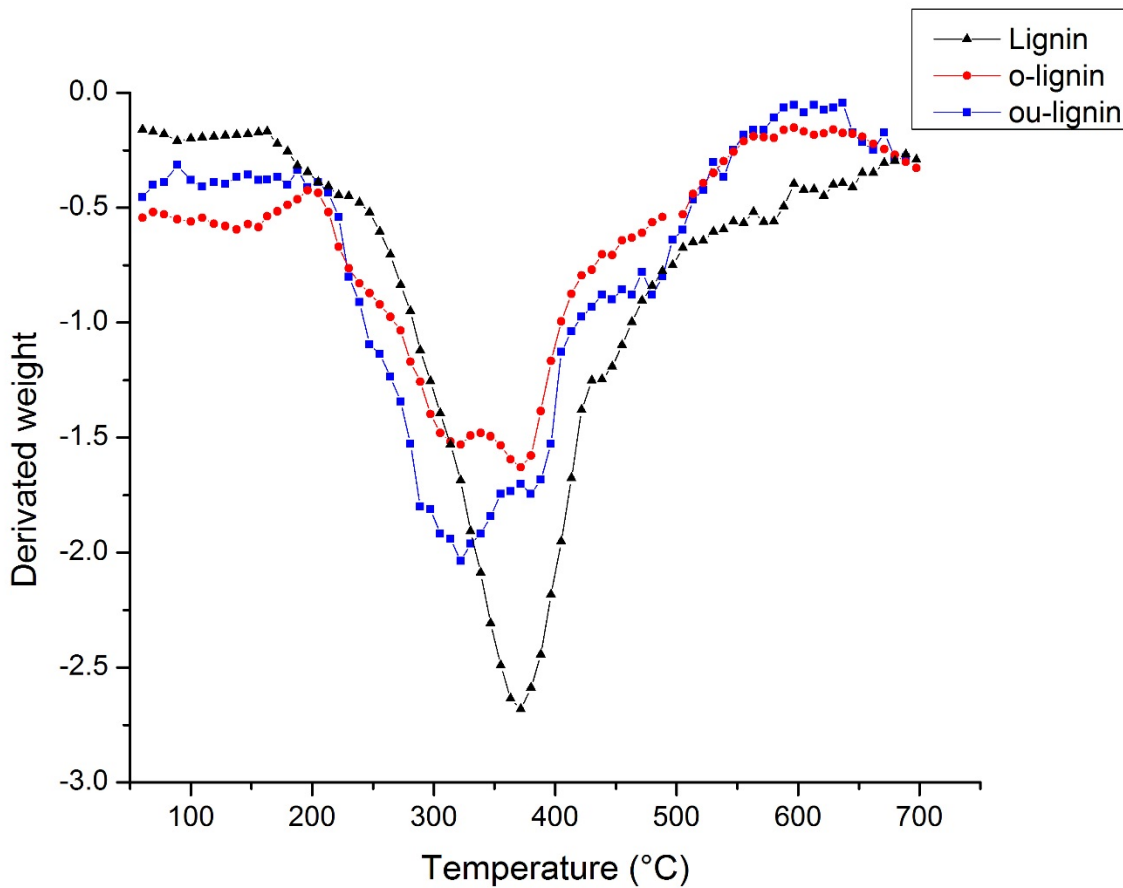
Figure 5-5 Fluorescence intensity of different protein-lignin dispersions of native camelina protein (P-CP), CP with lignin (P-CPL), CP wi1th OL (P-CPOL), and CP with UL (P-CPUL).

Figure 5-6 Rheological properties of CP-lignin adhesives. (a) Variation of storage modulus of different protein-lignin dispersions for the frequency sweep. (b) The apparent viscosity of different adhesive samples.
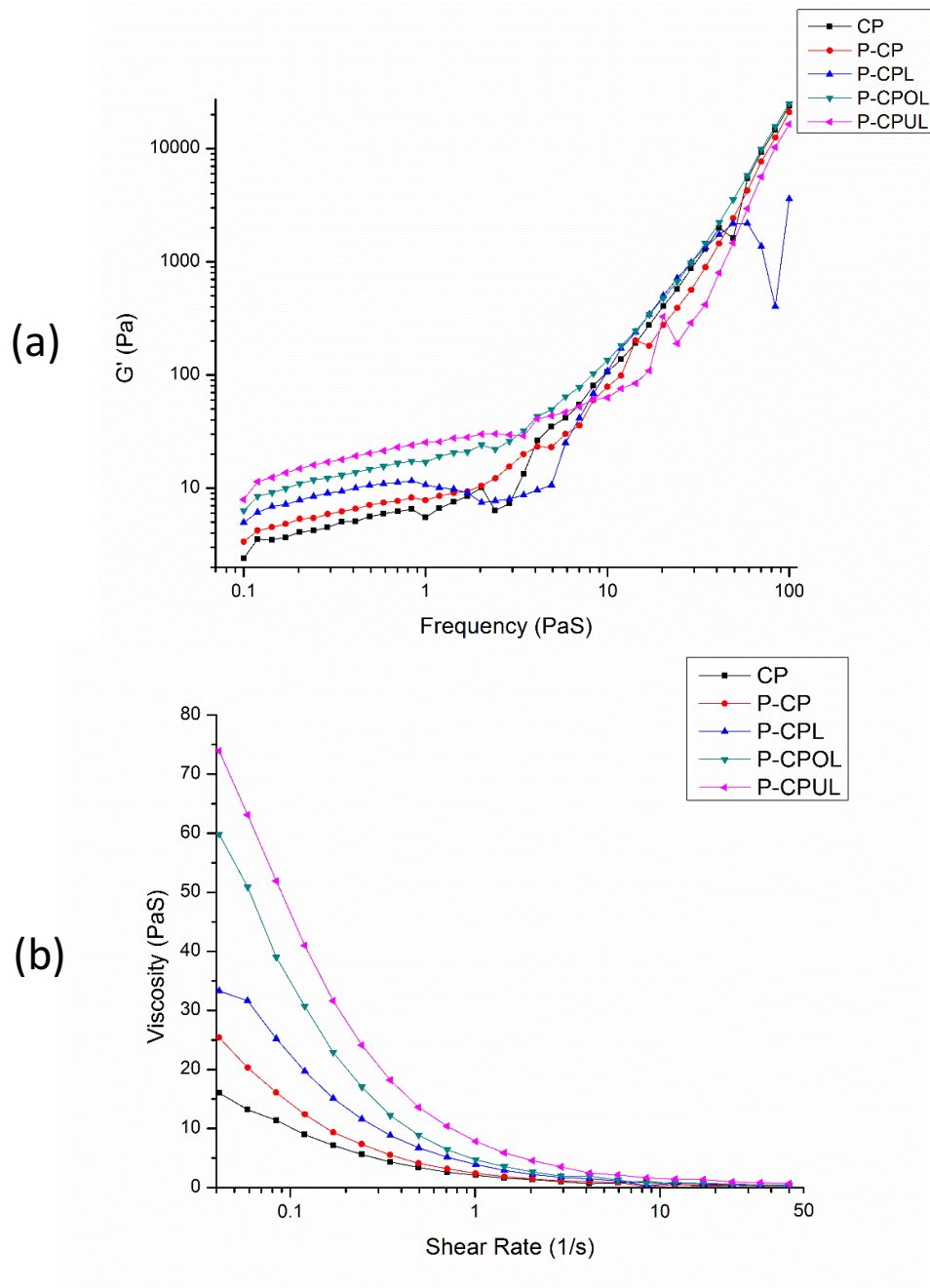
Figure 5-7 **Dry strength and wet shear strength of the different adhesive samples.**
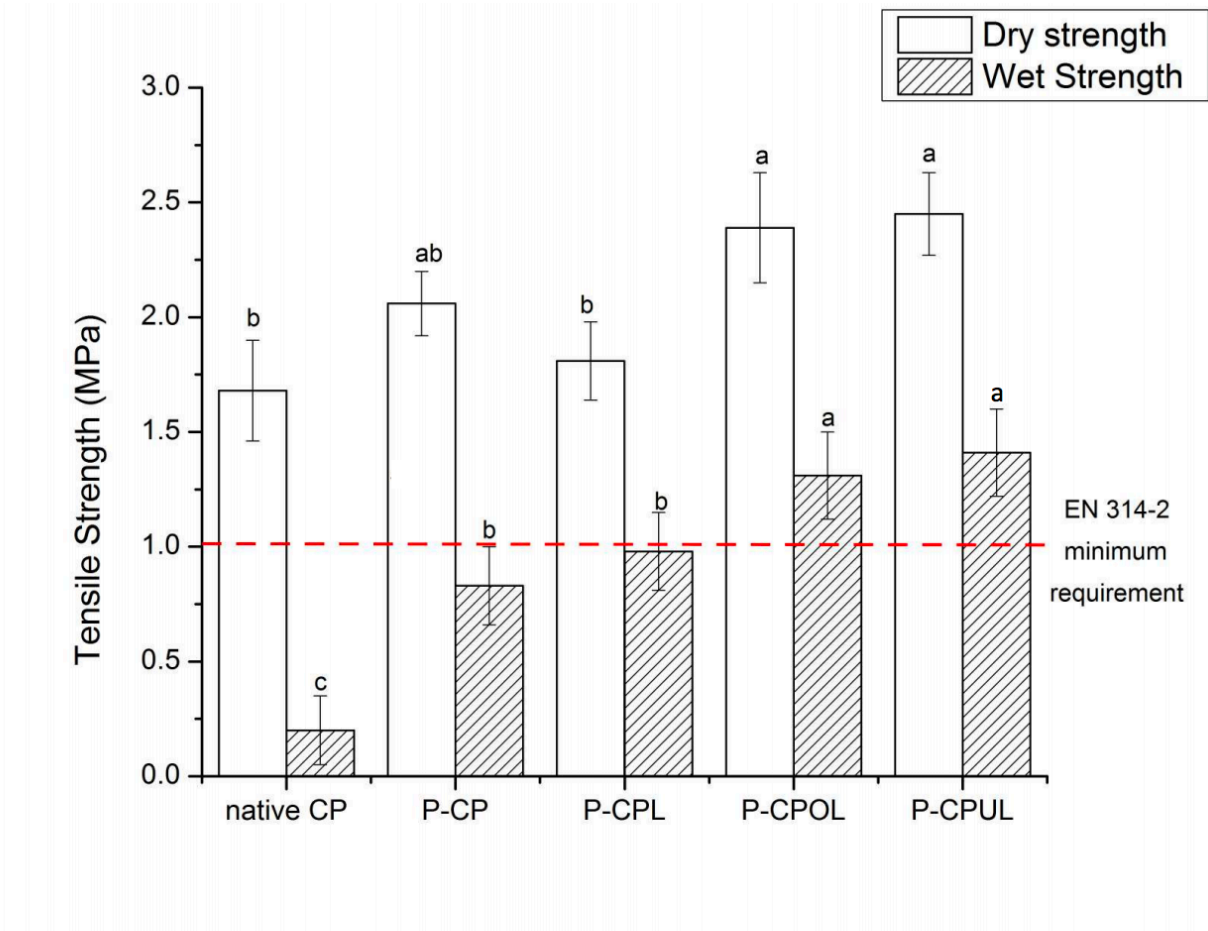
Letters indicate significant (p<0.05) difference within the same column.

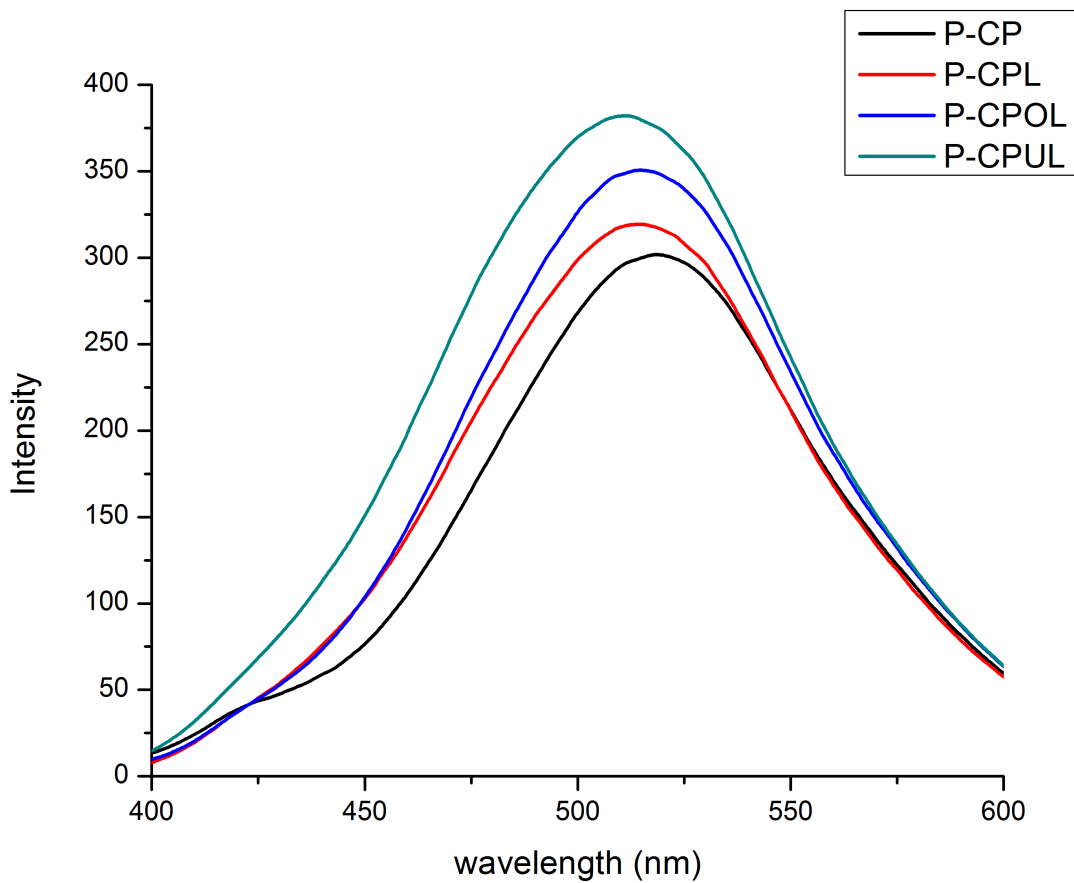**Table 5-1 Different Formulations of CP-lignin based Adhesives**

number	formulation	lignin content	notation
1	CP	0%	CP
2	CP cross-linked by PEGDE	0%	P-CP
3	CP/native lignin cross-linked by PEGDE	20%	P-CPL
4	CP/OL cross-linked by PEGDE	20%	P-CPOL
5	CP/UL cross-linked by PEGDE	20%	P-CPUL

Table 5-2 Rheological properties of different CP-lignin dispersions for frequency sweep

copolymer	[1] critical frequency f_c (PaS)	[2] modulus at f_c (Pa)
CP	1.00	6.5
P-CP	2.03	10.1
P-CPL	1.19	11.6
P-CPOL	2.42	22.1
P-CPUL	3.46	29.0

1. The frequency that protein structure broke down and G' began to increase sharply.

2. The modulus of the protein at the critical frequency.

Table 5-3 Three-cycle soak test evaluation of different CP-lignin adhesives

Samples	Wood pass the three-cycle wood soak test		
	1st round	2nd round	3rd round
CP	50%	25%	0%
P-CP	100%	100%	100%
P-CPL	100%	100%	75%
P-CPOL	100%	100%	100%
P-CPUL	100%	100%	100%

5.6 Reference

Aracri, E., Díaz Blanco, C., & Tzanov, T. (2014). An enzymatic approach to develop a lignin-based adhesive for wool floor coverings. *Green Chemistry*, *16*, 2597–2603. https://doi.org/10.1039/c4gc00063c

ASTM Standard Method D906-98.

Crestini, C., Pro, P., Neri, V., & Saladino, R. (2005). Methyltrioxorhenium: A new catalyst for the activation of hydrogen peroxide to the oxidation of lignin and lignin model compounds. *Bioorganic and Medicinal Chemistry*, *13*(7), 2569–2578. https://doi.org/10.1016/j.bmc.2005.01.049

Efhamisisi, D., Thevenon, M.-F., Hamzeh, Y., Karimi, A.-N., Pizzi, A., & Pourtahmasi, K. (2016). Induced Tannin Adhesive by Boric Acid Addition and Its Effect on Bonding Quality and Biological Performance of Poplar Plywood. *ACS Sustainable Chemistry & Engineering*, *4*(5), 2734–2740. https://doi.org/10.1021/acssuschemeng.6b00230

Gidh, A., Talreja, D., Vinzant, T. B., Williford, T. C., & Mikell, A. (2006). Detailed analysis of modifications in lignin after treatment with cultures screened for lignin depolymerizing agents. *Appl Biochem Biotechnol*, *131*(1–3), 829–843. https://doi.org/10.1385/ABAB:131:1:829

Gilca, I. A., Popa, V. I., & Crestini, C. (2015). Obtaining lignin nanoparticles by sonication. *Ultrasonics Sonochemistry*, *23*, 369–375. https://doi.org/10.1016/j.ultsonch.2014.08.021

Grossman, R. F., Nwabunma, D., Dufresne, A., Thomas, S., & Pothan, L. A. (2013). *Biopolymer nanocomposites: processing, properties, and applications* (Vol. 8). John Wiley & Sons.

Gui, C., Wang, G., Wu, D., Zhu, J., & Liu, X. (2013). Synthesis of a bio-based polyamidoamine-epichlorohydrin resin and its application for soy-based adhesives. *International Journal of Adhesion and Adhesives*, *44*, 237–242. https://doi.org/10.1016/j.ijadhadh.2013.03.011

Huang, J., Zhang, L., & Chen, F. (2003a). Effects of lignin as a filler on properties of soy protein plastics. I. Lignosulfonate. *Journal of Applied Polymer Science*, *88*(14), 3284–3290. https://doi.org/10.1002/app.12185

Huang, J., Zhang, L., & Chen, P. (2003b). Effects of Lignin as a Filler on Properties of Soy Protein Plastics . II . Alkaline Lignin. *J. Appl. Polym. Sci*, *88*(14), 3291–3297.

Kardos, N., Jean-ge, L., Goux-henry, C., Andrioletti, B., & Draye, M. (2015). H 2 O 2 ‐ Mediated Kraft Lignin Oxidation with Readily Available Metal Salts : What about the E ff

ect of Ultrasound ? Franc o. https://doi.org/10.1021/acs.iecr.5b00595

Li, N., Qi, G., Sun, X. S., Wang, D., Bean, S., & Blackwell, D. (2014). Isolation and Characterization of Protein Fractions Isolated from Camelina Meal. *Transactions of the ASABE*, *57*(2010), 169–178. https://doi.org/10.13031/trans.57.10455

Liu, D., Tian, H., Zhang, L., & Chang, P. R. (2008). Structure and Properties of Blend Films Prepared from Castor Oil-Based Polyurethane/Soy Protein Derivative. *Industrial & Engineering Chemistry Research*, *47*(23), 9330–9336. https://doi.org/10.1021/ie8009632

Liu, H., Li, C., & Sun, X. S. (2015). Improved water resistance in undecylenic acid (UA)-modified soy protein isolate (SPI)-based adhesives. *Industrial Crops and Products*, *74*, 577–584. https://doi.org/10.1016/j.indcrop.2015.05.043

Liu, Y., Hu, T., Wu, Z., Zeng, G., Huang, D., Shen, Y., … He, Y. (2014). Study on biodegradation process of lignin by FTIR and DSC. *Environmental Science and Pollution Research*, *21*(24), 14004–14013. https://doi.org/10.1007/s11356-014-3342-5

Luo, J., Luo, J., Yuan, C., Zhang, W., Li, J., Gao, Q., & Chen, H. (2015). An eco-friendly wood adhesive from soy protein and lignin: performance properties. *RSC Adv.*, *5*(122), 100849–100855. https://doi.org/10.1039/C5RA19232C

Mancera, A., Fierro, V., Pizzi, A., Dumar??ay, S., G??rardin, P., Vel??squez, J., … Celzard, A. (2010). Physicochemical characterisation of sugar cane bagasse lignin oxidized by hydrogen peroxide. *Polymer Degradation and Stability*, *95*(4), 470–476. https://doi.org/10.1016/j.polymdegradstab.2010.01.012

Napoly, F., Kardos, N., Jean-Gérard, L., Goux-Henry, C., Andrioletti, B., & Draye, M. (2015). H 2 O 2 -Mediated Kraft Lignin Oxidation with Readily Available Metal Salts: What about the Effect of Ultrasound? *Industrial & Engineering Chemistry Research*, *54*(22), 6046–6051. https://doi.org/10.1021/acs.iecr.5b00595

Qi, G., & Sun, X. S. (2010). Peel adhesion properties of modified soy protein adhesive on a glass panel. *Industrial Crops and Products*, *32*(3), 208–212. https://doi.org/10.1016/j.indcrop.2010.04.006

Reddy, N., Jin, E., Chen, L., Jiang, X., & Yang, Y. (2012). Extraction, characterization of components, and potential thermoplastic applications of camelina meal grafted with vinyl monomers. *Journal of Agricultural and Food Chemistry*, *60*(19), 4872–9. https://doi.org/10.1021/jf300695k

Ren, X., & Soucek, M. (2014). Soya-Based Coatings and Adhesives. In *ACS Symposium Series* (pp. 207–254). https://doi.org/10.1021/bk-2014-1178.ch010

Savy, D., & Piccolo, A. (2014). Physical-chemical characteristics of lignins separated from biomasses for second-generation ethanol. *Biomass and Bioenergy*, *62*(0), 58–67. https://doi.org/10.1016/j.biombioe.2014.01.016

Soria, A. J., McDonald, A. G., & Shook, S. R. (2008). Wood solubilization and depolymerization using supercritical methanol. Part 1: Process optimization and analysis of methanol insoluble components (bio-char). *Holzforschung*, *62*(4), 402–408. https://doi.org/10.1515/HF.2008.067

Sun, X. S. (2011). Soy Protein Polymers and Adhesion Properties. *Journal of Biobased Materials and Bioenergy*, *5*(4), 409–432. https://doi.org/10.1166/jbmb.2011.1183

Sun, Y.-G., Ma, Y.-L., Wang, L.-Q., Wang, F.-Z., Wu, Q.-Q., & Pan, G.-Y. (2015). Physicochemical properties of corn stalk after treatment using steam explosion coupled with acid or alkali. *Carbohydrate Polymers*, *117*, 486–493. https://doi.org/http://dx.doi.org/10.1016/j.carbpol.2014.09.066

Tortora, M., Cavalieri, F., Mosesso, P., Ciaffardini, F., Melone, F., & Crestini, C. (2014). Ultrasound driven assembly of lignin into microcapsules for storage and delivery of hydrophobic molecules. *Biomacromolecules*, *15*(5), 1634–1643. https://doi.org/10.1021/bm500015j

Tunick, M. H. (2011). Small-strain dynamic rheology of food protein networks. *Journal of Agricultural and Food Chemistry*, *59*(5), 1481–6. https://doi.org/10.1021/jf1016237

Wi, S. G., Cho, E. J., Lee, D.-S., Lee, S. J., Lee, Y. J., & Bae, H.-J. (2015). Lignocellulose conversion for biofuel: a new pretreatment greatly improves downstream biocatalytic hydrolysis of various lignocellulosic materials. *Biotechnology for Biofuels*, *8*(1), 1–11. https://doi.org/10.1186/s13068-015-0419-4

Xu, C., Arancon, R. A. D., Labidi, J., & Luque, R. (2014). Lignin depolymerisation strategies: towards valuable chemicals and fuels. *Chemical Society Reviews*, *43*(22), 7485–500. https://doi.org/10.1039/c4cs00235k

Zhao, Y., Jiang, Q., Xu, H., Reddy, N., Xu, L., & Yang, Y. (2014). Cytocompatible and water-stable camelina protein films for tissue engineering. *Journal of Biomedical Materials Research. Part B, Applied Biomaterials*, *102*(4), 729–36.

https://doi.org/10.1002/jbm.b.33053

Zheng, K. W., Zhang, J. Y., & Cheng, J. (2013). Morphology, Structure, Miscibility, and Properties of Wholly Soy-Based Semi-interpenetrating Polymer Networks from Soy-Oil-Polyol-Based Polyurethane and Modified Soy Protein Isolate. *Industrial & Engineering Chemistry Research*, *52*(40), 14335–14341. https://doi.org/10.1021/ie401791v

Zhu, X., Wang, D., & Sun, X. S. (2016). Physico-chemical properties of camelina protein altered by sodium bisulfite and guanidine-HCl. *Industrial Crops and Products*, *83*, 453–461. https://doi.org/10.1016/j.indcrop.2015.12.085

Chapter 6- CONCLUSION AND RECOMMENDATION

6.1 Conclusion

Camelina protein, extracted from the de-fatted meal, was modified by unfolding, crosslink and copolymerization treatment for improved water resistance and mechanical performance. The unfolding $NaHSO_3$ and Guanidine-HCl played an important role in disrupting camelina protein's secondary structures (namely destroy the disulfide bond and hydrogen bond respectively). The unfolded structures were confirmed by observing protein's increased free sulfydryl group and surface hydrophobicity. Accordingly, the viscosity, particle size decreased which consequently leaded to the improvement of protein resin's flow-ability. However, the denatured camelina protein exhibited reduced water resistance at high concentration of denaturing agents.

Then we attempted to increase the CP's water resistance by applying the coupling agent, Ethyl-3-(3-dimethyl-aminopropyl-1-carbodiimide) (EDC), to stabilize the protein structure. Covalent bonds formed between the free carboxyl groups and amino groups of CP peptide chains. This eventually leaded to CP's increased molecular weight and condensed microstructures. The cross-linked CP exhibited stronger intermolecular protein interaction (characterized by elastic modulus), increased viscosity and water resistance. Moreover, ultrasound treatment further enhanced the crosslink effect of EDC, resulting in CP's stronger aggregation behaviors and more compact protein structures. Accordingly, the elastic modulus, viscosity, and water resistance of ultrasound-pretreated CP exhibited further increase.

In addition, we attempted to develop the CP-lignin based copolymer to improve camelina protein's poor water resistance for wood adhesive. Kraft lignin was oxidized by H_2O_2 (induced by heat and ultrasound) and copolymerized with CP. The de-polymerized lignin with increased hydroxyl group exhibited stronger intermolecular interaction with CP than the pristine lignin. Thus, camelina protein exhibited obviously increased hydrophobicity and water resistance. For the best treatment condition, the wet shear adhesion strength of the copolymer increased from 0.28 MPa to 1.43 MPa (meet the industrial requirement), with all wood panels passing the three-cycle water soaking test.

6.2 Recommendation

Firstly, based on the results, incorporation of lignin as a hydrophobic enhancer to camelina protein was an effective and feasible method to improve its water resistance as wood adhesives. Thus, further research could focus on several other bio-based hydrophobic enhancers with higher reactivity than lignin, such as gallic acid. Secondly, the water-resistance of pristine camelina protein is too weak, which restricted its application as the industrial adhesive products. The investigation of camelina protein isolation or purification was necessary to find the optimized camelian protein fractions for wood adhesives. Thirdly, while the conditions of camelina protein modification and isolation were optimized, future work is suggested to use the camelina meal as the raw material; it is promising to stimulate the industrialization of camelina protein-based bioprocessing.

Abbreviations

CP: Camelina protein

CPI: Camelina protein isolate

CM: Camelina meal

DCM: Defatted camelina oil

CO: Camelina oil

UF: Urea-formaldehyde

PF: Phenol-formaldehyde

PVA: Polyvinyl acetate

SPA: Soy protein adhesive

SPI: Soy protein isolate

UA: Undecenoic acid

MSP: Modified soy protein

Gdm.Cl: Guanidine-HCl

SMCP: $NaHSO_3$-modified camelina protein

GMCP: Gdm.Cl-modified camelina protein

UCPI: Ultrasound-modified camelina protein isolate

EDC: N-(3-Dimethylaminopropyl)-N-ethylcarbodiimide hydrochloride

NHS: N-Hydroxysuccinimide

SEM: Scanning electron microscopy

TEM: Transmission electron microscopy

FTIR: Fourier transform infrared spectroscopy

TGA: Thermogravimetric analysis

OL: oxidized lignin

UL: ultrasound-induced oxidized lignin

DTG: Derivative thermogratimetry